On the Throughput of In-Band Full-Duplex Communication in Wireless Systems

by

Kudret Akçapınar

Submitted to
the Graduate School of Engineering and Natural Sciences
in partial fulfillment of
the requirements for the degree of
Master of Science

SABANCI UNIVERSITY

December 2015

ON THE THROUGHPUT OF IN-BAND FULL-DUPLEX COMMUNICATION IN WIRELESS SYSTEMS

APPROVED BY:

Assoc. Prof. Dr. Özgür Gürbüz
(Thesis Supervisor)

Prof. Dr. Özgür Erçetin

Prof. Dr. Elza Erkip

(Polytechnic Institute of NYU)

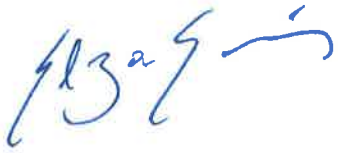

DATE OF APPROVAL:30.12.2015

On the Throughput of In-Band Full-Duplex Communication in Wireless Systems

Kudret Akçapınar

M.Sc. Thesis, 2015

Thesis Supervisor: Assoc. Prof. Dr. Özgür Gürbüz

Keywords: full-duplex, half-duplex, self-interference, power control, routing

Abstract

Proliferation of mobile devices and explosion in data intensive applications have led to serious spectrum crunch and stimulated the pursuit of new wireless communication techniques to utilize the scarce wireless spectrum assets more efficiently. As one of the promising technologies considered for next generation wireless communications, in-band full-duplex has been shown to have a great potential to alleviate this problem due to doubled spectral efficiency. Unlike half-duplex radios, which need to transmit and receive at different times, or out-of-band full-duplex radios, which devote different frequency bands to transmission and reception, in-band full-duplex radios are capable of simultaneously transmitting, while receiving over the same frequency band at the cost of self-interference that results.

In this thesis, via extensively conducted experiments, we compare the performance of in-band full-duplex with that of half-duplex in fundamental communication scenarios such as two way communication, one way two hop communication and two way two hop communication, clearly identifying the conditions under which in-band full-duplex outperforms half-duplex. Next, we extend our study to evaluate in-band full-duplex in multihop wireless networks, considering a linear topology. We obtain closed form analytical expressions for optimum transmission power policy in the two hop case and a linear programming and binary search based solution for the multihop case to compute the optimal transmission power levels. Our in-band full-duplex solution which takes into account full-interference is shown to outperform half-duplex transmission by a factor of 2.77 at low transmission power level, and by a factor of 1.81 at high transmission power level. We also

incorporate our power solution with routing algorithms for adhoc networks. We compare the end-to-end throughput performance of the proposed joint routing & power allocation solution to that of half-duplex, direct transmission and an existing one-hop interference based in-band full-duplex transmission strategy. Our numerical experiments considering practical, low power systems such as femto cells and Zigbee show that proposed joint routing & power control mechanism provides 30% throughput improvement, relative to the existing in-band full-duplex solution with one hop interference, while it offers five times throughput, relative to half-duplex transmission even for moderate ($80dB$) SI cancellation levels.

Kablosuz Sistemlerde Aynı Bant Tam-Çift Yönlü İletişimin Başarımı Üzerine

Kudret Akçapınar

M.Sc. Tez, 2015

Thesis Supervisor: Assoc. Prof. Dr. Özgür Gürbüz

Anahtar kelimeler: Tam-çift yönlü iletim, yarı-çift yönlü iletim, öz-girişim, güç kontrol, yol atama

Özet

Mobil cihazların ve veri tüketen uygulamaların çoğalması ciddi spektrum problemlerine yol açtı ve sınırlı olan spektrum varlıklarının daha verimli kullanmak için yeni kablosuz iletişim yöntemleri arayışını beraberinde getirdi. Gelecek nesil kablosuz iletişim için düşünülen, umut vaaden teknolojilerden biri olarak, aynı bant tam-çift yönlü kablosuz iletişimin, spektral verimliliği ikiye katladığı için, spektrum problemini hafifletmede büyük bir potansiyele sahip olduğu gösterildi. Farklı zamanlarda alım ve gönderim yapan yarım-çift yönlü radyolardan ve farklı frekans bantları üzerinden alım ve gönderim yapan tam-çift yönlü radyolardan farklı olarak, aynı bant tam-çift yönlü radyolar, özgirişim pahasına, aynı anda aynı frekans üzerinden alım ve gönderim yapma yeteneğine sahiptirler.

Bu tezde, kapsamlı olarak yapılmış deneyler aracılığı ile, tek atlamalı iki yönlü haberleşme, iki atlamalı tek yönlü haberleşme ve iki atlamalı iki yönlü haberleşme gibi temel iletişim senaryoları üzerinden, aynı bant tam-çift yönlü ve yarı-çift yönlü iletişimin, aynı bant tam-çift yönlü iletişimin yarı-çift yönlü iletişimin performansını geçtiği şartları açıkça belirterek, performans kıyaslamasını yapıyoruz. Sonra, çalışmamızı aynı bant tam-çift yönlü iletişimi, doğrusal bir topoloji düşünerek çok atlamalı kablosuz ağlarda incelemek için genişletiyoruz. En iyi iletim gücü seviyeleri hesaplaması için, iki atlamalı iletişim senaryosunda analitik ifadeler, çok atlamalı iletişim senaryosunda ise lineer programlama ve ikili arama tabanlı bir çözüm elde ediyoruz. Tam girişim modelini esas alan, önerdiğimiz aynı bant tam-çift yönlü iletim, düşük iletim güç seviyelerinde yarı-çift yönlü iletimin 2.77 katı

kadar, yüksek iletim gücü seviyelerinde ise 1.81 katı kadar performans sağlamaktadır. Ayrıca iletim gücü çözümümüzü, anlık ağlar için yol atama algoritması ile birleştiriyoruz. Önerdiğimiz bütünleşik yol atama ve güç tahsisi çözümümüzü, uçtan uca başarım performansı açısından, yarı-çift yönlü iletim, doğrudan iletim ve mevcut bir tam-çift yönlü iletim çözümü ile karşılaştırıyoruz. Femto hücreler ve Zigbee gibi pratik sistemleri düşünerek yaptığımız deneyler, önerdiğimiz tümleşik yol atama ve güç kontrol mekanizmasının, mevcut aynı bant tam-çift yönlü iletimden %30 daha fazla başarım, makul öz-girişim seviyesinde bile (80 dB) yarı-çift yönlü iletimin beş katı kadar başarım sağladığını göstermiştir.

Canım aileme. . .

Acknowledgements

I would like to express my deepest gratitude to

My advisor **Özgür Gürbüz** for her constant support all throughout my thesis study. From the beginning until the end of my master's program, she has always encouraged me to do what is necessary to do, motivating and showing me the right direction with her priceless guidance to surmount the obstacles I have encountered. It is undoubted that I could not have submitted this thesis without her persistent mentoring. Therefore, for all she did for me since the beginning, I am very much grateful to her,

My reading committee members, **Özgür Erçetin** and **Elza Erkip** for accepting to be in my jury and spending their valuable times,

Tonguç Ünlüyurt for his wise instructions for helping us with the solution of the optimization problem,

My colleagues at Telecommunications & Networking Laboratory for their perpetual cooperation in solving the problems I have confronted,

Tubitak for partially supporting our project with Grant No 113E222,

My family for disinterestedly being there to help and support me at all costs, at all times,

My nephew Yusuf for always enriching my life and cheering me up.

Contents

List of Figures

List of Tables

Chapter 1

Introduction

The total number of internet-connected wireless devices has tremendously increased in the last decade [2]. These devices have not only proliferated in numbers but also have become data-hungry because of the evolving context-rich applications, arising the natural necessity for improving wireless data rates. Take cell phones as an example: while a cell phone used to be a device used only for voice communication and text messaging, it has gradually turned into a device with which people can easily connect to the internet to reach the information they look for anytime, anywhere on earth. Anything that can be done on personal computers can now be easily done on mobile phones, from online banking to turning on a heater at home from work. We aim at highlighting the explosion in data demand and emphasizing the need for broadband wireless systems in the next section through the alarming statistics provided.

1.1 Increasing Data Demand

Advancements in mobile phone technology have made it possible to do what has usually been done with desktop computers on mobile devices as well, transforming them into bandwidth hungry devices [3]. Rapid proliferation of mobile devices and emergence of bandwidth intensive mobile applications have led to serious spectrum

crunch, creating an apprehension of whether the existing wireless technologies will be able to meet the ceaselessly growing demand in wireless data. As a result of rising number of mobile service subscribers and emergence of new trends such as Machine To Machine (M2M) communication and Internet Of Things (IoT), mobile data traffic has peaked and need for more bandwidth has increased more than ever. Just to highlight the booming wireless data traffic and seriousness of forthcoming spectrum scarcity, the following statistics provided by [2] may help appreciate quest for next generation wireless communication that responds to ever-increasing data consumption and allays the spectrum crunch mobile carrier companies and other commercial service providers have confronted.

- The total number of internet users was as small as 400 million in 2000, whereas it is expected to be 3.2 billion people all around the globe by the end of 2015.

- More than 7 billion people worldwide are expected to have access to mobile cellular services at the end of 2015, which is equivalent of 98% penetration.

- The proportion of internet-connected households is expected to climb up to 46% in 2015, which was as low as 18% in 2005.

- 3G population coverage has escalated to 69% in 2015, whereas only 45% of entire world population was covered in 2011.

These statistics undoubtedly point out that prevalence of wireless communication services has shown a massive uptrend since 2000. As this trend is assumed to continue even with a greater acceleration in the future, new technologies are required to fulfill the ever-growing data demand of users and to provide them a seamless service. In-band full-duplex (FD) wireless is one of the technologies that is considered as a candidate for future wireless technology, for instance, 5G mobile communication.

1.2 Motivation

Wireless spectrum is a quite limited, hence a significantly valuable asset, which sparks the competition between commercial service providers [4]. However, it has been well realized that the existing wireless spectrum has been almost completely exploited due to the increased wireless services, usage in the past 15 years.

Until recently, a long-held taboo in wireless communication was that a radio generally cannot achieve simultaneous transmission and reception on the same frequency band due to resulting high self-interference [5].

After the pioneering works conducted at Stanford University [6, 7] and Rice University [8], this assumption has been broken with the introduction of in-band full-duplex (FD) communication. This means that same capacities achieved with traditional half-duplex (HD) communication can be achieved occupying half of the total bandwidth only and hence the spectral efficiency is doubled by FD wireless technology. Consequently, using limited wireless spectrum assets in a more efficient way immediately alleviates the spectrum drought crisis. The significance of spectral efficiency can be more striking when considering the fact that bandwidth of 360.4 Mhz spectrum has been sold in an auction for $4.5G$ recently held in Turkey for 3.96 billion euros to the GSM operators [9]. Even from this single example, one can easily comprehend how important role FD wireless can potentially play in cellular mobile communication in terms of creating more wireless spectrum assets available.

Although we have so far discussed only about spectral efficiency enhanced by the in-band FD technology until now, it is not the only aspect we can benefit from it. In addition to spectral efficiency, in-band FD can also leverage the throughput performance of wireless networks, not only by improving overall data rate, but also mitigating the packet loss problem caused by hidden terminals. Plus, it is also possible with in-band FD to mitigate the loss of network throughput because of congestion and MAC scheduling, enabling nodes with congestion to forward their

packets, while simultaneously receiving [6]. Additionally, in-band FD communication has a potential to advance network secrecy. [10, 11, 12]. Consider two nodes trying to communicate with each other wirelessly, and an eavesdropper in the environment is trying to decode these nodes' messages. If both nodes are in-band FD enabled, then eavesdropper receives a sum signal, which is quite difficult to decode.

Our aim in this thesis is to investigate the performance gains of FD, considering different communication settings and determine the conditions, when FD can be preferred to HD. First, we focus on three fundamental scenarios, namely, bidirectional (two way) communication over a single hop, one way two hop communication i.e. relaying and two way two hop communication, i.e. two way relaying where we consider both HD and in-band FD implementations for the relay. As we look into the performance of HD and in-band FD in these communication models, we utilize an experimentally characterized, hence a quite realistic self-interference cancellation model.

Based on our findings, we extend our study to multihop communication scenarios where we commence our investigation by considering two hop communication of a source and destination via an in-band FD-enabled relay in a full-interference environment, and we present an optimal transmission power policy based on the closed form expressions we derive.

In the third part part of the thesis, based on our findings in two hop communication, assuming full-interference environment, we study multihop communication scenarios with more than 2 hops, where a source node sends its message to a destination node via multiple intermediate relays and delve into the issue of optimal transmission power allocation in multihop networks with full interference assumption. Finally, we consider routing with FD nodes in ad hoc networks. Two different subproblems are to be addressed at this point: 1) Finding the best path between source and destination nodes offering the highest end-to-end throughput 2) Transmission power allocation of the nodes selected on this path to get the maximum end-to-end throughput. The proposed solution is a joint strategy,

which couples our transmit power allocation policy with routing algorithms via a new metric. This solution is compared with existing in-band FD routing solution , which is based on a simple interference model, as well as some benchmark schemes, including HD routing.

1.3 Contributions of the Thesis

The contributions of the thesis can be summarized as follows:

- The performance of HD and in-band FD in bidirectional communication over a single hop is compared in detail under various settings, considering a realistic SI cancellation model for FD. The conditions under which in-band FD outperforms HD are identified.

- HD and in-band FD relaying performances are compared in one way and two way two hop relaying communication scenarios. Closed form integrals are employed to validate end-to-end average throughput in such networks.

- A closed form power allocation solution is derived and proposed for a one way relaying scenario, when source and destination nodes can hear each other.

- Packet streaming in a multihop linear chain topology has been investigated for HD and in-band FD relaying. Policies for optimum time sharing between the links for half-duplex and optimum transmission power for in-band FD are proposed. Performance of in-band FD and HD are compared with respect to several system parameters assuming full interference model. Our proposed FD transmission strategy outperforms HD transmission by up to 2.77 times at low power, by up 1.81 times at high power. For linear chain topologies, also a hybrid transmission strategy is introduced, which is shown to be superior to conventional HD transmission in most cases.

- Considering an adhoc wireless network with in-band FD relays, a routing strategy combined with optimal transmission power allocation policy is proposed and compared to the in-band FD routing scheme that is based on one hop interference model and direct link transmission, as well as optimized HD routing. Our proposed joint routing & power control mechanism provides 30% throughput improvement relative to the proposed solution with one hop interference model and it has also been shown to outperform HD transmission by up to five times, even in the case of moderate SI cancellation.

1.4 Outline of the Thesis

The rest of the paper is organized as follows: In Chapter 2, we provide background information on in-band FD wireless technology. In Chapter 3, we compare HD performance with that of FD in two way communication over a single hop in terms of achievable rates and identify the necessary conditions for in-band FD to outperform HD regarding achievable rate performance. Chapter 4 compares performance of one way and two way relaying communications. Chapter 5 is devoted to multihop networks, where first the optimal power allocation problem is studied and solved, and then a joint routing & power allocation scheme is proposed. The performance of proposed solution is investigated via detailed experiments with comparisons to existing schemes. Last chapter involves our conclusions and future direction of the study.

Chapter 2

Background

2.1 In-Band Full-Duplex Wireless Communications

A two-way (bidirectional) wireless communication usually occurs in two different ways: Half-duplex (HD) and Full-duplex (FD). In HD communication, transmission and reception are carried out orthogonally in time domain by so-called time-division duplexing (TDD) in order to avoid interference between transmit and receive antennas. Therefore, a HD radio either transmits or receives, but cannot do the both at a time. The arduous struggle for this duplexing type is the synchronization of the communicating stations with the same clock.

On the other hand, FD enabled radios are capable of transmitting and receiving at the same time. FD radios used to employ in frequency-division duplexing, where transmission and reception are achieved on non-overlapping frequency bands, allowing transmitting while simultaneously receiving. Assuming wireless channel may spread the signal bandwidth, in order to ensure that receive and transmit signals do not overlap with each other, guard frequency bands are put between these frequency channels. This type of FD communication where different frequency bands are used for transmission and reception is called out-of-band FD.

If the same frequency bands are used for both transmission and reception at the same time, then it is called in-band FD.

Unlike traditional HD and out-of-band FD communication systems which operate in TDD and FDD mode, respectively, in-band FD communication enables a transceiver to perform concurrent transmission and reception over the same frequency band. Since not a different frequency band is allocated for reception other than the one allocated for transmission, radio frequency bands are immediately utilized twice as efficiently as is done in HD communication [11]. As a consequence, in-band FD radios offer an alluring opportunity to double the capacity with respect to traditional duplexing schemes. Notwithstanding, due to simultaneous transmission and reception carried out over a common channel, an in-band FD radio hears also its own transmission, which blocks its reception to a great extend. Owing to the proximity of transmitter and receiver located closely in the radio, this undesired signal is much more dominant than the actual receive signal such that power gap between this undesired leakage and actual received signal is above $100dB$ [11]. This phenomena that reception is degraded by its own transmission is called self-interference, self-talk and sometimes loop-back interference and considered the most inevitable challenge in FD wireless communication. In addition to self-interference problem, inter node interference is another problem, particularly for relaying scenarios, as will be explained in the sequel. We give information about in-band FD wireless technology in the next sections, clearly explaining how it is designed, what challenges it brings with, how to overcome the issues and possible scenarios in which it is considered to take place. In the rest of the thesis, we use only FD to refer to in-band FD, not traditional out-of-band FD.

2.1.1 FD Radio Design

A FD radio can be implemented in two different ways [1] : 1) Separate antenna as in [13] and [14] or shared antenna as in [15] and [16]. These implementations are depicted in Figure 2.1. The main implementation distinction between separate

and shared antenna design is as follows: In separate antenna design, each TX/RX chain is terminated with a different antenna, whereas a TX and RX chain share a common antenna in shared antenna design, where receive and transmit signals are routed through a circulator.

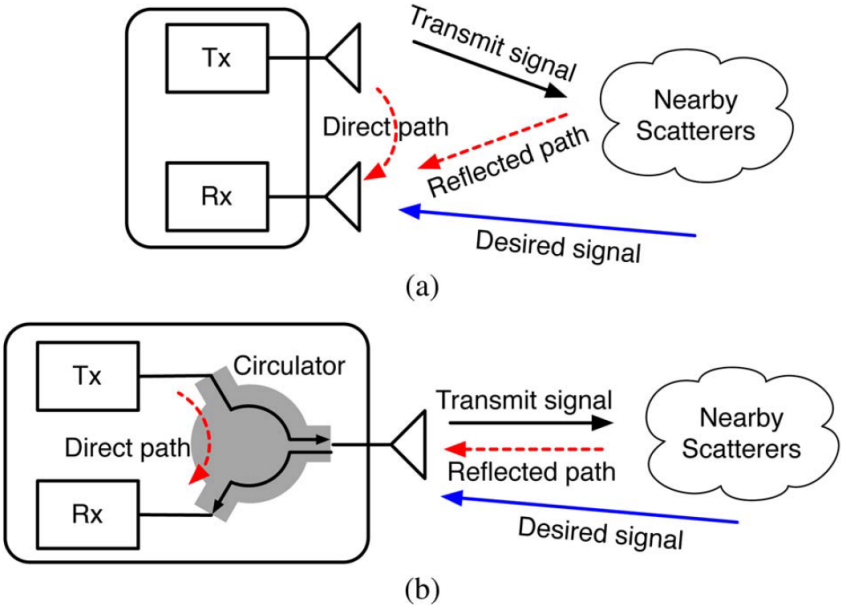

FIGURE 2.1: Different FD radio implementations : a) separate antenna b) shared antenna [1]

Note that if N antennas are allocated in a radio, then N RF chains are required in separate antenna implementation, while the total number of required RF chains is $2N$ in shared antenna design in addition to N circulators necessary to route receive and transmit signals.

2.1.2 Self-interference (SI) Cancellation Techniques

The biggest challenge in FD wireless is, with no doubt, self-interference (SI). It is a natural result of performing simultaneous transmission and reception at the same time over the same channel. As stated before, SI signal is much stronger than the desired signal being picked up by the receiver. As a result, success of the FD communication is determined dominantly by the SI cancellation capability of

a FD radio. The first solution to the problem of SI that comes to the mind would be subtracting transmitted signal from received signal as long as the transmitted signal is known by the receiver. Nevertheless, signal to be transmitted is passed through several blocks in the transmitter radio chain and each block affects the symbols in different ways, more specifically introduces a magnitude and phase change. As a result, the signal radiated from transmit antenna never looks like the same as intended transmit signal.

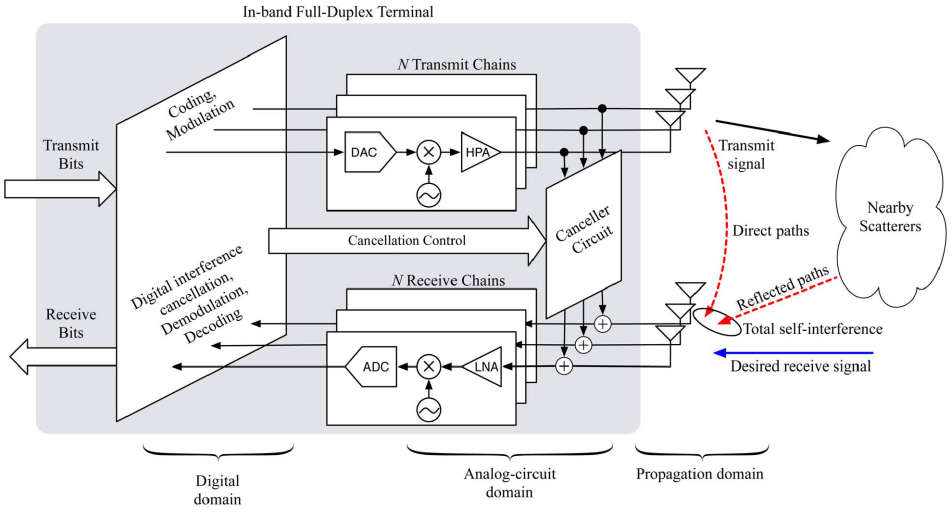

FIGURE 2.2: Structure of FD MIMO transceiver with separate transmit and receive antennas[1]

Figure 2.2 shows a typical structure of an in-band FD MIMO radio with separate receive and transmit antennas. On the transmitter side, transmit message is coded and modulated in digital domain. An DAC (Digital-to-analog converter) then converts baseband discrete samples into analog. Then these signals are up-converted to the carrier frequency and amplified by the virtue of HPA (High-power amplifier). Then this signal is sent into the air to propagate to the desired destination terminal. Remark that during the propagation of signal through these radio frequency radio blocks, none of the blocks works ideally since they introduce non-ideal behaviors [1]. This is what makes SI cancellation problematic in FD radio implementations. To achieve a perfect cancellation, the effect of each and every single block on the transmitted message must be perfectly estimated

since the success of the SI suppression is highly dependent on the accuracy of this estimation.

On the receiver side, stages are a bit different than the conventional radios due to SI cancellation operations. What happens on the receiver side is that electromagnetic waves are first detected by the receive antennas. Then initial analog cancellation is applied to the received signal. Next, signal is passed through an LNA (Low-noise amplifier), down-converter and ADC (Analog-to-digital convertor), respectively. In the final stage, signals are demodulated, decoded back. To further suppress the remaining SI, afterward digital cancellation techniques are applied.

One can notice from Figure 2.2 that SI may originate in two different forms: Direct-path SI and SI that is reflected from nearby obstacles. While it is straightforward to estimate the direct-path SI, channel state information (CSI) is required for predicting the channel between transmitter and nearby objects just outside the transceiver. As long as the transfer functions of the blocks in the TX chain is known, phase and gain introduced to transmit signal by these blocks can be obtained during the system design. Therefore, it is not quite challenging to predict direct-path SI. On the other hand, predicting the SI induced by reflecting nearby objects requires channel awareness since it is totally determined by the outside environment of the transceiver[1] and wireless channel, by its nature, is a linear time-invariant (LTI) system [5].

As seen from Figure 2.2, SI cancellation is performed in three different domains: Propagation domain, analog-circuit domain and digital domain. In propagation domain, the purpose is simply to increase the attenuation between transmit and receive antennas as in [17] and [6]. Using different polarizations (horizontal and vertical) and employing directional antennas are typical examples of prevalent propagation domain remedies for SI cancellation.

Another propagation domain cancellation technique is presented in [18], where two transmit antennas are placed d and $d+\lambda/2$ meters away from the receive antenna, respectively where λ is the wavelength of radio wave. Once two transmit antennas are located in this configuration, signals coming from two transmit antennas add

up in a destructive manner and cancel each other at the receiver creating a null position. This technique works impeccably given that transmitted signal is a single-band carrier. However, this cannot be the case for any communication systems. Once the transmit signal involves a band of frequencies, SI cancellation deteriorates depending on how wide the frequency band of the transmitted signal is.

The issue of frequency selectivity of this technique is addressed in [7] where a new design called "Balun" is introduced. In this new design, balanced/unbalanced transformers are used to invert transmit signal, mitigating the frequency selective characteristics of SI cancellation circuitry and hence providing a better suppression on SI. Similarly, [19] and [20] presents an antenna cancellation domain technique scaled for FD enabled MIMO radios.

Followed by antenna domain cancellation, analog domain cancellation techniques are applied. What basically happens at the analog domain cancellation stage, transmit signal is fed into an analog circuit that subtracts it from the received signal in RF domain. This step is obligatory because ADCs have a dynamic range that limits the maximum peak voltage it can pick up. Without a cancellation in analog domain, input signal to ADC would be out of range due to strong SI signal. For this reason, a reduction on received signal is necessary before it is fed into ADC as input.

As previously stated, during the propagation of transmit signal through the radio blocks, transmit signal is transformed into a form which in fact does not look like the intended transmitted signal since these blocks introduce a gain and phase shift to the transmited signal. As a result, for the analog cancellation to be successful, the effect of these blocks in the TX chain should be well characterized in terms of gain and phase so that exact copy of the SI signal emitted from transmit antenna could be created and subtracted from receive signal. [21] presents an optimal tuning of gain and phase shift for analog SI cancellation where these parameters are tuned through a multi-tapping tuning algorithm. In papers such as [22] and

[23] channel estimation error and its effect on system performance is investigated in different FD scenarios.

To maintain a successful FD communication, even combination of propagation and analog domain suppression techniques is considered insufficient in reducing SI down to acceptable levels and digital cancellation techniques are used in order to further eliminate residual amount of SI. Followed by down-converting, analog base-band receive signal is converted digital and advanced DSP algorithms are applied on the digital samples in the third and the last stage of SI cancellation, in an effort to further suppress residual SI. [24], [25], [26], [27], [28], [20] and [29] are suggested to get to know more about SI cancellation.

2.2 Related Work On The Analysis of FD

FD wireless technology offers a potential to double the spectral efficiency, enabling radios to perform simultaneous transmission and reception over the same frequency band. However, spectral efficiency can be doubled in ideal case only, in which SI is completely suppressed. Because of vigorous effect of SI, that is about $100dB$ stronger than desired received signal, decoding capability of the radios is degraded to a great extend, impeding a proper reception. In order for a radio to perform a successful FD communication, SI must be reduced down to acceptable levels.

Because of challenges in suppressing SI signal that is million to billion times stronger than the desired signal receive antenna is trying to pick up, FD wireless has not caught sufficient amount of attention and has not shown to be realizable until the recently conducted studies where FD operation had been made possible by combination of successive advanced SI cancellation techniques.

When it comes to the scenarios to which FD technology can be applicable, followings are the potential communication types where spectral efficiency can be leveraged by FD technology: 1) bidirectional communication as in [30], 2) Two-hop relaying communication as in [31], [32], [33], [34], 3) Cellular communication

with a FD base station serving uplink and downlink users simultaneously as descibed in [35]. In addition to these scenarios, mesh networks are also considered to potentially benefit from FD technology.

The performance of FD communication has been evaluated for various scenarios and different SI cancellation models. In [23], HD and FD bidirectional communications over a single hop are compared in the presence of channel estimation errors and closed form expressions for ergodic capacities for bidirectional FD communication are provided for different combining schemes. An analysis for FD bidirectional wireless communication can be found in [36], where a closed form outage probability is proposed in the case of imperfect SI cancellation, and validated via simulations. In this study, Rayleigh fading for channel between nodes and Rician fading for the SI channels are considered for channel modeling and it is showed that as the Rician parameter K increases, the outage probability increases.

In our previously published conference paper [30], we investigate the sum rate performance of bidirectional HD and FD communication. We analyze the total system throughput when these nodes are HD and FD enabled in an effort to identify the conditions under which FD outperforms HD. By making use of the SI cancellation model given in [37] to mathematically quantify magnitude of residual SI, in these comparisons we look at the several system parameters, such as transmission powers of nodes, SI cancellation levels, number of antennas employed in each node, clearly identifying the circumstances under which FD communication yields a better performance.

In [38], bidirectional communication between two MIMO nodes with statistical queuing constraints is investigated, while a decision making strategy between two modes, HD and FD, is proposed so as to offer higher throughput under constraints on the buffer overflow probability. In [39], a study on FD Multiple Input Multiple Output (MIMO) radios is presented, basically showing how a FD radio with a single antenna (shared antenna design), as in [16], can be transformed into a FD MIMO radio. When multiple antennas are employed to operate in FD, two distinct interference take place: self-talk and cross-talk. While cross-talk corresponds to

interference caused by other co-located transmit antennas in the radio, self-talk is defined as the leakage from the transmit chain into the receive chain of the same antenna because of the imperfect isolation in the circulator.

In [35] a power controlled medium access control (MAC) scheme is proposed for relaying in cellular network scenarios, where the relay is an access point (AP). In this MAC scheme, the AP is assumed to operate in FD mode. While an uplink user is transmitting to the AP, it also interferes with the downlink user that the AP is transmitting to. The optimum transmission power levels for the uplink user and the AP are obtained via a heuristic solution and power control is implemented in the MAC protocol.

In [40], one way two hop communication is studied with channel estimation errors in the presence of loop-back interference in order to come up with capacity cut-set bounds for both HD and FD functioning relay. An effective transmission power policy is proposed for the relay to maximize this bound, and performance of FD relaying with optimal power control is compared with HD relaying. Another relaying communication in a cellular environment is investigated in [41], where a hybrid scheduler is presented, that is capable of switching between HD and FD to give the maximum system throughput in an opportunistic fashion. In addition to decision of duplexing mode, scheduler selects the best uplink and downlink users based on their channel status at each time slot. The performance of such scheduler is compared with a traditional HD scheduler, and a pure FD scheduler has been shown to outperform conventional HD scheduler by a factor of 1.81 times.

In [42], two hop communication with a FD relay is investigated and it is showed that the relay should employ power control in order to maximize system throughput. In [31], power control is used, such that the relay scales its power with respect to the source to achieve maximum Degree of Freedom (DoF) when the relay operates in decode-and-forward mode. The relaying scenario is investigated from the perspective of end-to-end throughput and DoF, comparing HD and FD relaying via the empirical residual SI model from [37]. In [43], a two way relaying network is investigated. For an efficient transmission strategy, an analog network coding

scheme is introduced, where the interference in the physical layer signal level is turned into an advantage. In the proposed method, two users send their signals to an AP, in the first phase of communication, creating a MAC channel, hence the AP receives the sum signal. In the second phase, the AP broadcasts this sum signal to both users, who can extract desired signal by the virtue of what is called analog network coding techniques. Similarly, in [44], a two way HD relaying communication is analyzed, where source and destination nodes are assumed to hear each other. Similarly, in this study too, physical layer network coding is considered as in [43]. Here, the outage probability and the system throughput are taken as performance criteria for comparisons between HD and FD. FD relaying is shown to be better than HD relaying even if SI is not completely canceled at the FD relay.

In [45], a power optimal routing scheme is evaluated in fading wireless channels, where the fading of the channel is assumed to follow Nakagami-m distribution. In the proposed algorithm, end-to-end outage probability is taken as the constraints of the problem and kept below a certain threshold, while the aim is to minimize the weighted power sum of the relay nodes. In [46], a modified version of the Dijkstra's algorithm for routing, and a recursion based optimal transmit power allocation scheme for maximum end-to-end throughput is introduced, assuming a simplified interference model, where only one hop interference is considered. Then, this simplified model is applied to the networks with full interference model, where a node hears every other nodes in the network. The performance gap between the optimal solution and the proposed solution has been shown to be bounded by a constant.

Chapter 3

FD over A Single Hop: Bidirectional Communication

Single hop two way communication is the building block of numerous contemporary communication systems, therefore play a significant role. This model may represent an indoor wi-fi link between a modem and a device, where they are simultaneously uploading and downloading data. We devote this chapter to scrutinizing FD in single hop two way communication model and we evaluate the performance FD in comparison to HD, comparing their performances in terms of achievable rates offered by each duplexing scheme.

3.1 Channel Model

Two wireless nodes A and B are communicating with each other as shown in Figure 3.1. We investigate this communication model in two scenarios: 1) when both nodes are HD functioning and 2) when they are both FD functioning.

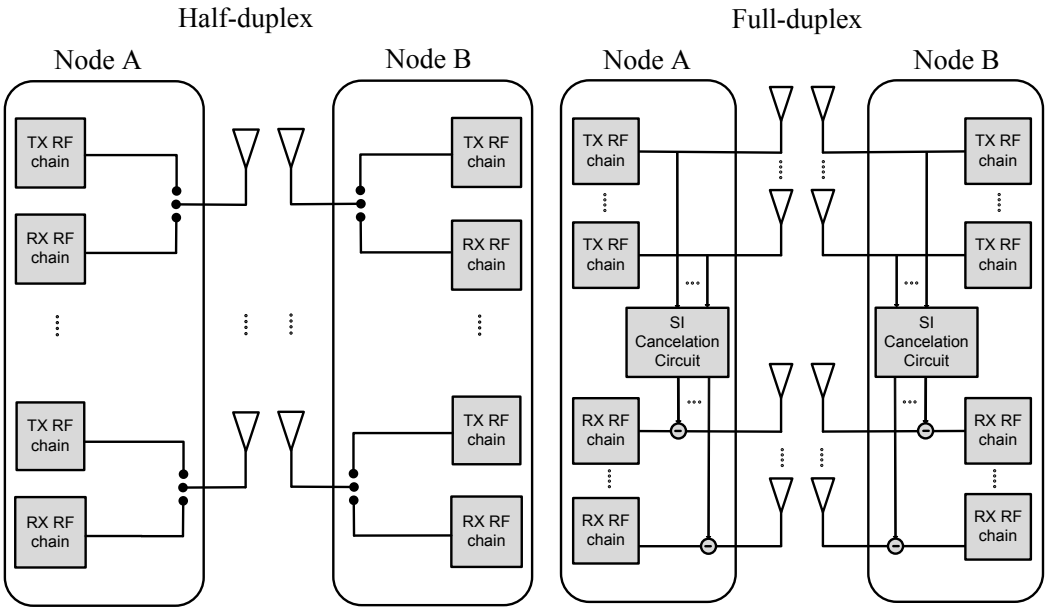

FIGURE 3.1: Bidirectional communication in HD and FD modes

In order to refrain from repetition, rather than giving different channel models for HD and FD, we opt to use a unified channel model, which is valid for both types of duplexing schemes. On the left side of Figure 3.1, architecture for HD radio and on the right side separate antenna design based FD radio architecture are shown. The nodes are considered to be equipped with multiple antennas and the channel between the nodes is modeled as Rayleigh fading Multi Input Multi Output (MIMO) channel with AWGN at the receiver. Consider a scenario where node A is transmitting to node B. Assuming that node A transmits with t_A and node B receives over r_B antennas, then the received signal at node B can be expressed follows

$$\mathbf{y}_B = \sqrt{K}\mathbf{H}_{AB}\mathbf{x}_A + \mathbf{i}_B + \mathbf{w}_B \tag{3.1}$$

where $\mathbf{H}_{AB} \in \mathbf{C}^{r_B \times t_A}; \mathbf{x_A} \in \mathbf{C}^{t_A \times 1}; \mathbf{y}_B, \mathbf{n}_B, \mathbf{i}_B \in \mathbf{C}^{r_B \times 1}$. Here $\mathbf{x}_A$ denotes the vector of transmitted symbols, $\mathbf{w}_B$ denotes the AWGN noise term with variance of σ_B^2 and $\mathbf{i}_B$ is the SI signal with a power of I_B for the FD mode. $\mathbf{H}_{AB}$ denotes the channel fading coefficients of the wireless link between nodes A and B. For Rayleigh fading, entries of $\mathbf{H}_{AB}$ are assumed to have circularly symmetric complex Gaussian distribution [5]. The channel state information is assumed to be available

only at the receiver (CSIR). The size of the channel matrices depends on the number of the transmit and receive antennas employed at the nodes. Note that for HD operation, term I_B is zero. With P_A specified as transmission power and letting K as the parameter that characterizes the path loss between nodes, the Signal to Interference and Noise Ratio (SINR) at the receiver is

$$\Gamma_{AB} = \frac{KP_A}{(\sigma_B^2 + I_B + Q_B)}. \tag{3.2}$$

As in [47], the average achievable rate from node A to node B, R_{AB} is obtained as follows

$$R_{AB} = \mathbb{E}\left[\log\det\left(\mathbf{I} + \frac{\Gamma_{AB}}{t_A}\mathbf{H}_{AB}\mathbf{H}_{AB}^*\right)\right]. \tag{3.3}$$

3.2 SI Cancellation Model

In order to accurately assess the performance of HD and FD communication, we need a model that represents the amount of remaining SI after successive cancellation steps are applied. Also, this model should be mathematically tractable so that it could be utilized in the calculation of the average achievable rates. For this purpose, we employ an empirical model in [37], which is based on extensive experiments performed on real FD devices. According to this model, the average power of the residual SI is modeled as a function of transmit power, P_T as follows

$$I(P_T) = \frac{P_T^{(1-\lambda)}}{\beta\mu^{\lambda}} \tag{3.4}$$

Here β represents the SI suppression due to passive cancellation, while μ and λ values depend on the active cancellation technique. Note that this model has non-linear characteristics with respect to transmission power. For the FD radio implementations in [37], μ and β are set to $13dB$ and $38dB$, respectively while λ is found in the range $0 \leq \lambda \leq 1$.

3.3 Comparing FD with HD

In order to make a fair performance comparison between HD and FD communication models, radio resources must be kept identical for both duplexing schemes. Keeping in mind that in a radio the dominant resources are antennas and RF chains, we investigate two implementations for FD: *Antenna conserved* FD where in reference to HD, number of antennas is kept equal to the number of antennas of HD mode and *RF chain conserved* FD where the number of RF chains in the two modes is kept equal. As an example, consider a HD radio with N antennas. Since in HD radios each antenna is terminated with 2 RF chains, one for TX and one for RX, there are total of $2N$ RF chains in this HD radio. To fairly compare this radio with its FD counterpart, we either compare it with a FD radio with N antennas (Antenna Conserved FD implementations) or $2N$ RF chains (RF chain conserved FD implementations). We use AC to denote antenna conserved FD and RC to denote RF chain conserved FD. While considering AC FD, if r antennas are used for reception, then remaining $(N - r)$ antennas are used for transmission. Whereas for the RC FD, if r antennas are used for reception, in addition to r down-converting RF chains, r RF chains are necessary for analog cancellation. Remaining $2N-2r$ RF chains can be allotted to TX antennas, hence the number of TX antennas would be $2N - 2r$, making total number of antennas available $2N - r$. Antenna numbers for the aforementioned implementations are summarized n in a more organized way in Table 3.1.

Table 3.1: Number of antennas in HD, AC FD and RC FD

	number of RX antennas	number of TX antennas	Total number of antennas
HD	r	N-r	N
AC FD	r	N-r	N
RC FD	r	2N-2r	2N-r

3.4 HD Achievable Rates

In the HD mode, nodes A and B take turn for transmission and one receives as other is transmitting. Figure 3.2 shows the typical data flow in a two way

communication over a single when the nodes are in HD mode. Node A transmits to node B at certain time slots, as shown in Figure 3.2(a). This flow is reversed during the rest of the time, as shown in figure 3.2(b). However, they never transmit at the same time slot because of the HD limitation. Note that N_A and N_B denote the number of antennas of each node.

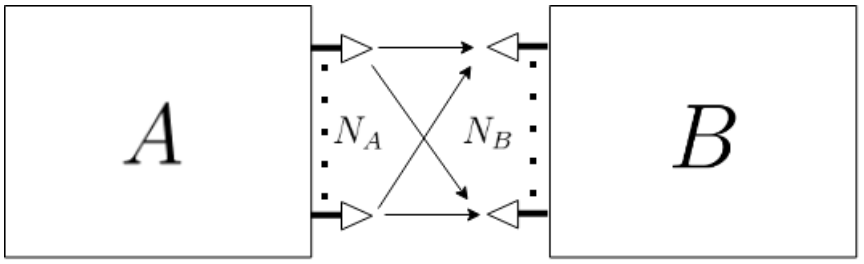

(a)

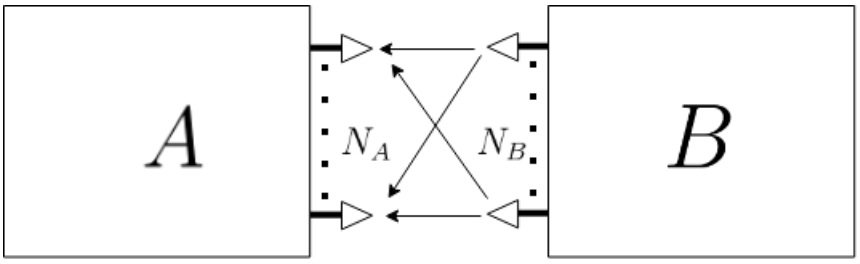

(b)

FIGURE 3.2: (a) First phase, A transmitting to B, (b) Second phase, B transmitting to A

When nodes A and B communicate in HD mode, they need to apply time division duplexing (TDD) for transmission at alternating time slots. Let us assume that for a τ fraction of total communication time, node A transmits, and in the remaining fraction $1-\tau$, node B transmits. Revisiting on the SNR expression given in (3.2), the average rate achieved by HD from node A to node B, R_{AB} and the rate in the reverse direction are calculated as

$$R_{AB}^{HD} = \tau \mathbb{E}\left[\log\det\left(\mathbf{I} + \frac{\Gamma_{AB}}{N_A}\mathbf{H}_{AB}\mathbf{H}_{AB}^{*}\right)\right], \tag{3.5}$$

$$R_{BA}^{HD} = (1-\tau)\,\mathbb{E}\left[\log\det\left(\mathbf{I} + \frac{\Gamma_{BA}}{N_B}\mathbf{H}_{BA}\mathbf{H}_{BA}^{*}\right)\right], \tag{3.6}$$

where $\mathbf{I}$ denotes the identity matrix, with $\mathbf{I} \in \mathbf{C}^{N_B \times N_B}$ for (3.5) and $\mathbf{I} \in \mathbf{C}^{N_A \times N_A}$ for (3.6). In the case of symmetrical channels, τ is set to 0.5. On the other hand, in case of asymmetrical channels, we set τ to a value that produces equal link rates in each direction so as to make equal rates for each direction as follows

$$\tau = \frac{\mathbb{E}\left[\log\det\left(\mathbf{I} + \frac{\Gamma_{BA}}{N_B}\mathbf{H}_{BA}\mathbf{H}_{BA}^*\right)\right]}{\mathbb{E}\left[\log\det\left(\mathbf{I} + \frac{\Gamma_{AB}}{N_A}\mathbf{H}_{AB}\mathbf{H}_{AB}^*\right)\right] + \mathbb{E}\left[\log\det\left(\mathbf{I} + \frac{\Gamma_{BA}}{N_B}\mathbf{H}_{BA}\mathbf{H}_{BA}^*\right)\right]} \tag{3.7}$$

(3.7) states that the total communication time is shared between nodes inversely proportional to their respective link rates. The sum rate of this network is obtained as

$$R_{sum}^{HD} = R_{AB}^{HD} + R_{BA}^{HD} \tag{3.8}$$

Note that to maximize R_{sum}^{HD}, both nodes should use their maximum powers : $P_A = P_{Amax}$ and $P_B = P_{Bmax}$.

3.5 FD Achievable Rates

When nodes A and B operate in FD mode, they are able to transmit to each other at the same time over the same frequency band. This is achieved by devoting some antennas and RF chains to reception and some to transmission for separate antenna FD implementations [1]. This way, a node becomes capable of FD communication at the cost of SI. In Figure 3.3, information flow in a typical two way FD communication scenario over a single hop is illustrated. Here t_A and r_A denote the number of transmit and receive antennas at node A, respectively. Similarly, t_B and r_B denote the number of antennas at node B. Dotted arrows in each node represent the SI channel.

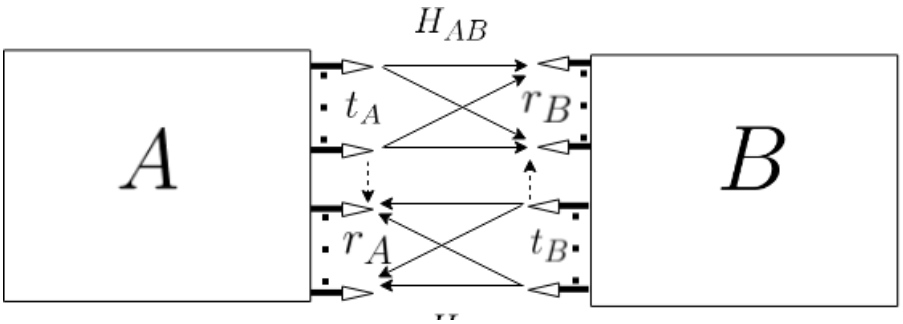

FIGURE 3.3: TWC when both nodes operate in FD

Average achievable link rates in each direction are computed by

$$R_{AB}^{HD} = \mathbb{E}\left[\log\det\left(\mathbf{I} + \frac{\Gamma_{AB}}{t_A}\mathbf{H}_{AB}\mathbf{H}_{AB}^{*}\right)\right], \tag{3.9}$$

$$R_{BA}^{HD} = \mathbb{E}\left[\log\det\left(\mathbf{I} + \frac{\Gamma_{BA}}{t_B}\mathbf{H}_{BA}\mathbf{H}_{BA}^{*}\right)\right], \tag{3.10}$$

where $\mathbf{I} \in \mathbf{C}^{r_B \times r_B}$ for (3.9) and $\mathbf{I} \in \mathbf{C}^{r_A \times r_A}$ for (3.10). The sum rate of this network is obtained as

$$R_{sum}^{FD} = R_{AB}^{FD} + R_{BA}^{FD} \tag{3.11}$$

3.6 Simulation Results

We investigate a rather simple example scenario to observe which duplexing scheme works more satisfactorily in two way communication over a single hop. In this example scenario, nodes A and B are equipped with 3 antennas if they are HD operating. On the other hand, in AC FD they have 2 receive and 1 transmit antennas. In RC FD they have 2 receive and 2 transmit antennas as in Table 3.1. Figures 3.4, 3.6, 3.7 are all obtained for these settings, whereas 3.5 shows the sum rates for different number of antennas numbers for investigating the effect of number of antennas on the FD gain. In all simulations performed, noise variances at the nodes are taken to be $\sigma_A^2 = \sigma_B^2 - 50dB$. Path loss attenuation between nodes is set as $K = -50dB$.

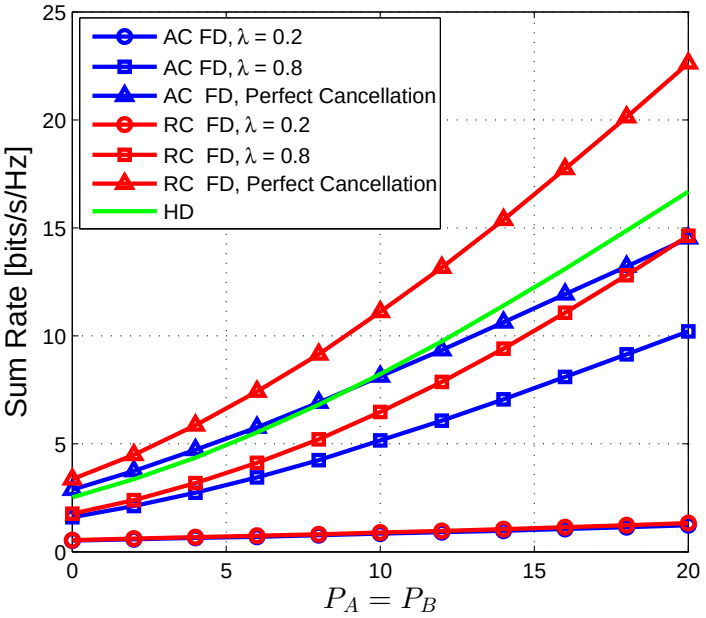

FIGURE 3.4: Sum rates of HD and FD with different SI cancellation levels with respect to the transmission powers

Figure 3.4 shows the sum rate performance of HD, AC FD and RC FD implementations under different SI suppression levels. Since λ is a parameter that captures the quality of SI cancellation, the performance of both AC FD and RC FD implementations are improved with higher λ values. Antenna conserved FD, performs only slightly better than HD at low transmit power levels, while it performs strictly below HD at high transmit power levels, even in the case of perfect SI cancellation (i.e., $\lambda = \infty$ in (3.4)). The RC FD implementation provides superior performance over HD, when the SI is perfectly suppressed; however it performs below HD even for the case of low residual SI (i.e., $\lambda = 0.80$). Note that, the case of perfect SI cancellation presents the upper bound for FD performance, which is quite loose, since the actual sum rate is considerably lower. Since better performance is observed with RC FD relative to AC FD, we focus on the RF chain conserved FD implementation in the remaining experiments.

Next, we consider different number of antennas employed at the nodes, in an effort to see the effect of number of antennas on the performance of FD. For this purpose, we consider two different levels of SI cancellation: Poor ($\lambda = 0.2$) and

good ($\lambda = 0.8$). Figure 3.5 shows the gain of FD mode over HD, which is found by dividing the FD achievable rate of FD mode by the rate of HD mode, considering different number of antennas per node as well as transmission power levels. The value $N_A = N_B$ is the number of antennas per node, when they communicate in HD mode. In the corresponding RC FD implementation, a node X employs $2N_X - r$ antennas, allocating $2N_X - 2r$ antennas for transmission and r antennas for reception. As the figure clearly depicts, the FD gain is almost independent of the number of antennas employed in the nodes. It can also be noted that, when SI cancelation is poor, increasing the transmission power results in lower FD gain, while it is improved with transmission power in case of good SI cancelation. This is because with poor cancelation, the effect of SI gets more severe with increasing power, causing further degradation on the performance of FD.

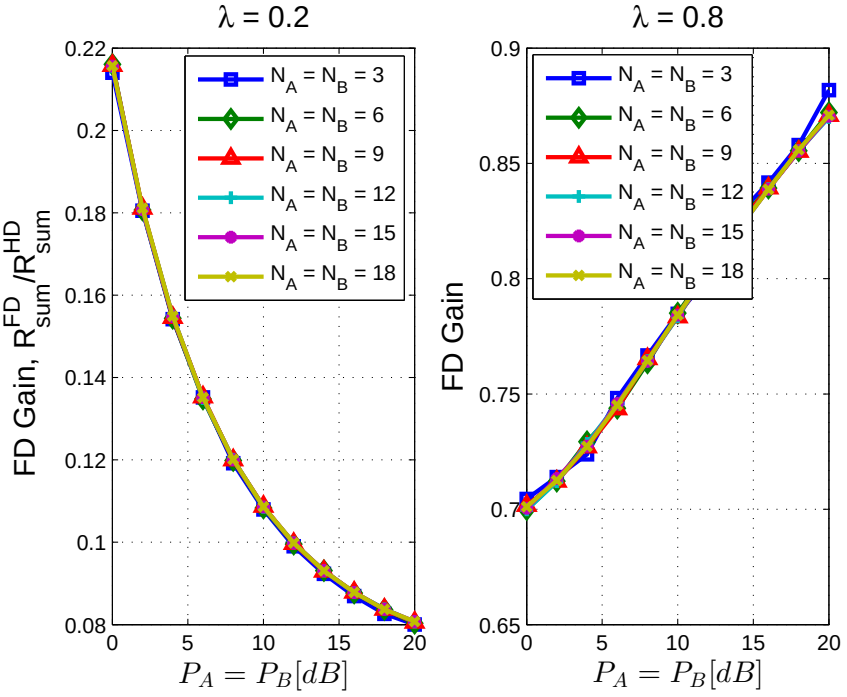

FIGURE 3.5: Gain of RC FD over HD with respect to different number of antennas under low and high SI cancellation, $r_A = t_A = r_B = t_B = \frac{2N_A}{3} = \frac{2N_B}{3}$

In Figure 3.6, we investigate the effect of SI suppression on the sum rate, when P_A and P_B are both kept constant, as $P_A = P_B = 10$ dB. This figure enable us to see the threshold λ value, over which RC FD performs better than HD. Naturally, the performance of HD mode does not change with λ, as shown by the red line in

the figure. The sum rate of RC FD mode increases with increasing λ, as depicted by the blue curve. The intersection of the two curves correspond to the so-called threshold, referred as λ_{thr} in the rest of paper. This value, in fact, denotes the level at which RC FD and HD yield the same performance, for $\lambda < \lambda_{thr}$, $R^{FD} < R^{HD}$, and for $\lambda > \lambda_{thr}$, $R^{FD} > R^{HD}$.

We further investigate the relation between the transmission power of nodes and λ_{thr} in Figure 3.7. As it can be seen from this figure, λ_{thr} drops with increasing $P_A = P_B$. Though not shown, in our numerical experiments, we were able to observe that for very (unrealistically) high power levels (such as 100 dB), and we observed that λ_{thr} converges to 0.75. Figure 3.7 also implies that a desired FD gain can be obtained by increasing transmission power of nodes. Hence, one can improve the performance of a given RC FD implementation, by increasing the transmission power, even when SI cancelation capability is not good enough.

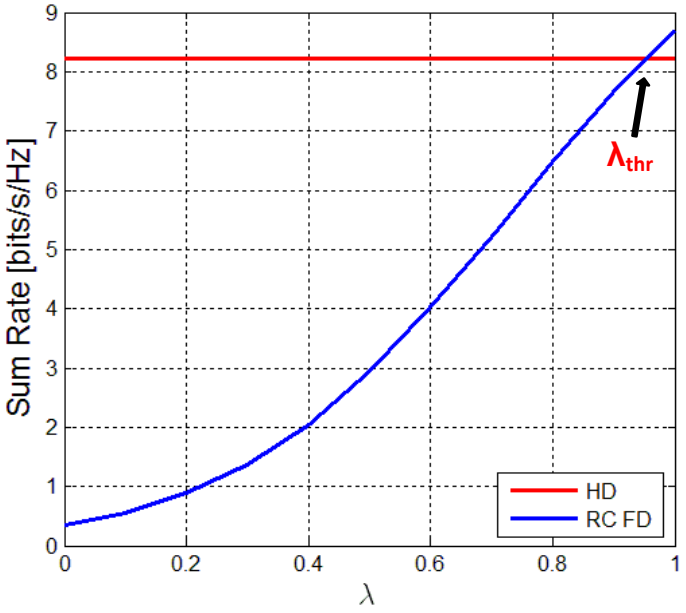

FIGURE 3.6: Effect of SI cancellation on sum rate performance of FD, $P_A = P_B = 10dB$, $r_A = t_A = r_B = t_B = 2, N_A = N_B = 3$

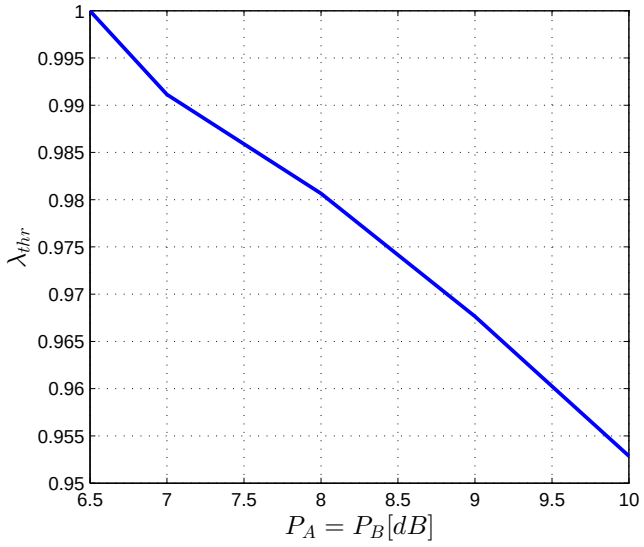

FIGURE 3.7: λ_{thr} with respect to transmission power of nodes, $r_A = t_A = r_B = t_B = 2, N_A = N_B = 3$

In Figure 3.8, the sum rate, R_{sum}^{FD} is plotted for varying values of P_A and P_B, selected independently in their respective ranges, $P_A \leq P_{Amax}, P_B \leq P_{Bmax}$. Figure 3.8(a) shows the performance for a poor cancellation and 3.8(b) shows a good SI cancellation performance, respectively. As indicated by Figure 3.8(b), increasing either P_A or P_B always ameliorates the sum rate when SI cancellation is good, since the sum rate is increasing with respect to both P_A and P_B. However, this is not always the case for poor SI cancellation, as shown by Figure 3.8(a). When SI cancellation is poor, the sum rate reaches its maximum value with asymmetrical transmission power levels, i.e., when one of the nodes transmits at $20dB$ and the other one transmits at $0dB$. In a nutshell, transmission power assignment of nodes can be critical in FD wireless networks if SI cancellation is poor. On the other hand, the nodes should use their maximum power to get the best sum rate performance, as long as SI is reduced to acceptable levels with a good SI cancellation, since a node's own transmission does not significantly deteriorate its reception in this case.

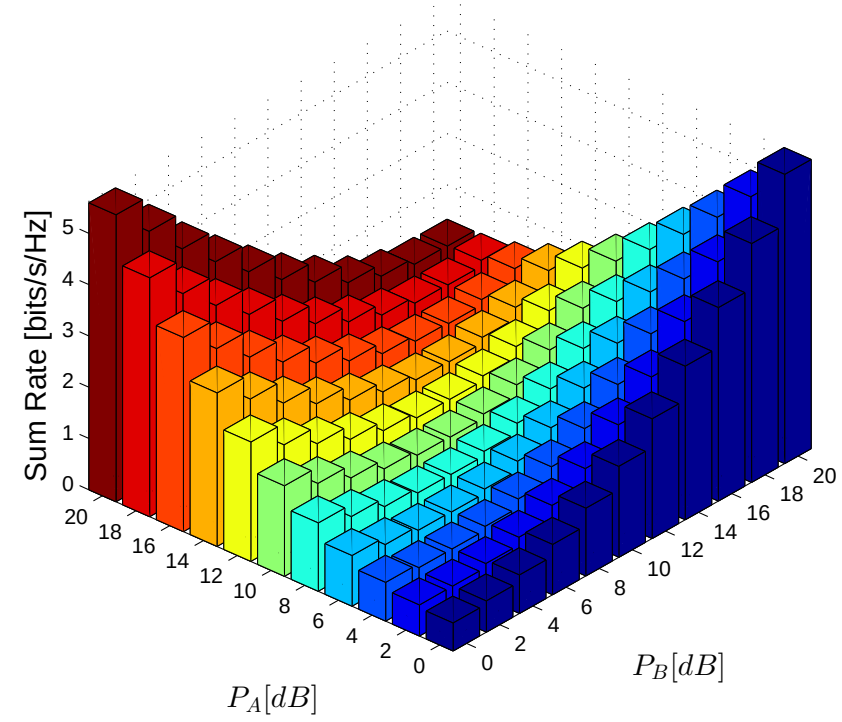

(a)

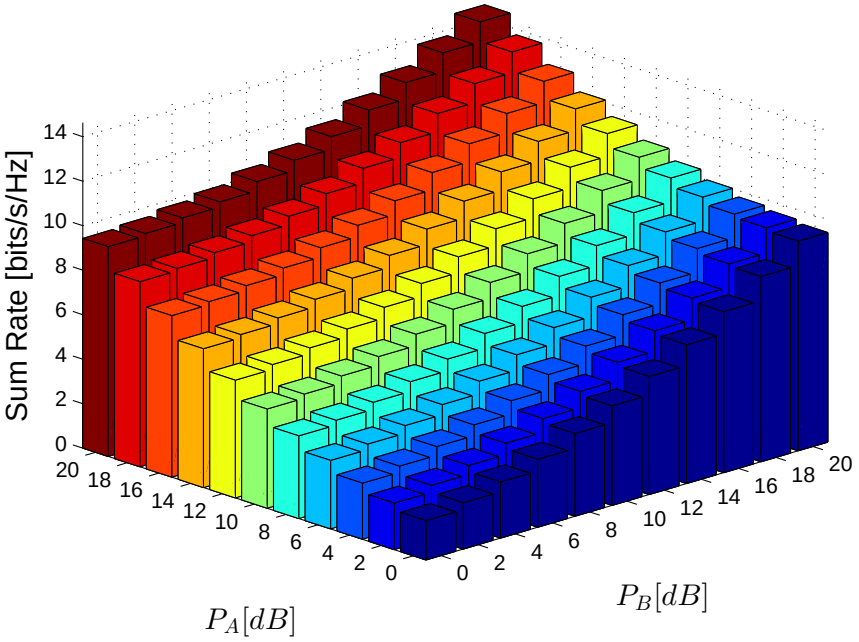

(b)

FIGURE 3.8: Achievable sum rate of FD mode with respect to P_A and P_B, $P_{Amax} = P_{Bmax} = 20dB$ under two different level of SI suppression, (a) $\lambda = 0.2$ (Poor SI cancellation) (b) $\lambda = 0.8$ (Good SI cancellation)

Note that, the finite SNR results presented here are more pessimistic, but more realistic for FD mode, as compared to our initial results in [30], since here the RC FD implementation is modeled in a more realistic fashion with smaller number of transmit antennas, unlike [30].

Our results indicates that even with perfect SI cancellation, AC FD performance slightly surpasses that of HD. On the other hand, we observe a significant capacity enhancement, magnitude of which is substantially dependent on the intensity of the residual SI. We also show what is the minimum SI cancellation requirement for FD to outperform HD. Furthermore, we demonstrate that minimum SI cancellation requirement is a function of transmission powers of the nodes, i.e. a FD radio with a poor SI cancellation performance can be still able to perform better than its HD counterpart at high transmission power levels. Our investigation on the effect of the number of antennas on the sum rate has shown that FD gain over HD gain does not have anything to do with antenna numbers. We have also showed the significance of power control in FD bidirectional communication.

Chapter 4

FD over Two Hops: Relaying Scenarios

In this chapter, we investigate the one way and two FD communications over two hops. We use the same channel and SI cancellation models described in Section 3.1 and Section 3.2.

4.1 One Way Communication

In this setting, node A acts as a source node and aims to deliver its message to a destination node B via an intermediate relay node R, which forwards the data from A to B. Here, nodes A and B are both assumed to operate in HD and they have N_A and N_B antennas, respectively. Additionally, no direct link is assumed between nodes A and B, thus node B cannot hear node A's transmission. The relay is assumed to employ in decode-and-forward (DAF) protocol for forwarding. A real-life example of this scenario is an access point forwarding one station's message to another station.

4.1.1 HD Achievable Rates

If the relay is HD functioning, nodes A and R cannot transmit at the same time. For this reason, flow of the information from source node A to destination node B occurs in two phases. First, node A transmits to node R, as shown in Figure 4.1(a) and in the second phase node R forwards what it received from node A in the first phase to node B, as shown Figure 4.1(b).

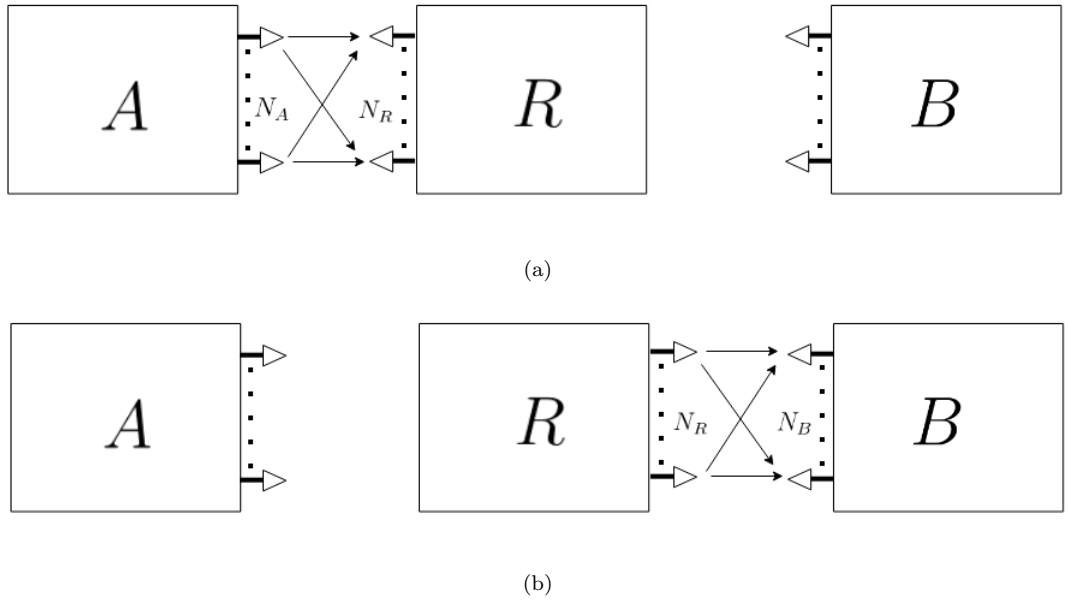

FIGURE 4.1: (a) First phase, A transmitting to R , (b) Second phase, R transmitting to B

Owing to HD constraints at the relay, it needs to devote different time slots to transmission and reception. Assuming τ fraction of total communication being dedicated for relay's reception, average achievable rate of link between A and $R$is as follows

$$R_{AR}^{HD} = \tau \mathbb{E}\left[\log\det\left(\mathbf{I} + \frac{\Gamma_{AR}}{N_A}\mathbf{H}_{AR}\mathbf{H}_{AR}^{*}\right)\right], \tag{4.1}$$

Similarly, the rate achievable over the relay to B link is given by

$$R_{RB}^{HD} = (1-\tau)\mathbb{E}\left[\log\det\left(\mathbf{I} + \frac{\Gamma_{RB}}{N_R}\mathbf{H}_{RB}\mathbf{H}_{RB}^{*}\right)\right]. \tag{4.2}$$

By optimizing over τ, the end-to-end average achievable rate for HD relaying can be found as

$$R_{AB}^{HD} = \max_{0 \leq \tau \leq 1} \min \left\{ R_{AR}^{HD}, R_{RB}^{HD} \right\}. \tag{4.3}$$

Note that in (4.3) increase in τ leads to increase in R_{AR}^{HD}, yet decrease in R_{RB}^{HD}. As a result, in this maxmin problem, we can infer that optimum τ should hold $R_{AR}^{HD} = R_{RB}^{HD}$. Thus, optimal τ, denoted by τ_{opt} is given by

$$\tau_{opt} = \frac{\mathbb{E}\left[\log\det\left(\mathbf{I} + \frac{\Gamma_{RB}}{N_R}\mathbf{H}_{RB}\mathbf{H}_{RB}^{*}\right)\right]}{\mathbb{E}\left[\log\det\left(\mathbf{I} + \frac{\Gamma_{AR}}{N_A}\mathbf{H}_{AR}\mathbf{H}_{AR}^{*}\right) + \log\det\left(\mathbf{I} + \frac{\Gamma_{RB}}{N_R}\mathbf{H}_{RB}\mathbf{H}_{RB}^{*}\right)\right]} \tag{4.4}$$

4.1.2 FD Achievable Rates

When the relay has FD capability, it can transmit and receive at the same time. While receiving i^{th} packet from source node A with its r antennas, it forwards the previously received $(i-1)^{th}$ packet to destination node B with its t antennas unlike in section 4.1.1. This causes relay to hear its own transmission as SI. Information flow in FD relay is shown in Figure 4.2. Here, r denotes the number of receive antennas and t denotes the number of antennas assigned for transmission at the relay. N_A and N_B denote the number of antennas at node A and B, respectively.

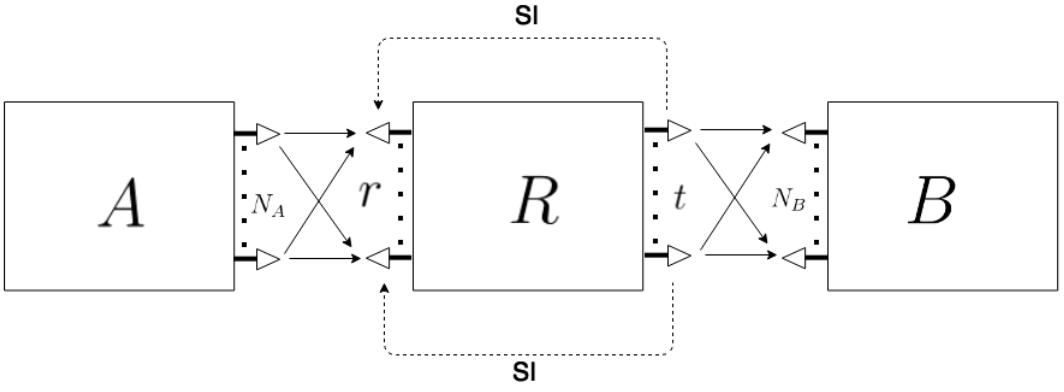

FIGURE 4.2: Information flow when the relay is FD

In this case, the link rates are given b

$$R_{AR}^{FD} = \mathbb{E}\left[\log\det\left(\mathbf{I} + \frac{\Gamma_{AR}}{N_A}\mathbf{H}_{AR}\mathbf{H}_{AR}^{*}\right)\right], \tag{4.5}$$

$$R_{RB}^{FD} = \mathbb{E}\left[\log\det\left(\mathbf{I} + \frac{\Gamma_{RB}}{t}\mathbf{H}_{RB}\mathbf{H}_{RB}^{*}\right)\right]. \tag{4.6}$$

Let us recall that number of transmit antenna is $t = (N_R - r)$ for the AC FD and $t = (2N_R - 2r)$ for the RC FD implementations. We assume that relay can optimally allocate the number of receive antennas so as to maximize the average rate achievable from node A to node B. Furthermore, depending upon the average SINR at the relay and SNR at B, the excess power at the relay can have a negative impact on the achievable rate due to increased SI. Note that from SINR expression, SINR at the relay decreases as the relay power P_R increases given that transmission power of node A, P_A is held constant. Thus, with the increase in P_R for constant P_A, R_{AR}^{FD} decreases while R_{RB}^{FD} increases. Therefore, relay's transmission power should be optimally set in order to get the maximum achievable end-to-end throughput. Mathematically, this corresponds to

$$R_{FD}^{AD} = \max_{P_R \leq P_{Rmax}} \min\left\{R_{AR}^{FD}, R_{RB}^{FD}\right\}. \tag{4.7}$$

4.1.3 A Closed Form Expression for Rate Calculations

We have noticed that it is possible to obtain closed form expressions that give the average achievable end-to-end throughput, when nodes A and B are both equipped with a single antenna, in other words, when links $A \longrightarrow R$ and $R \longrightarrow B$ are Single Input Multiple Output (SIMO) and Multiple Input Single Output (MISO) channels, respectively. Consider a MISO channel between relay with N_R transmit antennas and node B with 1 receive antenna. The average achievable rate of this link is calculated by

$$R_{RB} = \mathbb{E}\left[\log\det\left(\mathbf{I} + \frac{\Gamma_{RB}}{N_R}\mathbf{H}_{RB}\mathbf{H}_{RB}^{*}\right)\right]. \tag{4.8}$$

Here $Z = \mathbf{H}_{RB}\mathbf{H}_{RB}^{*}$ is called Wishart matrix, and remark that in case nodes A and B are equipped with single antenna, $Z = \mathbf{H}_{RB}\mathbf{H}_{RB}^{*}$ becomes a number. Then, the rate expression calculates the expectation of a function of Z, a random variable representing the channel. Denoting any single channel between node R and node B by h_i where $i \in \{1, 2, ..., N_R\}$. After a simple manipulation, we obtain

$$\mathbf{H}_{RB}\mathbf{H}_{RB}^{*} = \|h_1\|^2 + \|h_2\|^2 + ... + \|h_{N_R}\|^2 = \sum_{i}^{N_R} \|h_i\|^2 \tag{4.9}$$

Let x and y denote the real and imaginary parts of the channel coefficient as $h_i = x + iy$. By our assumptions we know that $x, y \sim \mathcal{N}(0, \vartheta^2)$. This implies that each $\|h_i\|$ is a Rayleigh random variable and $\|h_i\|^2$ is an exponentially distributed random variable with a mean of $\frac{1}{2\vartheta^2}$. Either taking multiple convolutions or using characteristic function method [48], the distribution of the Wishart Matrix is derived as

$$f_Z(z) = \frac{z^{(N_R-1)} e^{-\frac{z}{2\vartheta^2}}}{(2\vartheta^2)^{N_R}\,(N_R-1)!} \tag{4.10}$$

As long as node B has single antenna, (4.8) boils down to

$$R_{RB} = \mathbb{E}\left[\log\left(1 + \frac{\Gamma_{RB}}{N_R} z\right)\right]. \tag{4.11}$$

Defining $X = \log\left(1 + \frac{\Gamma_{RB}}{N_R} z\right)$, the distribution function of the term inside the expectation in (4.11) is obtained as follows

$$f_X(x) = \frac{(2^x - 1)^{N_R - 1}\, 2^{x - N_R} {N_R}^{N_R} ln2}{\Gamma_{RB}^{N_R} \vartheta_{RB}^{2N_R}\,(N_R-1)!} e^{\frac{(1-2^x)N_R}{2\Gamma_{RB}\vartheta_{RB}^2}} \tag{4.12}$$

Average achievable link rate, R_{AR} is found as

$$R_{RB} = \int_0^{\infty} x \frac{(2^x - 1)^{N_R - 1}\, 2^{x - N_R} {N_R}^{N_R} ln2}{\Gamma_{RB}^{N_R} \vartheta_{RB}^{2N_R}\,(N_R-1)!} e^{\frac{(1-2^x)N_R}{2\Gamma_{RB}\vartheta_{RB}^2}} dx \tag{4.13}$$

Note also that 4.12 could have been computed by following as well

$$R_{RB} = \int_0^{\infty} \log\left(1 + \frac{\Gamma_{RB}}{N_R} z\right) f_Z(z)\, dz \tag{4.14}$$

When same steps are followed as above, R_{AR} is calculated as

$$R_{AR} = \int_0^\infty x \frac{(2^x - 1)^{N_R - 1} \, 2^{x - N_R} ln2}{\Gamma_{AR}^{N_R} \vartheta_{AR}^{2N_R} \, (N_R - 1)!} e^{\frac{(1-2^x)}{2\Gamma_{AR}\vartheta_{AR}^2}} dx \tag{4.15}$$

Above expression have been validated by our simulations results. In [49], more general closed form expressions for achievable MIMO channel rate with any number of receive and transmit antenna are provided, where Laguerre polynomials are utilized.

4.1.4 Simulation Results

We take a simple scenario to compare FD performance with that of HD, discussing different system parameters and their effects on the performance through the simulations. In this scenario, while P_A is set to its maximum level ($10dB$), transmit power of the relay is computed optimally according to relay's transmission power.

In order to highlight the significance of power control mechanism in relaying scenarios, we plot rates from A to B with both power control and without power control, as function of relay transmission power, P_R in Figure 4.3. When power control is applied at the relay, it computes the best transmission power level and transmits at that power level. On the other hand, in the case of no power control, relay uses its maximum power budget for transmission, i.e., $P_R = P_{Rmax}$. As the Figure 4.3 clearly points out, unless power control is applied R_{AB}^{FD}, indicated by red curve, starts falling. Yet, this is not the case when it comes to power control scheme. Even though P_{Rmax} is increased, P_R remains same by the virtue of power control mechanism applied. Figure 4.3 suggests that optimal relay transmission power corresponds to the x-coordinate of the intersection point of R_{AR}^{FD} and R_{RB}^{FD} curves. If no intersection point exists, then R_{AR}^{FD} curve is always above R_{RB}^{FD} curve, and in that case relay should transmit at its maximum power.

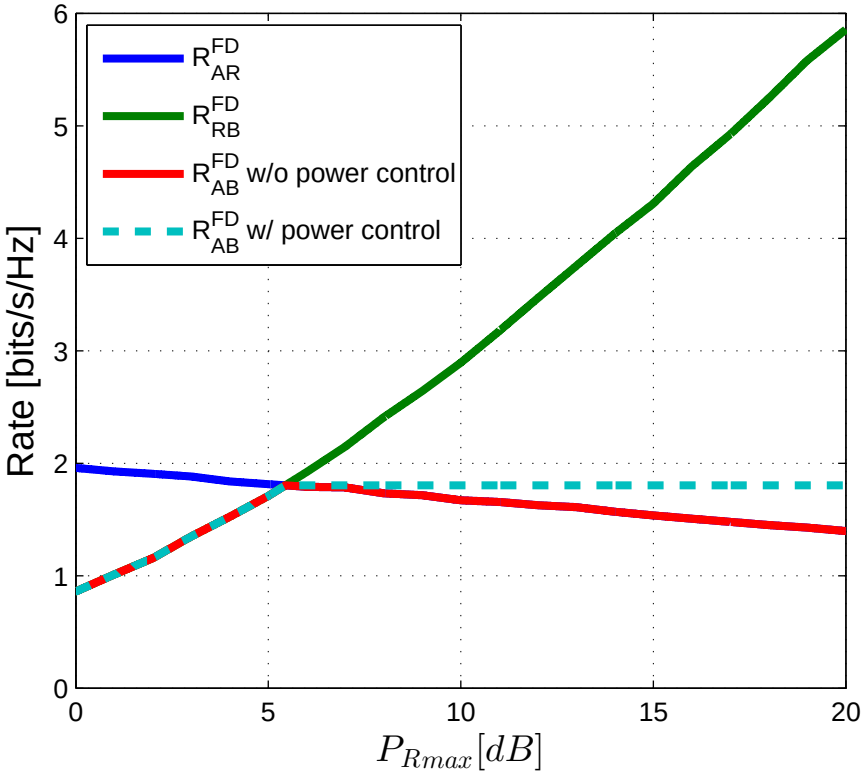

FIGURE 4.3: Importance of power control, ($P_{Amax} = 10dB, N_A = N_B = r = t = 1, \lambda = 0.8$)

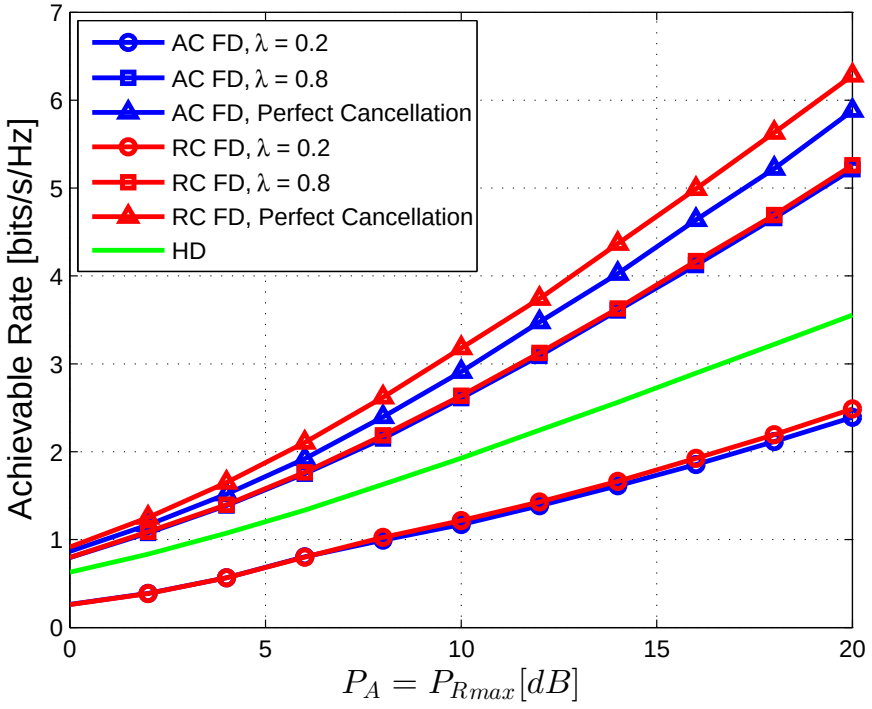

FIGURE 4.4: End-to-end rate w.r.t $P_A = P_{R_{max}}$

In Figure 4.4, end-to-end throughput performances of HD, AC FD and RC FD with respect to $P_A = P_{Rmax}$ are plotted, considering three different level of SI cancellation for FD: poor, good and perfect. In each one of FD relaying scenario, relay is assumed to be applying power control. In this simple scenario, nodes A and B have a single antenna. Relay is equipped with three antennas if it is HD, two receive one transmit antennas if it is RC FD, and two receive two transmit antennas if it is RC FD, as explained in Table 3.1 in Section 3.3. As obviously seen from Figure 4.4, FD RC and FD AC shows a superior performance to HD under good and perfect SI cancellation, whereas situation is the opposite in the case of poor SI cancellation. The fact that both FDs outperform HD when $\lambda = 0.8$, reveal that even with imperfect SI cancellation, FD still could offer a better throughput performance than HD.

4.2 Two Way Communication

In this scenario, nodes A and B exchange their information bidirectionally, via an intermediate decode-and-forward relay node, R. As in one way relaying, nodes A and B are assumed to be HD and they have N_A and N_B antennas, respectively. Similarly, the relay has r receive antennas and t transmit antennas and it can optimally allocate its resource for maximum throughput. Again, no direct link is assumed between nodes A and B. A realistic example for this scenario can be two stations on earth trying to communicate bidirectionally with each other via a satellite, without a direct link between them.

In the next sections, we obtain the achievable rates for the two way two hop communication, i.e., two way relaying, considering the relay's operation in HD and FD modes. Note that, since the capacity of the two way relay channel in HD mode is not known, and there are many strategies such as decode-and-forward [50] and physical network coding [51], we compute the average achievable rates for HD relay as an upper bound of all existing schemes.

4.2.1 HD Achievable Rates

When relay is HD constrained, instead of four-phase transmission, we consider an efficient transmission strategy, namely analog network coding as described in [43, 51]. In this strategy, communication is performed in two phases. First, both nodes transmit to the relay at the same time. The relay receives the sum of signals from both terminals, which is the superposition of A's and B's transmit signals. During the second phase, the relay broadcasts this sum signal. Each node will be able to decode other's message simply by subtracting its own message from the received signal. Note that for such scheme to work, the nodes should possess the channel state information and store their transmitted signals. The first phase can be considered as the Multi Access Channel (MAC) phase, while second phase is the broadcast (BC) phase. These phases are demonstrated in Figure 4.5 (a) and (b).

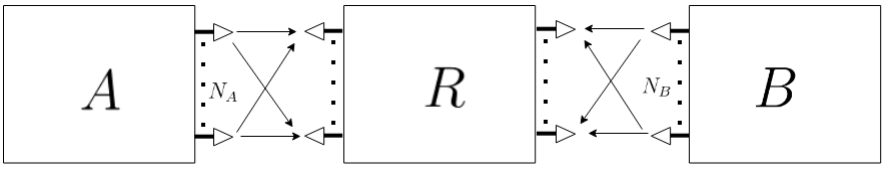

(a)

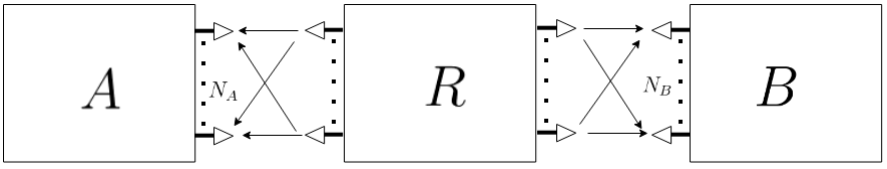

(b)

FIGURE 4.5: (a) First phase, A and B transmitting to R (MAC), (b) Second phase, R broadcasting (BC)

For calculating the average achievable rates, we will use two phase MAC-BC strategy in [50]. During the MAC phase, both of the nodes transmit their respective messages to the relay. The achievable rates during MAC phase from the nodes A

and B to the relay are found as

$$\begin{aligned} R_{AR} &\leq I\left(\mathbf{y}_R; \mathbf{x}_A | \mathbf{x}_B\right) \\ R_{BR} &\leq I\left(\mathbf{y}_R; \mathbf{x}_B | \mathbf{x}_A\right) \\ R_{MAC} &\leq I\left(\mathbf{y}_R; \mathbf{x}_A, \mathbf{x}_B\right) \end{aligned} \tag{4.16}$$

During the second phase, the relay broadcasts the sum signal to both nodes, such that each node can recover other node's message by applying analog network coding techniques discussed in [43]. Then the achievable rates in this phase are calculated by

$$\begin{aligned} R_{RA} &\leq I\left(\mathbf{y}_A; \mathbf{x}_R\right) \\ R_{RB} &\leq I\left(\mathbf{y}_B; \mathbf{x}_R\right) \end{aligned} \tag{4.17}$$

Assume that MAC phase lasts for τ fraction of total communication time and BC phase for remaining fraction $(1-\tau)$. Then, based on the mutual information expressions given in equations 4.16 and 4.17, rate region achievable during MAC phase is given by followings

$$\begin{aligned} R_{AR}^{HD} &= \tau \mathbb{E}\left[\log\det\left(\mathbf{I} + \frac{\Gamma_{AR}}{N_A}\mathbf{H}_{AR}\mathbf{H}_{AR}^*\right)\right], \\ R_{BR}^{HD} &= \tau \mathbb{E}\left[\log\det\left(\mathbf{I} + \frac{\Gamma_{BR}}{N_B}\mathbf{H}_{BR}\mathbf{H}_{BR}^*\right)\right], \\ R_{MAC} &\leq \tau \mathbb{E}\left[\log\det\left(\mathbf{I} + \frac{\Gamma_{AR}}{N_A}\mathbf{H}_{AR}\mathbf{H}_{AR}^* + \frac{\Gamma_{BR}}{N_B}\mathbf{H}_{BR}\mathbf{H}_{BR}^*\right)\right]. \end{aligned} \tag{4.18}$$

Note that omitting the sum rate constraint from the MAC phase gives the cut-set upper bound[52]. The achievable rates during BC phase are given by

$$\begin{aligned} R_{RA}^{HD} &= (1-\tau)\,\mathbb{E}\left[\log\det\left(\mathbf{I} + \frac{\Gamma_{RA}}{N_R}\mathbf{H}_{RA}\mathbf{H}_{RA}^*\right)\right], \\ R_{RB}^{HD} &= (1-\tau)\,\mathbb{E}\left[\log\det\left(\mathbf{I} + \frac{\Gamma_{RB}}{N_R}\mathbf{H}_{RB}\mathbf{H}_{RB}^*\right)\right]. \end{aligned} \tag{4.19}$$

Then, end-to-end rate in both directions are given by

$$R_{AB}^{HD} = \min\left\{R_{AR}, R_{RB}\right\},$$
$$R_{BA}^{HD} = \min\left\{R_{BR}, R_{RA}\right\}. \tag{4.20}$$

The achievable sum rate is calculated by optimizing over the fraction of time spent between two phases

$$R_{sum}^{HD} = \max_{0\leq\tau\leq1}\left(R_{AB}^{HD} + R_{BA}^{HD}\right). \tag{4.21}$$

4.2.2 FD Achievable Rates

Two way two hop communication with a FD relay takes place in two phases with the following information flow $A \longrightarrow R \longrightarrow B$ in first and $B \longrightarrow R \longrightarrow A$ in the second phase, respectively. In each phase, the relay operates in FD mode, allowing simultaneous reception and transmission. The information flow is same as one way relaying with FD relay, other than flow being reversed in the second phase. A diagram depicting information flow in this communication scenario is given in Figure 4.6.

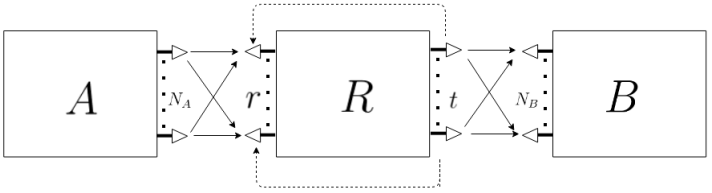

(a)

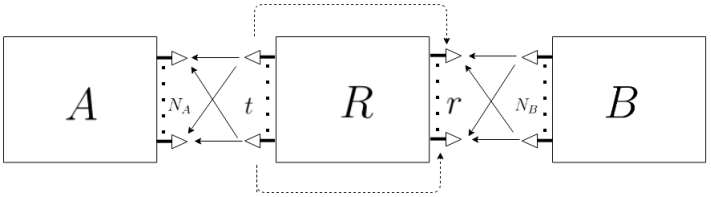

(b)

FIGURE 4.6: (a) First phase, A transmitting to B through R, (b) Second phase, B transmitting to A through R

Let us assume that τ denotes the fraction of total communication period devoted to first phase. Two way communication over two hop with FD relay consists of two phases. Let us assume that τ fraction of total communication period is devoted to the first phase, direction of flow is reversed in the remaining fraction $(1-\tau)$ of the time. Then achievable average rates are calculated through the following expressions

$$\begin{aligned}
R_{AR}^{FD} &= \tau\mathbb{E}\left[\log\det\left(\mathbf{I}+\frac{\Gamma_{AR}}{N_A}\mathbf{H}_{AR}\mathbf{H}_{AR}^{*}\right)\right],\\
R_{RB}^{FD} &= \tau\mathbb{E}\left[\log\det\left(\mathbf{I}+\frac{\Gamma_{RB}}{t}\mathbf{H}_{RB}\mathbf{H}_{RB}^{*}\right)\right],\\
R_{BR}^{FD} &= (1-\tau)\,\mathbb{E}\left[\log\det\left(\mathbf{I}+\frac{\Gamma_{BR}}{N_B}\mathbf{H}_{BR}\mathbf{H}_{BR}^{*}\right)\right],\\
R_{RA}^{FD} &= (1-\tau)\,\mathbb{E}\left[\log\det\left(\mathbf{I}+\frac{\Gamma_{RA}}{t}\mathbf{H}_{RA}\mathbf{H}_{RA}^{*}\right)\right].
\end{aligned} \tag{4.22}$$

End-to-end average achievable rate is given by following expressions

$$\begin{aligned}
R_{AB}^{FD} &= \tau \max_{P_{R1}\leq P_{Rmax}} \min\{R_{AR}, R_{RB}\},\\
R_{BA}^{FD} &= (1-\tau) \max_{P_{R2}\leq P_{Rmax}} \min\{R_{BR}, R_{RA}\}.
\end{aligned} \tag{4.23}$$

where P_{R1} and P_{R2} denote the relay's transmission power in the first and second phase of the communication, respectively. In order to create symmetrical link rates, τ is adjusted such that end-to-end rates in each direction are equalized, $R_{AB}^{FD} = R_{BA}^{FD}$. Therefore, we set τ to $\frac{R_{BA}^{FD}}{R_{AB}^{FD}+R_{BA}^{FD}}$. Sum rate is given by

$$R_{sum}^{FD} = \left(R_{AB}^{FD} + R_{BA}^{FD}\right). \tag{4.24}$$

4.2.3 Results

We take the same test scenario as in 4.1. Our aim is to compare sum rates achieved by HD with those of AC FD and RC FD implementations for different transmission powers. As seen from Figure 4.7, FD does not show a better performance even in the absence of SI. The reason why maximum achievable performance of FD

does not outperform HD is that HD can serve both terminals at the same time in MAC and BC phases, giving rise to doubling the spectral efficiency. Consequently, FD and HD offer almost the same throughput performance at their best cases. Therefore, considering extra cost that comes with FD deployment, we conclude that FD may not be good strategy to go with since it also does not offer a improved throughput. Remark that FD performance can be leveraged by making nodes A and B both FD-enabled. However, the case where all the nodes are FD enabled is beyond the scope of our study.

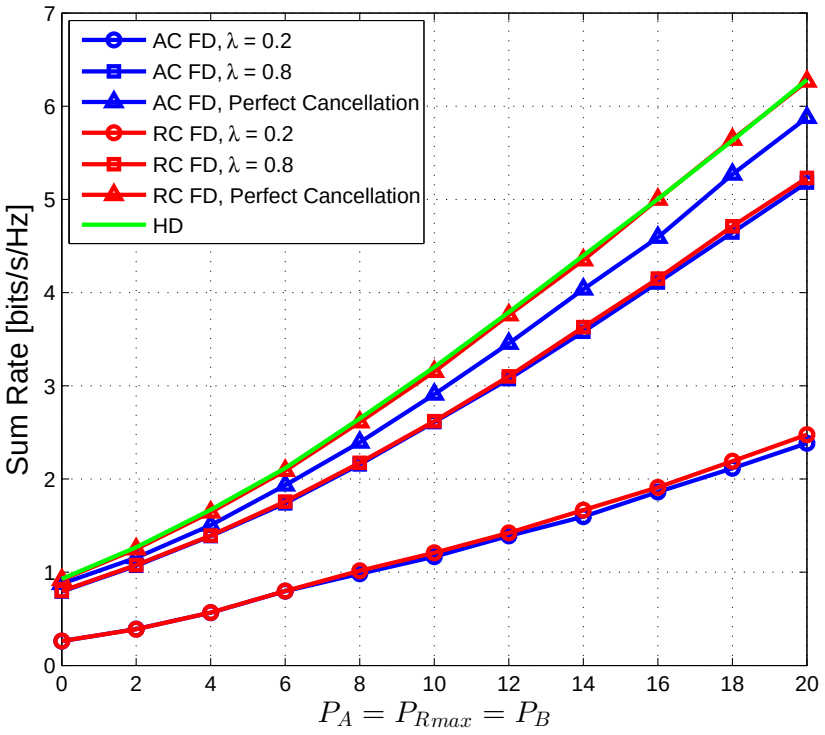

FIGURE 4.7: Sum rate with respect to $P_A = P_{Rmax} = P_B$

Chapter 5

FD in Multihop Networks

In this chapter, we evaluate FD in multihop wireless scenarios such as wireless ad hoc networks. We consider one way communication between a source node and a destination node across multiple intermediate nodes, assuming a full-interference model, where all nodes can hear each other. In this problem, the aim is to connect source and destination nodes to each other via the best route with the highest end-to-end throughput. Once the route between source and destination nodes is found, unselected nodes in the network are assumed to remain idle (performing no transmission). Since a single flow case is studied, the problem boils down to a one way multihop communication problem.

In the investigated network model, if all the nodes operate in conventional HD mode, then they simply need to apply time division, since a node cannot transmit and receive simultaneously. On the other hand, if the intermediate nodes are FD enabled, then the selected nodes (on the route) can all transmit & receive at the same time. To offer a complete solution to the problem of one way multihop communication in ad hoc networks, we take a step-by-step approach. In the first step, we revisit the one way communication over two hops investigated in Chapter 4, with the condition that destination node can hear both the source and the relay nodes. We obtain analytical expressions for optimal transmission power policy. Then, we extend our solution to the multihop relay networks. The power control solution we obtain for multihop relay network constitutes a base for the

power allocation problem in FD ad hoc networks with a single pair of source and destination.

5.1 Channel Model

As summarized in [1], FD communication is best suited for short distance wireless systems such as femto cells because of SI cancellation challenges at high transmit power levels. Therefore, we consider low transmission power, low noise power, short distance wireless communication scenarios. Unlike in Chapter 3 and Chapter 4, in this chapter, a node is able to hear the other nodes in the network since we assume that nodes are placed in a small area, justifying the full-interference model.

For the wireless channels between the nodes, we assume all the channels to be non-fading, hence only path loss is considered. Furthermore, all the nodes in the network are assumed to have a single antenna. If a node is operating in HD mode, its antenna is connected to either transmit RF chain or receive RF chain by a means of a switch. For FD nodes, we assume a shared antenna design, where an antenna is shared by transmit and receive RF chains, similar to the design in [53]. Note that, from the perspective of radio resources, antenna and RF chain requirements are the same for both HD and shared antenna FD implementations except for 1) additional hardware for digital cancellation and 2) circulator used for isolation between transmit and receive RF chains.

Considering a point-to-point communication channel over which node A is transmitting to node B, the communication between these nodes could either be carried out in HD mode or FD mode depending upon scenario being investigated. Recall that since nodes are equipped with one antenna only, all the channels investigated in this chapter represent a SISO channel. The received signal model at node B can be written as follows

$$\mathbf{y}_B = \sqrt{K_{AB}}\mathbf{x}_A + \mathbf{i}_B + \sum_{j\in\Pi} \mathbf{q}_{j,B} + \mathbf{w}_B. \tag{5.1}$$

Here K_{AB} denotes the path loss attenuation of the link between nodes A and B. $\mathbf{x}_A$ denotes the vector of transmitted symbols, $\mathbf{w}_B$ denotes the AWGN noise term, and $\mathbf{i}_B$ is the SI signal with power of I_B if node B is operating in FD mode and $\mathbf{q}_{j,B}$ represents the interference signal from transmission of node $j \in \Pi_B$ on node B with a power of $Q_{j,B}$, where Π_B denotes the set of nodes causing interference on node B. In the case of HD operation, the terms $\mathbf{i}_B$ and $\sum_{j\in\Pi} \mathbf{q}_{j,B}$ are both zero. The Signal to Interference and Noise Ratio (SINR) at the receiver is given by

$$\Gamma_{AB} = \frac{K_{AB}P_A}{\left(\sigma_B^2 + I_B + \sum_{j\in\Pi_B} Q_{j,B}\right)}. \tag{5.2}$$

where σ_B^2 denotes the variance of the noise at node B. Thus, the achievable throughput from A to B, R_{AB} is given by

$$R_{AB} = \log\left(1 + \Gamma_{AB}\right). \tag{5.3}$$

5.2 SI Cancellation Model

FD radios with shared antenna design achieve simultaneous transmission and reception over the same frequency by the virtue of a simple circulator as in [54]. Yet, since perfect isolation is not realizable, there is always a leakage from TX chain into RX chain in the circulator, creating SI. The essential function of the circulator is to route RX and TX signals, and minimize the leakage as much as possible. How much of the transmitted signal leaks into the receive chain is completely determined by the performance of this circulator. We represent this undesired energy leakage, i.e. SI, through a simple mathematical model, as in [35], to facilitate the

task of obtaining the closed form rate expressions and later solving optimization problems. This SI model is defined as follows

$$I = \beta P_T \tag{5.4}$$

dB-converted version of (5.4) is

$$I(dB) = \beta(dB) + P_T(dB) \tag{5.5}$$

For instance, the case when $\beta = 10^{-6}$ corresponds to $60dB$ cancellation or $\beta = 0$ indicates perfect cancellation. Notice that, unlike the experimentally characterized nonlinear residual SI model used in Chapter 3 and Chapter 4, SI cancellation model given in (5.4) is linear. Because of the linear characteristics of SI model in (5.4), it facilitates analytical manipulations and solutions of the optimization problem for power control.

Both SI cancellation models have their own advantages/disadvantages. Since we focus on the gain of FD in previous chapters, we prefer to employ the first nonlinear model to obtain more realistic results in basic scenarios. On the other hand, it is more advantageous to use the linear model for an analytical approach to the multihop problem. Note that when $\lambda = 0$, nonlinear SI cancellation model becomes the linear SI cancellation. Therefore, the linear residual SI model is only a special case of nonlinear SI model with $\lambda = 0$. While the performance of SI cancellation is captured by λ in the non-linear residual SI model, it is characterized by a multiplier, β in the linear model.

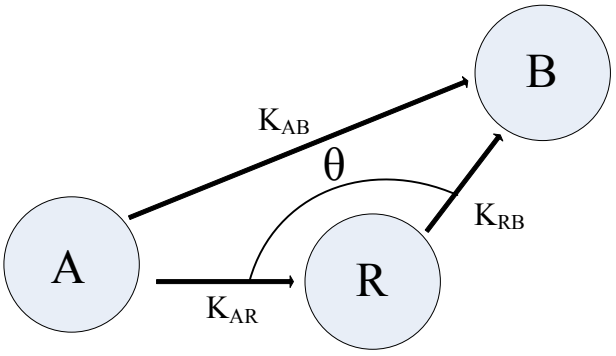

FIGURE 5.1: One way relaying revisited

5.3 Relaying Revisited: Optimal Power Assignment Policy

We study one way two hop communication discussed in Chapter 4 under the new channel and system model assumptions in this section. Let us assume that terminal A, as the source terminal, wishes to send its message to destination terminal B via an intermediate relay terminal, R which assists forwarding from A to B, as described in Figure 5.1. In this scenario, the relay is assumed to employ decode-and-forward protocol. With the full-interference assumption, all nodes hear each other, but node B cannot decode node A's signal over the direct path, so it needs the relay. As a real life example of this scenario, we can think of an access point (or base station) forwarding an uplink user's message to another user over the downlink channel. When the relay operates in HD mode, an uplink user and a downlink user cannot be served at the same time. If the relay, on the other hand, operates in FD mode, it is capable of performing transmission and reception concurrently. We also assume that multi packet reception is also not possible at any of the nodes.

Nodes A and R are power limited such that $P_A \leq P_{Amax}$ and $P_R \leq P_{Rmax}$ where P_A and P_R denote the actual transmit power at which nodes A and R operate, respectively while P_{Amax} and P_{Rmax} are the maximum transmit power of the respective nodes. In below sections, we explain how we obtain achievable rates in both HD and FD relaying scenarios.

5.3.1 HD Achievable Rates

If the relay is HD functioning, then links $A \longrightarrow R$ and $R \longrightarrow B$ must be active at alternating time slots, implying that A and R cannot transmit at the same time. For this reason, the flow of the information from source node, A to destination node, B occurs in two phases. First, A transmits to R and in the second phase R forwards what it received from A to B. SNR at the nodes is then given by

$$\Gamma_{AR} = \frac{K_{AR} P_A}{\sigma_R^2}, \tag{5.6}$$

$$\Gamma_{RB} = \frac{K_{RB} P_R}{\sigma_B^2}. \tag{5.7}$$

where K_{AR} and K_{AR} represent the path loss attenuation of the respective links. σ_R^2 and σ_B^2 are the variance of the noise at node R and node B, respectively. When the relay operates in HD mode, it needs to devote different time slots to reception and transmission. Assuming fraction τ of total communication time is dedicated to transmission of source, rate achieved from A to R is obtained as

$$R_{AR}^{HD} = \tau \log\left(1 + \Gamma_{AR}\right), \tag{5.8}$$

and the rate achievable over the link R to B link is given by

$$R_{RB}^{HD} = (1 - \tau) \log\left(1 + \Gamma_{RB}\right). \tag{5.9}$$

By optimizing over τ, the end-to-end achievable average rate for HD relaying is obtained as

$$R_{AB}^{HD} = \max_{0 \leq \tau \leq 1} \min\left\{R_{AR}^{HD}, R_{RB}^{HD}\right\}. \tag{5.10}$$

Note that in (5.10) increase in τ results in increase in R_{AR}^{HD}, yet decrease in R_{RB}^{HD}. As a consequence, in this maxmin problem, optimal τ, denoted by τ_{opt} should

satisfy $R_{AR}^{HD} = R_{RB}^{HD}$. Thus, τ_{opt} is given by

$$\tau_{opt} = \frac{\log\left(1+\Gamma_{RB}\right)}{\log\left(1+\Gamma_{AR}\right)+\log\left(1+\Gamma_{RB}\right)} \tag{5.11}$$

Note that, according to our system model, destination node B can only hear (i.e., sense) but cannot decode node A's transmission. Hence node B cannot take advantage of the transmitted signal in the first phase and it can extract information only from relay's transmission as in [35], resulting in the rate expression in 5.10.

5.3.2 FD Achievable Rates

When the relay operates in FD mode, it is capable of transmitting and receiving at the same time. While receiving i^{th} packet from the source node A, relay can forward the previously received $(i-1)^{th}$ packet to the destination node B. As a result, links $A \longrightarrow R$ and $R \longrightarrow B$ are active at the same time unlike in HD relaying. This causes SI at relay node, R. Meanwhile, the node B receives $(i-1)^{th}$ packet from R, also hearing from the transmission of the i^{th} packet from node A. Note that, node B hears (i.e., senses) but cannot decode A's transmission, and since none of the nodes have multi packet reception capability, node A's transmission is treated as interference at node B. Signal to Noise and Interference Ratio at nodes R and B are then given by

$$\Gamma_{AR} = \frac{K_{AR}P_A}{\sigma_R^2 + I} = \frac{K_{\mathrm{AR}}P_A}{\sigma^2 + \beta P_R}. \tag{5.12}$$

$$\Gamma_{RB} = \frac{K_{RB}P_R}{\sigma_B^2 + Q} = \frac{K_{\mathrm{RB}}P_R}{\sigma^2 + K_{AB}P_A}. \tag{5.13}$$

where I denotes the power of interference signal at node R and Q denotes the power of inter node interference signal. It is assumed that noise variance at nodes R and B are equal ($\sigma_R^2 = \sigma_B^2 = \sigma^2$). β is the parameter that captures the amount of isolation between TX and RX RF chains of the FD relay, as in (5.4). Here K_{AR}, K_{RB} and K_{AB} are path losses for links $A \longrightarrow R$, $R \longrightarrow B$ and $A \longrightarrow B$,

respectively. Using Shannon capacity equations, achievable rates of each link are calculated as follows

$$\begin{aligned} R_{AR}^{FD} &= \log\left(1+\Gamma_{AR}\right), \\ R_{RB}^{FD} &= \log\left(1+\Gamma_{RB}\right). \end{aligned} \tag{5.14}$$

Since the relay operates in decode-and-forward manner, the end-to-end throughput from A to B is the minimum of R_{AR}^{FD} and R_{RB}^{FD} and is maximized over P_A and P_R

$$R_{AB}^{FD} = \max_{\substack{P_A \leq P_{Amax} \\ P_R \leq P_{Rmax}}} \min\left\{R_{AR}^{FD}, R_{RB}^{FD}\right\}. \tag{5.15}$$

Lemma 5.1. *For optimal end-to-end throughput, achievable link rates R_{AR}^{FD} and R_{RB}^{FD} should be equal by adjusting the transmission power levels, P_A and P_B.*

Proof. The rate of link $A \longrightarrow R$ increases with P_A and decreases with P_R monotonically. Likewise, the rate of link $R \longrightarrow B$ increases with P_R and decreases with P_A monotonically. Additionally, the end-to-end rate is the minimum of these link rates. Therefore, end-to-end throughput is maximized when the link rates are equalized, which equivalently means, when SNRs at nodes R and B are equal. Assuming that P_A and P_R can be adjusted continuously, there has to be a pair (P_A, P_R), which yields the equal link rates ($R_{AR} = R_{RB}$). □

Lemma (5.1) has been proven by a game theoretical approach in earlier works on relaying such as [55], [56], [57], [58]. The game here is that there are two users who have the common objective, which is to maximize end-to-end throughput. Since the bargain parameters (P_A and P_R) are both continuous, there has to be a Nash equilibrium, and this equilibrium is reached, when rates are equalized. The lemma has also been validated with numerical observations as well. Having said that, by equating Γ_{AR} and Γ_{RB}, we obtain following

$$\frac{K_{AR}P_A}{\sigma^2+\beta P_R} = \frac{K_{RB}P_R}{\sigma^2+K_{AB}P_A} \tag{5.16}$$

Note that equation (5.16) constitutes a quadratic equation for P_A and P_R. Solving it with respect to P_A, we get the following roots:

$$P_{A_1} = \frac{-\sqrt{K_{\mathrm{AR}}}\sqrt{4\beta K_{\mathrm{AB}}K_{\mathrm{RB}}P_R^2 + 4\sigma^2 K_{\mathrm{AB}}K_{\mathrm{RB}}P_R + \sigma^4 K_{\mathrm{AR}}} - \sigma^2 K_{\mathrm{AR}}}{2K_{\mathrm{AB}}K_{\mathrm{AR}}} \tag{5.17}$$

$$P_{A_2} = \frac{\sqrt{K_{\mathrm{AR}}}\sqrt{4\beta K_{\mathrm{AB}}K_{\mathrm{RB}}P_R^2 + 4\sigma^2 K_{\mathrm{AB}}K_{\mathrm{RB}}P_R + \sigma^4 K_{\mathrm{AR}}} - \sigma^2 K_{\mathrm{AR}}}{2K_{\mathrm{AB}}K_{\mathrm{AR}}} \tag{5.18}$$

Obviously, P_{A1} turns out to be negative. Since this is not possible, we choose P_{A2} as the solution to the equation (5.16). Plugging P_A into Γ_R or Γ_B, one can obtain the equal SNR levels $\Gamma_{AR} = \Gamma_{RB}$ as follows

$$\frac{2\sqrt{K_{\mathrm{AR}}}K_{\mathrm{RB}}P_R}{\sqrt{4K_{\mathrm{AB}}K_{\mathrm{RB}}P_R\left(\beta P_R + \sigma^2\right) + \sigma^4 K_{\mathrm{AR}}} + \sigma^2\sqrt{K_{\mathrm{AR}}}}, \tag{5.19}$$

which is a function of only one parameter, P_R. Our aim is now to find the best P_R value, which will maximize Γ_{AR} or Γ_{RB} (Recall that $\Gamma_{AR} = \Gamma_{RB}$). Taking the first derivative of (5.19) with respect to P_R, $\frac{d\Gamma_{AR}}{dP_R}$ is calculated as follows

$$\frac{d\Gamma_{AR}}{dP_R} = \frac{2\sigma^2\sqrt{K_{\mathrm{AR}}}K_{\mathrm{RB}}\left(\sqrt{K_{\mathrm{AR}}}\sqrt{4K_{\mathrm{AB}}K_{\mathrm{RB}}P_R\left(\beta P_R + \sigma^2\right) + \sigma^4 K_{\mathrm{AR}}} + 2K_{\mathrm{AB}}K_{\mathrm{RB}}P_R + \sigma^2 K_{\mathrm{AR}}\right)}{\sqrt{4K_{\mathrm{AB}}K_{\mathrm{RB}}P_R\left(\beta P_R + \sigma^2\right) + \sigma^4 K_{\mathrm{AR}}}\left(\sqrt{4K_{\mathrm{AB}}K_{\mathrm{RB}}P_R\left(\beta P_R + \sigma^2\right) + \sigma^4 K_{\mathrm{AR}}} + \sigma^2\sqrt{K_{\mathrm{AR}}}\right)^2} \tag{5.20}$$

and noting that β and all the path loss coefficients are positive, we realize that (5.20) is positive, implying that equal SNR level is always increasing with respect to P_R, clearly for positive P_R values. Hence, the solution for P_R is on the boundary, implying that the relay should use its maximum power level i.e. $P_R = P_{Rmax}$ in order to get the achievable maximum throughput. Node A, on the other hand, needs to adjust its transmission power according to (5.18). Hence, optimal power transmission levels are found as

$$P_R = P_{R_{max}}$$

$$P_{A_2} = \frac{\sqrt{K_{\mathrm{AR}}}\sqrt{4\beta K_{\mathrm{AB}}K_{\mathrm{RB}}P_R^2 + 4\sigma^2 K_{\mathrm{AB}}K_{\mathrm{RB}}P_R + \sigma^4 K_{\mathrm{AR}}} - \sigma^2 K_{\mathrm{AR}}}{2K_{\mathrm{AB}}K_{\mathrm{AR}}} \tag{5.21}$$

If this solution is not feasible for P_A, in other words, if P_{A2} found in (5.21) turns

out to be larger than P_{Amax}, then P_A is maximized, $P_A = P_{A_{max}}$ and P_R is obtained from the equation (5.21) in the same manner as follows

$$P_R = \frac{\sqrt{K_{\mathrm{RB}}}\sqrt{4\beta P_A^2 K_{\mathrm{AB}} K_{\mathrm{AR}} + 4\beta\sigma^2 P_A K_{\mathrm{AR}} + \sigma^4 K_{\mathrm{RB}}} - \sigma^2 K_{\mathrm{RB}}}{2\beta K_{\mathrm{RB}}} \tag{5.22}$$

In Algorithm 1, we provide the pseudo code of the complete procedure for optimal transmission power strategy for one way two hop relaying communication scenario.

$P_R = P_{Rmax}$; $P_A = \frac{\sqrt{K_{\mathrm{AR}}}\sqrt{4\beta K_{\mathrm{AB}} K_{\mathrm{RB}} P_R^2 + 4\sigma^2 K_{\mathrm{AB}} K_{\mathrm{RB}} P_R + \sigma^4 K_{\mathrm{AR}}} - \sigma^2 K_{\mathrm{AR}}}{2K_{\mathrm{AB}} K_{\mathrm{AR}}}$;
if $P_A \leq P_{Amax}$ **then**
  exit;
else
  $P_A = P_{Amax}$;
  $P_R = \frac{\sqrt{K_{\mathrm{RB}}}\sqrt{4\beta P_A^2 K_{\mathrm{AB}} K_{\mathrm{AR}} + 4\beta\sigma^2 P_A K_{\mathrm{AR}} + \sigma^4 K_{\mathrm{RB}}} - \sigma^2 K_{\mathrm{RB}}}{2\beta K_{\mathrm{RB}}}$;
end

Algorithm 1: Algorithm Implementation of the Optimal Power Assignment

Comparison with One Way Relaying

Here, we elaborate on how our solution in this section can be related to one way relaying scenario provided in Chapter 4. Note that the difference between the scenarios evaluated in this section and one way relaying in Chapter 4 is SI and interference models. In order to understand the effect of inter node interference, letting $K_{AR} = K_{RB} = \sigma^2 = \beta = 1$, we plot P_A as a function of P_R based on equation (5.21) in Figure 5.2 for different K_{AB} values. As clearly depicted in the figure, as K_{AB} gets smaller, the optimal and feasible solution is obtained as $P_A = P_{Amax} = 10dB$ and P_R is obtained via equation (5.22). When $K_{AB} = 0$, we obtain the one way relaying scenario as in Section 4.1, where destination node B does not hear source node A. Furthermore, considering the same SI model given in (5.4) and equating SNR levels at relay and B, we obtain the following:

$$\frac{K_{AR} P_A}{\sigma^2 + \frac{P_R^{(1-\lambda)}}{\beta\mu^{\lambda}}} = \frac{K_{RB} P_R}{\sigma^2} \tag{5.23}$$

Substituting the same parameter settings that were used in obtaining Figure 4.3 (i.e., $\sigma^2 = K_{AR} = K_{RB} = -50dB, P_{Amax} = 10dB$), and solving for P_R in equation (5.23), we get $P_R = 5.44dB$, which is exactly same as the x-coordinate of the intersection point of R_{AR}^{FD} and R_{RB}^{FD} curves in Figure 4.3. Hence, we conclude that solution for full-interference model is consistent with the power control result obtained in Section 4.1.

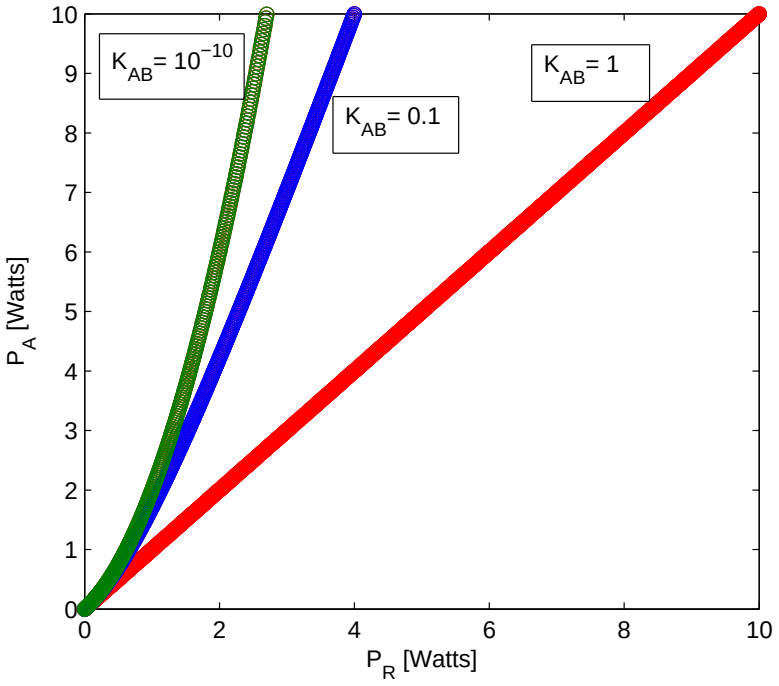

FIGURE 5.2: Effect of inter node interference channel, K_{AB}

5.3.3 Numerical Results

In our experiments, we consider the system model in Figure 5.1, assuming different levels of SI suppression for FD. We evaluate the effect of maximum transmission power, distances and angle between the nodes on the end-to-end throughput for HD and FD operation. In all simulations performed in this section, noise variance, σ^2 and path loss exponent, α are taken to be $100dBm$ and 4, respectively.

In Figure 5.3, the end-to-end throughput of the investigated relaying system as a function of maximum transmission power is shown. One can note from Figure 5.3

that HD underperforms FD when SI cancellation is strong enough (e.g $100dB$). On the other hand, FD does not show a satisfactory performance in the case of 20 and 60 dB suppression levels.

In Figure 5.4, we investigate how the end-to-end throughput is affected by the change in θ in a fixed distance and fixed maximum power levels. Obviously, there is no interference in HD mode. Therefore, HD performance is not changed with the change in θ. Notwithstanding, since θ changes the distance between nodes A and B, affecting the severity of the interference from A to B, end-to-end throughput performance of FD relaying is highly dependent on θ. As θ increases, nodes A and B get far away from each other, leading to smaller amount of inter node interference. Again, when SI cancellation is poor ($20dB$ and $60dB$), we do not observe any gain by FD over HD. However, with sufficient SI cancellation ($75dB$ and $100dB$), one can find a threshold θ after which FD performs better. More specifically, FD gain reaches to 160% under $75dB$ SI suppression, while FD under $100dB$ SI suppression almost doubles the HD performance.

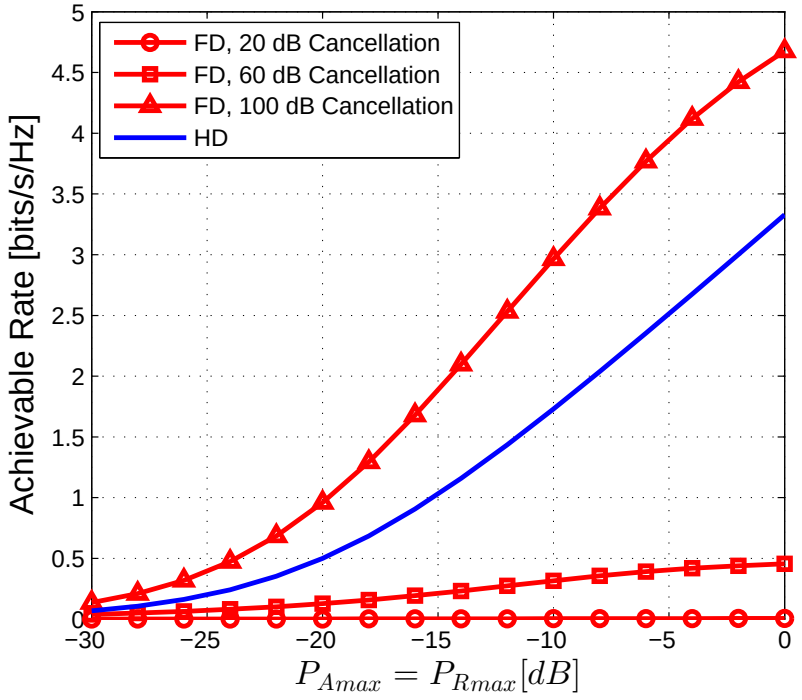

FIGURE 5.3: End-to-end throughput with respect to transmission powers of nodes A and R, $\theta = \pi$, $d_{AR} = d_{RB} = 100m$, $\alpha = 4$

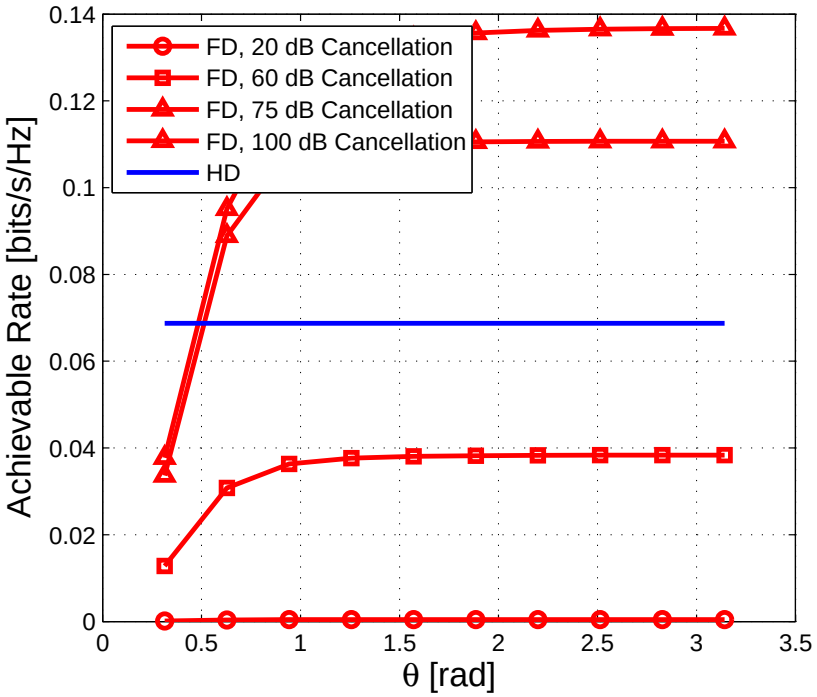

FIGURE 5.4: End-to-end throughput with respect to θ (θ given in radians), $d_{AR} = d_{RB} = 100m, P_{Amax} = P_{Rmax} = 0dBm$, $\alpha = 4$

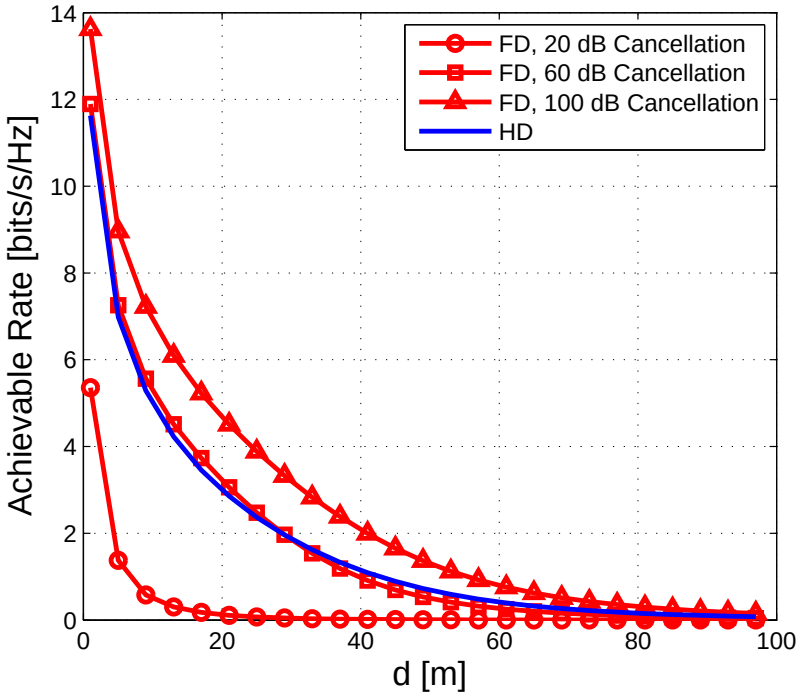

FIGURE 5.5: End-to-end throughput with respect to $d_{AR} = d_{RB}$, $\theta = \pi$ (θ given in radians) , $P_{Amax} = P_{Rmax} = 0dBm$, $\alpha = 4$

In Figure 5.5, the relationship between end-to-end throughput and inter node distance, $d_{AR} = d_{RB} = d$ is evaluated. Here we fix θ to π, and maximum node transmission power to $0dBm$. We can see from Figure 5.5 that as long as FD radio has a good SI cancellation capability (e.g. $100dB$ SI cancellation), it always achieves a better performance for the indicated distances. FD under $60dB$ cancellation shows almost same performance as HD does. On the other hand, if SI cancellation capability is poor (e.g. $20dB$ SI cancellation), then a huge performance gap is observed between HD and FD.

In conclusion, we look into FD performance, considering different level of SI suppression through an example test scenario, suitable for FD operation (low transmission power, small distance). Our investigation on the effect of critical system parameters on the FD performance has shown that FD outperform its HD counterpart under good SI suppression. The gain achieved by FD over HD has observed to approach to 2 as the residual amount of SI approaches to zero. .

5.4 Power Control for FD in Multihop Networks

Having obtained a formulation for optimal power policy to achieve the maximum end-to-ed throughput in one way two hop relaying networks, we extend this problem to one way multihop communication in linear network topologies in this section. The system model of the network we evaluate in this section is demonstrated in Figure 5.6.

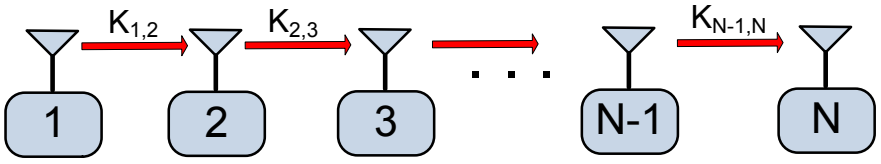

FIGURE 5.6: One way multihop communication system model in a linear network

In this scenario, a source node (labeled by 1) wishes to deliver its packets to a destination node (labeled by N), which is d meters away from the source node, through multiple relay nodes $(2, 3, \ldots, N-1)$, as shown in Figure 5.6. An arbitrary node $i, \forall i \in \{1, \ldots, N-1\}$ in this network has a transmission power budget, denoted by P_{imax} and the transmission power at which node i operates is denoted by $P_i \leq P_{imax}$. When all the relays operate in HD, each link should become active at different times. However, when relays are FD capable, all transmits at the same time. Again, we assume that all nodes hear, i.e. sense each other's transmission, but packet reception (i.e., decoding) is possible only between one hop neighbors, and the nodes do not have multi packet reception capability.

5.4.1 HD Achievable Rates

We consider a conventional HD transmission strategy, where each node takes the possession of the channel at different times, by taking turns, avoiding any possible inter node interferences. Therefore, each link must be active at different time slots. In this case, the total communication time should be divided between these links, leading to time division multiple access (TDMA). Assuming that the link from node $(i-1)$ to i is active for a fraction, τ_{i-1} of total communication time, and also that entire communication lasts one time unit, then we have $\sum_{i=1}^{N-1} \tau_i = 1$. Neglecting the overheads such as ACK, random back-offs, etc..., which are necessary for medium access control, and assuming pure TDMA, and assuming that each node suffers from AWGN with same variance, σ^2, the throughput of link from node $(i-1)$ to node i, $R_{i-1,i}$ is then given by

$$R_{i-1,i} = \tau_{i-1} log\left(1 + \frac{K_{i-1,i} P_{i-1}}{\sigma^2}\right), \forall i \in \{2, \ldots, N\}, \tag{5.24}$$

and the end-to-end throughput is found and maximized as follows

$$\begin{aligned} \underset{\tau_i}{\text{maximize}} \quad & min\left\{R_{1,2}, R_{2,3}, \ldots R_{N-1,N}\right\} \\ \text{subject to} \quad & \sum_{i=1}^{N-1} \tau_i = 1. \end{aligned} \tag{5.25}$$

Lemma 5.2. *On a given a path, for maximizing end-to-end throughput, all the link rates should be all equal to each other:* $R_{i,i+1} = R, \forall i \in \{1, 2, ..., N-1\}$.

For rate equalization, the total communication time should be divided by allocating times to the links inversely proportional to their respective physical rates. This implies that links with higher physical rates should get smaller amount of communication time. The same proof for Lemma 5.1 can be used for Lemma 5.2 as well.

For 2-hop case, $R_{max}^{HD} = \frac{R_1 R_2}{R_1+R_2}$ with optimal τ values calculated as, $\tau_1^* = \frac{R_2}{R_1+R_2}$ and $\tau_2^* = \frac{R_1}{R_1+R_2}$. For 3-hop communication case, maximum end-to-end throughput is given by $R_{max}^{HD} = \frac{R_1 R_2 R_3}{R_1 R_2 + R_1 R_3 + R_2 R_3}$. By induction, on a N-hop route, after optimally distributing τ_is among the links, maximum end-to-end throughput is calculated as

$$R_{max}^{HD} = \frac{\prod_{i=2}^{N} R_{i-1,i}}{\sum_{i=2}^{N} \prod_{\substack{j=2 \\ j \neq i}}^{N} R_{i-1,i}} \tag{5.26}$$

5.4.2 FD Achievable Rates

When the intermediate relays are FD, they transmit simultaneously, while receiving. Since we assume full-interference model, each node, in addition to SI, is subject to inter node interference because of transmission of other nodes. In this case, the achievable rate between two FD nodes $(i-1)$ and i is given by

$$R_{i-1,i} = log\left(1 + \frac{K_{i-1,i} P_{i-1}}{\sigma^2 + \beta P_i + \sum\limits_{\substack{j=1 \\ j \neq i, j \neq i-1,}}^{N-1} K_{j,i} P_j}\right). \tag{5.27}$$

Note that term $\sum_{\substack{j=1 \\ j\neq i, j\neq i-1,}}^{N-1} K_{j,i}P_j$ is the total amount of interference at node i induced by other transmitting nodes. We assume that each node suffers from AWGN with same variance, σ^2. Thus, the end-to-end throughput is obtained from the following optimization problem:

$$\begin{aligned} &\underset{P_i,\forall i\in\{1\ldots,N-1\}}{\text{maximize}} && min\left\{R_{1,2}, R_{2,3}, \ldots R_{N-1,N}\right\} \\ &\text{subject to} && P_i \leq P_{max}, \forall i \in \{1\ \ldots, N-1\}\,. \end{aligned} \tag{5.28}$$

Although the problem of optimal transmission power assignment for FD node in multihop networks has been attempted in the literature as in [46], a complete solution for the full-interference model does not exist, to the best of our knowledge. In [59], the same problem has been approached by formulating the optimization problem given in (5.28), considering outage probabilities as the constraints. In [46], Ramirez et al consider a simplified model to come up with a solution to the problem, where they only consider self and one-hop interference from neighboring nodes. It is shown for this simplified interference model that, in order to maximize the end-to-end throughput, all the link rates (hence equivalently SNRs) should be equal and at least one of the nodes should transmit at its maximum power. They propose a recursive procedure, in which rate of the last link in the network forms a base solution for the recursion.

Their proposed solution can be briefly formulated as follows: Assume that SNR of the each node is equal to w. Considering SNR at destination node, we get $w = \frac{K_{N-1,N}P_{N-1}}{\sigma^2}$ or $P_{N-1} = \frac{w\sigma^2}{K_{N-1,N}}$ as the base to the recursion. The power of node i in the network is given by

$$P_i = \frac{w\left(\sigma^2 + \beta P_{i+1} + K_{i+2,i+1}P_{i+2}\right)}{K_{i,i+1}} \tag{5.29}$$

As seen from equation (5.29), transmission power of node i is a function of P_{i+1} and P_{i+2} owing to self- and one hop interference. Using (5.29), polynomial expressions as a function of w for each P_i is derived. Then each P_i is individually considered

to be equal to P_{max} and maximum real root of the polynomial is found for each P_i. This is repeated for every $P_i = P_{max}$ and minimum of these maximum real roots are picked as the maximum SNR. As the final stage of the procedure, calculated w values are plugged into equation (5.29) and optimal transmission power for each node is individually calculated.

Simplified interference model (one hop interference) based solution is applied into networks with full-interference model in [46], and it is shown that as the network size increases the gap between the optimal solution and the solution obtained from the simplified model tends to converge to a constant.

In our work, we develop a complete solution for the optimal power policy, considering the full-interference model. We start with a two hop network of three nodes, then grow the network size to four, finally we provide a generic solution for the networks of any size with full-interference model.

Two Hop Network: In the case of two hop scenario, optimization problem given in (5.28) becomes as follows

$$\begin{aligned} \underset{P_1,P_2}{\text{maximize}} \quad & min\left\{log\left(1+\frac{P_1K_{1,2}}{\sigma^2+\beta P_2}\right), log\left(1+\frac{P_2K_{2,3}}{\sigma^2+P_1K_{1,3}}\right)\right\} \\ \text{subject to} \quad & P_1 \leq P_{max} \\ & P_2 \leq P_{max}. \end{aligned} \tag{5.30}$$

Objective function of (5.30) is nonlinear because of both logarithmic expressions and minimum operation. To make it linear, we define $z = \min\{R_{1,2}, R_{2,3}\}$ and carry the objective function to the constraints, and hence get rid of minimum operation. Note that there are only two possibilities in this case: 1) $z = log\left(1+\frac{P_1K_{1,2}}{\sigma^2+\beta P_2}\right)$ and $z \leq log\left(1+\frac{P_2K_{2,3}}{\sigma^2+P_1K_{1,3}}\right)$, 2) $z \leq log\left(1+\frac{P_1K_{1,2}}{\sigma^2+\beta P_2}\right)$ and

$z = log\left(1 + \frac{P_2 K_{2,3}}{\sigma^2 + P_1 K_{1,3}}\right)$. Therefore, we can divide the problem into two subproblems, where all the constraints are linear with respect to P_1 and P_2, as follows

$$\begin{aligned} \underset{P_1,P_2}{\text{maximize}} \quad & z_1 \\ \text{subject to} \quad & -K_{1,2}P_1 + \beta(2^{z_1} - 1)P_2 = (1 - 2^{z_1})\sigma^2 \\ & P_1 K_{1,3}(2^{z_1} - 1) - P_2 K_{2,3} \leq (1 - 2^{z_1})\sigma^2 \\ & P_1 \leq P_{max} \\ & P_2 \leq P_{max}. \end{aligned} \tag{5.31}$$

$$\begin{aligned} \underset{P_1,P_2}{\text{maximize}} \quad & z_2 \\ \text{subject to} \quad & -K_{1,2}P_1 + \beta(2^{z_2} - 1)P_2 \leq (1 - 2^{z_2})\sigma^2 \\ & P_1 K_{1,3}(2^{z_2} - 1) - P_2 K_{2,3} = (1 - 2^{z_2})\sigma^2 \\ & P_1 \leq P_{max} \\ & P_2 \leq P_{max}. \end{aligned} \tag{5.32}$$

The maximum end-to-end throughput from node 1 to 3 is the maximum of z_1 and z_2,

$$R_{1,3} = max\left\{z_1, z_2\right\}. \tag{5.33}$$

Three Hop Network: In the case of three hop scenario, we revisit (5.28) and linearize the problem by defining $z = \min\left\{R_{1,2}, R_{2,3}, R_{3,4}\right\}$, which also implies that there exists only 3 possibilities: 1)$z = R_{1,2}$, $z \leq R_{2,3}$ and $z \leq R_{3,4}$ 2)$z \leq R_{1,2}$, $z = R_{2,3}$ and $z \leq R_{3,4}$ 3) $z \leq R_{1,2}$, $z \leq R_{2,3}$ and $z = R_{3,4}$. This leads us to divide the problem into three subproblems as follows

$$
\begin{aligned}
\underset{P_1,P_2,P_3}{\text{maximize}} \quad & z_1 \\
\text{subject to} \quad & -K_{1,2}P_1 + \beta(2^{z_1}-1)P_2 + K_{3,2}(2^{z_1}-1)P_3 = (1-2^{z_1})\sigma^2 \\
& K_{1,3}(2^{z_1}-1)P_1 - K_{2,3}P_2 + \beta(2^{z_3}-1)P_3 \leq (1-2^{z_1})\sigma^2 \\
& K_{1,4}(2^{z_1}-1)P_1 + (2^{z_1}-1)P_2K_{2,4} - K_{3,4}P_3 \leq (1-2^{z_1})\sigma^2 \\
& P_1 \leq P_{max} \\
& P_2 \leq P_{max} \\
& P_3 \leq P_{max}.
\end{aligned} \tag{5.34}
$$

$$
\begin{aligned}
\underset{P_1,P_2,P_3}{\text{maximize}} \quad & z_2 \\
\text{subject to} \quad & -K_{1,2}P_1 + \beta(2^{z_2}-1)P_2 + K_{3,2}(2^{z_2}-1)P_3 \leq (1-2^{z_2})\sigma^2 \\
& K_{1,3}(2^{z_2}-1)P_1 - K_{2,3}P_2 + \beta(2^{z_3}-1)P_3 = (1-2^{z_2})\sigma^2 \\
& K_{1,4}(2^{z_2}-1)P_1 + (2^{z_2}-1)P_2K_{2,4} - K_{3,4}P_3 \leq (1-2^{z_2})\sigma^2 \\
& P_1 \leq P_{max} \\
& P_2 \leq P_{max} \\
& P_3 \leq P_{max}.
\end{aligned} \tag{5.35}
$$

$$
\begin{aligned}
\underset{P_1,P_2,P_3}{\text{maximize}} \quad & z_3 \\
\text{subject to} \quad & -K_{1,2}P_1 + \beta(2^{z_3}-1)P_2 + K_{3,2}(2^{z_3}-1)P_3 \leq (1-2^{z_3})\sigma^2 \\
& K_{1,3}(2^{z_3}-1)P_1 - K_{2,3}P_2 + \beta(2^{z_3}-1)P_3 \leq (1-2^{z_3})\sigma^2 \\
& K_{1,4}(2^{z_3}-1)P_1 + (2^{z_3}-1)P_2K_{2,4} - K_{3,4}P_3 = (1-2^{z_3})\sigma^2 \\
& P_1 \leq P_{max} \\
& P_2 \leq P_{max} \\
& P_3 \leq P_{max}.
\end{aligned} \tag{5.36}
$$

Note here also that all the constraints of the maximization problem are linear with respect to P_1, P_2 and P_3. The maximum end-to-end throughput from node 1 to 4 is the maximum of z_1, z_2 and z_3:

$$R_{1,4} = max\left\{z_1, z_2, z_3\right\}. \tag{5.37}$$

To find the z_i values, we increase z_i until the constraints are no longer satisfied and pick the maximum z_i as the solution. In the numerical experiments, we have observed that optimal z_i values found turn out to be equal to each other, implying that solutions are all on the boundary, which also agree with Lemma 5.1. Therefore, we conclude that, as in the case of one way two hop relaying, all of the link rates on a given path should be equal in the multihop communication scenario.

Network of any size: Now, we can generalize the problem to the network with any size, N. In this case, our objective function will be $z = \min\left\{R_{1,2}, \ldots, R_{N-1,N}\right\}$. Because of rate equalization, we also know that $z = R_{1,2} = R_{2,3} = \ldots = R_{N-1,N}$. We can get rid of logarithms by employing $z = \log\left(1 + \frac{K_{i-1,i}P_{i-1}}{\sigma^2+Q_i}\right) \forall i \in \{2 \ldots N\}$, where Q_i denotes the total amount of inter node interference on the i^{th} node induced by other nodes in the network. Let us assume that all the nodes have the same SI cancellation capability with SI cancellation parameter β. Then, the total interference including SI at the i^{th} node is given by

$$Q_i = \sum_{\substack{j=1 \\ j\neq i-1}}^{N-1} K_{j,i}P_j, \forall i \in \{2, \ldots, N\} \tag{5.38}$$

Note that $K_{i,i}$ denotes the SI cancellation parameter for node i, which is assumed to equal to β ($K_{i,i} = \beta, \forall i \in \{2, \ldots, N\}$). Hence, the rate of the link between nodes $(i-1)$ and i, $R_{i-1,i}$ is given by

$$R_{i-1,i} = \log\left(\frac{K_{i-1,i}P_{i-1}}{\sigma^2 + Q_i}\right) \forall i \in \{2, \ldots, N\} \tag{5.39}$$

Letting $z = R_{i-1,i}, \forall i \in \{2, \ldots, N\}$, we get

$$(2^z - 1)Q_i - K_{i-1,i}P_{i-1} \leq (1 - 2^z)\sigma^2, \forall i \in \{2, \ldots, N\} \tag{5.40}$$

Expanding interference term as in 5.38, we obtain

$$(2^z - 1)\left(\sum_{\substack{j=1 \\ j\neq i}}^{N-1} K_{j,i}P_j\right) - K_{i-1,i}P_{i-1} = (1 - 2^z)\sigma^2, \forall i \in \{2, \ldots, N\} \tag{5.41}$$

The optimization problem given in (5.28) can be rewritten in the form of matrix as follows

maximize z

subject to

$$\begin{bmatrix} -K_{1,2} & K_{2,2}(2^z-1) & K_{3,2}(2^z-1) & \cdots & K_{N-1,2}(2^z-1) \\ K_{1,3}(2^z-1) & -K_{2,3} & K_{3,3}(2^z-1) & \cdots & K_{N-1,3}(2^z-1) \\ K_{1,4}(2^z-1) & K_{2,4}(2^z-1) & -K_{3,4} & \cdots & K_{N-1,4}(2^z-1) \\ \vdots & \vdots & \vdots & \vdots & \vdots \\ K_{1,N}(2^z-1) & K_{2,N}(2^z-1) & K_{3,N}(2^z-1) & \cdots & -K_{N-1,N} \end{bmatrix} \begin{bmatrix} P_1 \\ P_2 \\ P_3 \\ \vdots \\ P_{N-1} \end{bmatrix} = \begin{bmatrix} \sigma^2(2^z-1) \\ \sigma^2(2^z-1) \\ \sigma^2(2^z-1) \\ \vdots \\ \sigma^2(2^z-1) \end{bmatrix}$$

$$\begin{bmatrix} P_1 \\ P_2 \\ P_3 \\ \vdots \\ P_{N-1} \end{bmatrix} \leq \begin{bmatrix} P_{1max} \\ P_{2max} \\ P_{3max} \\ \vdots \\ P_{N-1max} \end{bmatrix}$$

Note that, optimization problem (5.28) given in matrix form becomes completely linear and linear programming (LP) tools can be utilized to solve it. In order to find a solution to this problem, we employ a binary search algorithm, where we increase the value of z starting from 0 until the constraints do not provide a feasible region any more. We define the limits for the search interval as: $z \in [0, u]$ where u is defined as

$$u = \min\left\{\log\left(1 + \frac{P_{max}K_{1,2}}{\sigma^2}\right), \ldots, \log\left(1 + \frac{P_{max}K_{N-1,N}}{\sigma^2}\right)\right\}. \tag{5.42}$$

Initially, current lower limit of of the interval,a is set to zero ($a = 0$) and upper limit, b is set to u ($b = u$). The search procedure starts from the middle of the interval, i.e. from $z = \frac{a+b}{2}$, then the constraints are checked with the newly updated z value. If there is a feasible region of powers, obtained by the constraints, current lower limit of the interval is updated to z. If not, the current upper limit of the interval is updated to z. In the next iteration, z is set to middle of current interval. Therefore, during the execution of the algorithm z is shifted to the right as long as constraints form a non-empty feasible region. Conversely, z is shifted to the left if the feasible region is an empty set. Note that constraints form a linear systems of equations. In each iteration, the algorithm checks feasibility with the newly assigned z value. For feasibility check, we use linear programming tools. Once the length of current interval, denoted by $L = |b - a|$ goes down below a certain tolerance, ϵ, the algorithm terminates.

Input: Channel coefficients, P_{max}, σ^2, ϵ
Output: R_{max}^{FD}
for $i = 1$ ***to*** $N - 1$ **do**
  $R(i) = \log\left(1 + \frac{P_{max} K_{i,i+1}}{\sigma^2}\right)$
end
$a = 0$;
$b = \min\{R\}$;
$z = \frac{b}{2}$;
while *1* **do**
  if *feasible region is non-empty* **then**
    $a = z$;
  else
    $b = z$;
  end
  $z = a + \frac{b-a}{2}$;
  $L = |a - b|$;
  if $L \leq \epsilon$ *and feasible region is non-empty* **then**
    break ;
  end
end
$R_{max}^{FD} = z$;

Algorithm 2: Pseudo Code of the Search Algorithm

Although the search procedure is known to always converge, how many steps it takes for algorithm to converge to a solution is determined by the initial length of

the interval and ϵ. Since power can be continuously adjusted, a power assignment solution that will equalize the link rates does exist. Therefore, search procedure always converges to a solution within a given resolution. The pseudo code of the proposed search algorithm is given in Algorithm 2.

5.4.3 Numerical Results

In this section, we compare the performance of HD transmission, direct transmission, FD transmission suggested in [46] and our proposed FD transmission strategy for multihop communications in linear network topologies with full-interference, considering different system parameters. In our experiments, we consider a hybrid transmission strategy as in [60], which takes advantage of FD capability, in an attempt to reduce severity of the inter node interference. In this strategy, the network is divided into many source-relay-destination subnetworks with a FD functioning relay between source and destination. These subnetworks become active, taking turn and hence operating at different time slots, basically applying TDMA. This strategy requires some nodes to be able to perform HD and some to have FD capability. Therefore, we will call it "Hybrid" strategy. For our experiments, system parameters are assigned as follows (unless otherwise stated in figure captions):

TABLE 5.1: System parameters

$P_{max} = 0dBm$	Maximum transmission power per node
$N = 20$	Number of nodes in the network
$d = 250m$	Source-destination separation
$\alpha = 4$	Path loss exponent of the environment
$\beta = -80dB$	SI suppression

First of all, we validate the accuracy of the proposed power allocation solution with the closed form analytical expressions we have derived in Section 5.3 for two hop communication scenarios. As apparently seen from Figure 5.7, the achievable rates obtained by the analytical expressions (optimal solution described in Algorithm 1) and our proposed transmission power policy, described in Algorithm 2

perfectly overlaps, revealing that our proposed power allocation scheme computes the optimal solution for transmission powers.

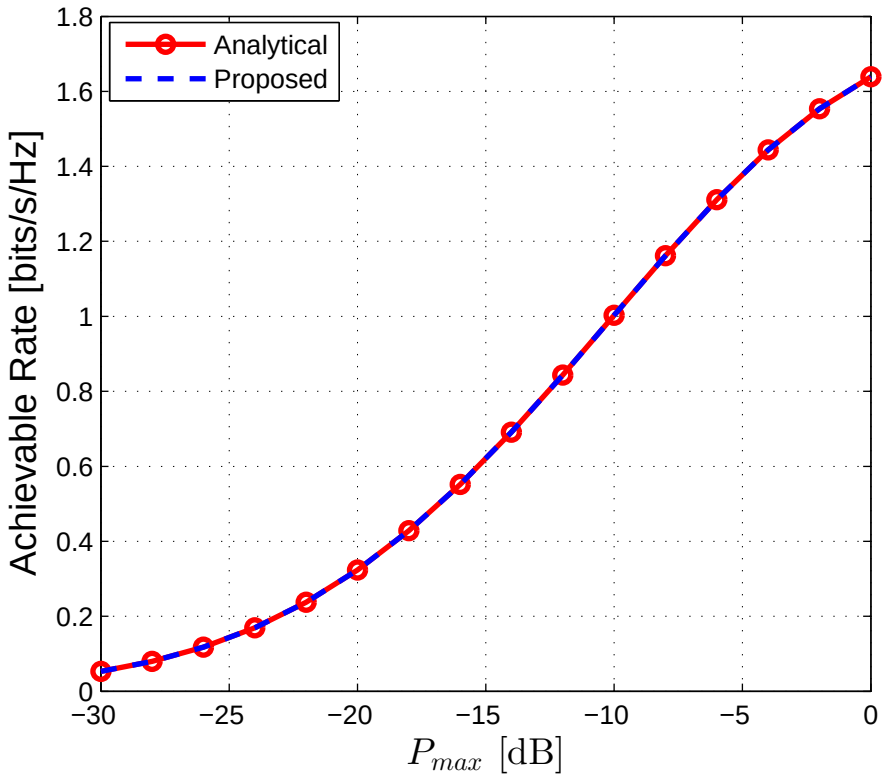

FIGURE 5.7: End-to-end throughput with respect P_{max}, $N = 3, \alpha = 4, d = 250m, \beta = 10^{-8}$

Figure 5.8 shows the end-to-end throughput with respect to the number of nodes in the network. As apparently seen from the figure, our proposed FD transmission shows the best performance among the other schemes. In the investigated scenario, FD gain over HD is observed to go up to 300% for large network sizes. Hybrid transmission performance is on the other hand turns out to be lower than that of Ramirez's FD, yet higher than that of HD. This scheme can be applied when all intermediate nodes cannot be FD enabled.

In Figure 5.9, we investigate the effect of maximum transmission power per node, P_{max} on the throughput performance of the network. Again, for the demonstrated range of P_{max}, our solution offers the best performance. It is worth noting that in our proposed FD and hybrid transmission strategies, the throughput never decreases with increasing P_{max}. This is because of optimal power control mechanism

applied, which considers the full-interference model. Nevertheless, this is not the case for FD transmission strategy proposed in [46] since their solution is based on the simplified (one hop interference) model.

In Figure 5.10, the throughput performances of aforementioned transmission strategies are plotted as a function of separation between source node and destination node. As in previous figure, Figure 5.10 also shows that our proposed FD solution yields the best performance among the others. In Figure 5.11, we investigate the effect of path loss exponent, α on the throughput. Figure 5.11 indicates that our proposed FD exhibits a better performance than FD solution proposed in [46] for all α values. Remark also that both FD transmission strategies offer a better throughput performance for greater α values. This can be illustrated by the inter node interference diminishing with the increasing path loss attenuation.

End-to-end throughput is plotted in Figure 5.12 (a) and (b) as a function of SI cancellation parameter, β for low and high transmission power levels, respectively. It is obvious that all the FD performances ameliorate with a stronger SI suppression. However, the achievable rate does not change after a certain level of SI in both figures. In Figure 5.12 (a), our proposed FD transmission almost triples the HD performance, while in Figure 5.12 (b), we observe that our proposed FD achieves a more than %80 throughput improvement over HD. Note also that, again our proposed FD solution always works better than FD solution suggested in [46].

In a nutshell, we have investigated the performance of different FD transmission strategies in different test scenarios, considering several system parameters and compare them with traditional HD transmission strategies. Our extensive investigation on these parameters has shown that, proposed transmission power policy yields the optimal transmission power levels, producing the best end-to-end throughput performance in linear network topologies among the other evaluated transmission strategies in the case of good SI suppression. We have also observed that FD gain over HD is highly dependent on these parameters. In the investigated test scenario, it has been noted that under $80dB$ cancellation, FD gain over HD

reaches up to %300 as the network size grows. We have also observed that $60dB$ cancellation is quite efficient suppression to maintain a successful FD operation.

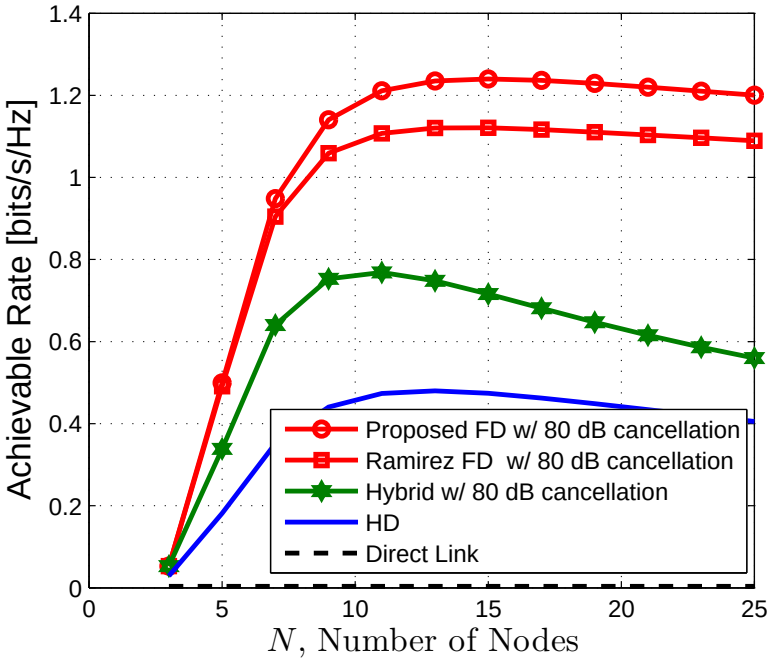

FIGURE 5.8: End-to-end throughput with respect to node density, $P_{max} = 0dBm, \alpha = 4, d = 250m, \beta = -80dB$

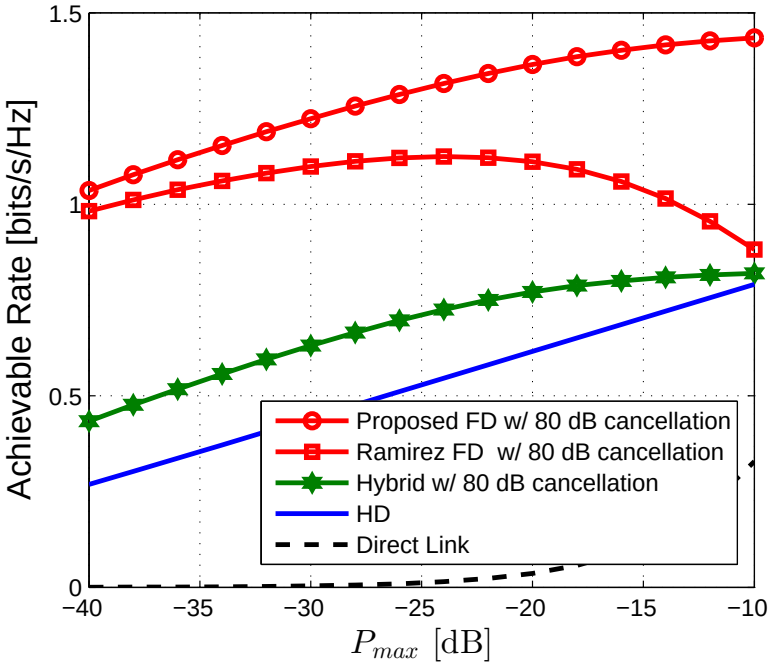

FIGURE 5.9: End-to-end throughput with respect to P_{max}, P_{max}, $N = 20, d = 250m, \alpha = 4, d = 250m, \beta = -80dB$

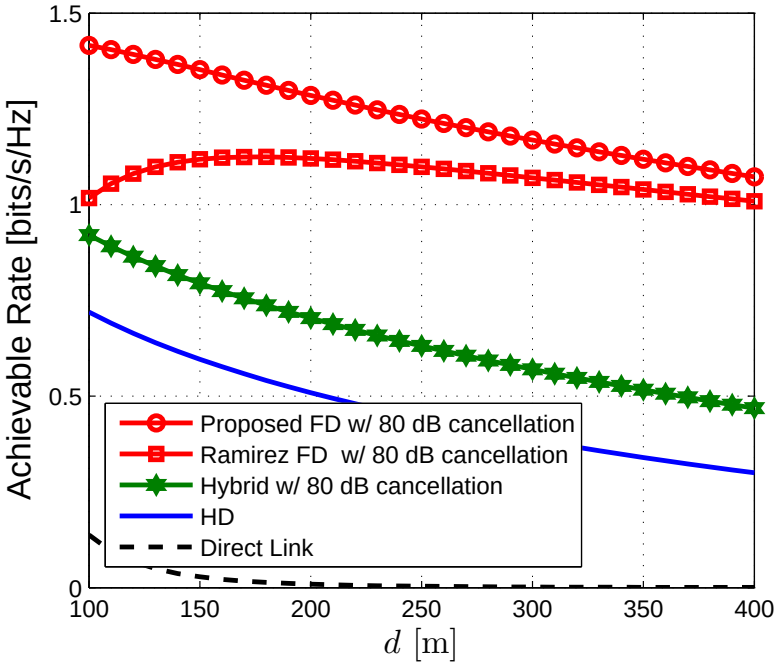

FIGURE 5.10: End-to-end throughput with respect to side length of the square region, d, $P_{max} = 0dBm, N = 20, \alpha = 4, \beta = -80dB$

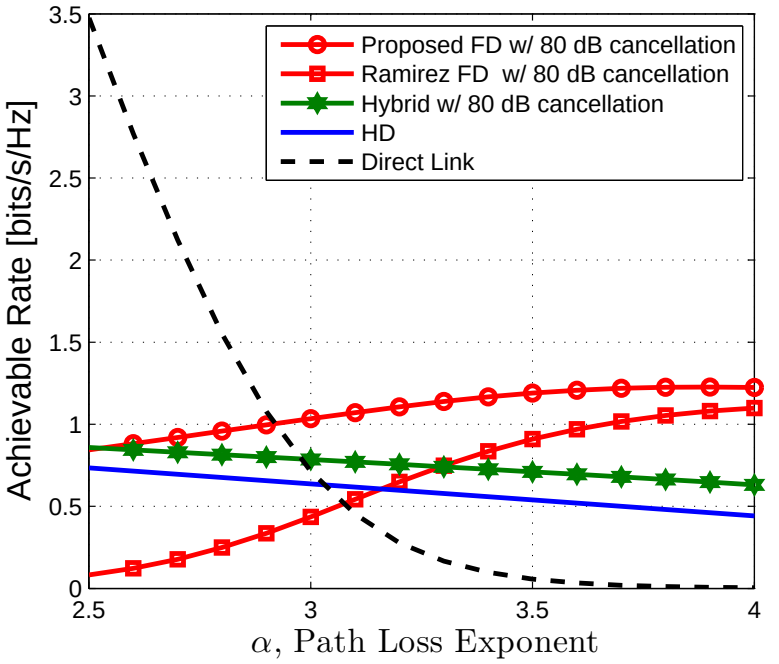

FIGURE 5.11: End-to-end throughput with respect to path loss exponent α, $P_{max} = 0dBm, N = 20, d = 250m, \beta = -80dB$

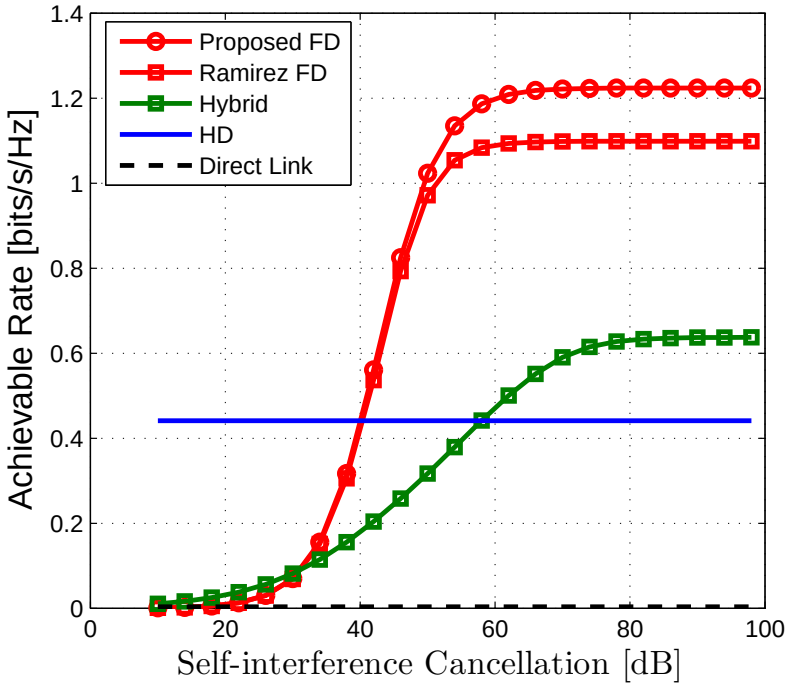

(a)

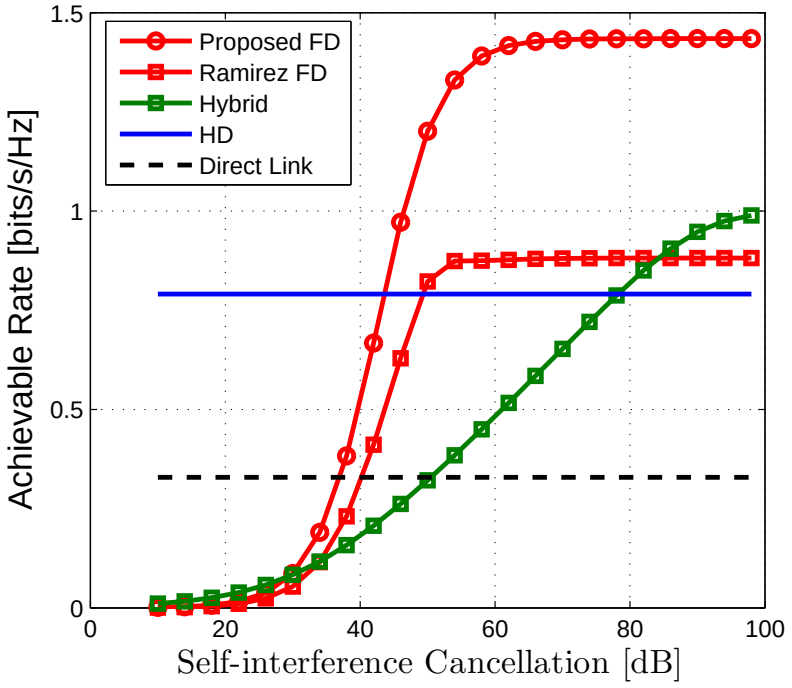

(b)

FIGURE 5.12: End-to-end throughput with respect to SI suppresion level, $\beta, N = 20, \alpha = 4, d = 250m$ (a) $P_{max} = 0dBm$ (Low power) (b) $P_{max} = 20dBm$ (High power)

5.5 Joint Routing & Power Control

In section 5.4, we mainly focused on the transmission power control mechanism which maximizes end-to-end throughput of a FD (linear) network. In this section, we will incorporate our power assignment solution with routing so as to determine the best path yielding the highest throughput between the source and destination nodes in a given network.

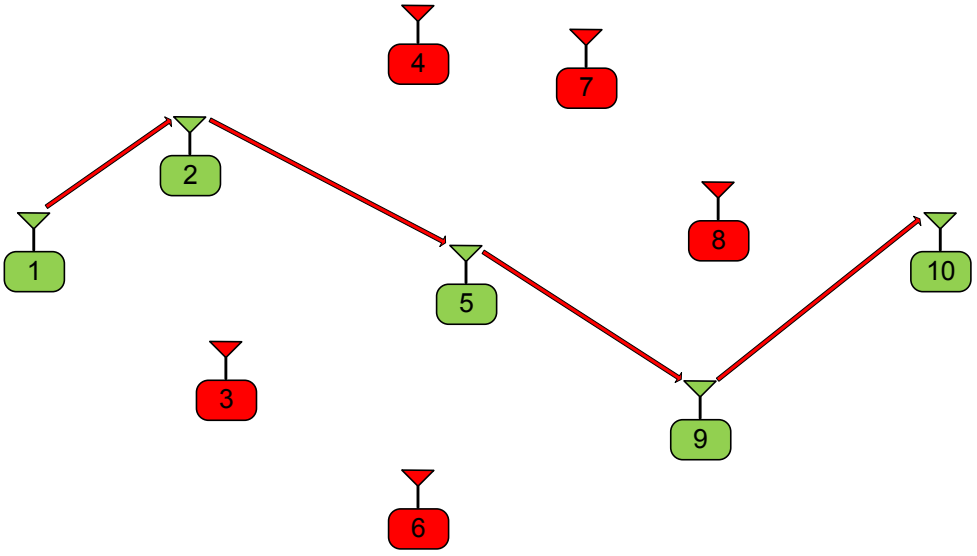

FIGURE 5.13: An example path

Consider a network, as shown in Figure 5.13, where source node 1 forwards its data via the intermediate relays with decode-and-forward protocol to destination node 10. For streaming packets from the source node to the destination node, the data flow can take place over candidate paths. Note that, in this network, several possible candidate paths connecting source and destination nodes exist. An example path is shown in Figure 5.13, where transmitting nodes are colored in green, while the idle nodes are colored in red.

Our aim is to find the best path with the highest end-to-end throughput between source and destination nodes. Clearly, routing for HD and FD forwarding of packets emerge into different optimization problems, as will be studied in the sequel.

5.5.1 HD Achievable Rates

In a network consisting of HD relay nodes, the connection between source and destination node is to be established over the optimal link producing the highest throughput, while sharing the channel via TDMA since only one relay can transmit at a time. All the other relays that are not included in the selected path remain idle all throughout the communication as we consider a single flow. On the selected path, transmission from the source node to the destination node is carried out as described in Section 5.4. In order to determine the optimal path, all possible candidate paths should be considered, with optimum time assignment. However, since this requires all the candidate routes to be visited, it is computationally costly and computation time grows drastically as the network size grows. For this reason, we consider two different routing schemes for HD communication that are not optimal but quite efficient in terms of computational performance.

Basic Routing Algorithm

This routing algorithm is quite similar to Dijkstra's shortest path algorithm except for its objective function. In Dijkstra's shortest path algorithm, the objective is to find the shortest path between two node in a network, while here the objective is to find the path with the highest throughput. In conventional Dijkstra's algorithm, the costs are the arc lengths (distances) and the objective function is the summation of the link costs, whereas in the considered problem, link rates are the costs and objective function is the minimum of the link rates. For a detailed knowledge on Dijkstra's shortest path algorithm, see [61].

Assuming that all nodes transmit with maximum power without interfering each other, and that they are subject to same amount of noise with power σ^2, the rate of a link between two arbitrary nodes i and j can be obtained as follows

$$R_{i,j} = \log\left(1 + \frac{P_{max}K_{i,j}}{\sigma^2}\right) \forall i, j \in \{1, \ldots, N\}\,. \tag{5.43}$$

These link rates are given as input to Dijkstra's algorithm, and they are utilized as the metric for routing, so as to find the path with the highest end-to-end rate, as described by the pseudo code provided in Algorithm 3.

Calculate $R_{i,j} \forall i, j \in \{1, \ldots, N\}$ via (5.43)
$S = \emptyset, \overline{S} = \{1, \ldots, N\}$;
$C(1) = \infty, \mathbf{P}(1) = 0$;
$C(i) = 0, \forall i \in \{2, \ldots, N\}$;
while $N \in \overline{S}$ **do**
  Let $i \in \overline{S}$ be a node for which $C(i) = \max\left\{C(j), \forall j \in \overline{S}\right\}$;
  $S = S \cup \{i\}$;
  $\overline{S} = \overline{S} - \{i\}$ **for** $j \in A(i)$ **do**
    if $C(j) < \min\{C(i), R_{i,j}\}$ **then**
      $C(j) = \min\{C(i), R_{i,j}\}$;
      $\mathbf{P}(j) = i$;
    end
  end
end

Algorithm 3: Basic Routing Algorithm without Time Allocation

Algorithm 3 returns a path through which source and destination nodes can communicate with. The algorithm executes as follows: two sets S and $\overline{S}$ are created. At the initialization step, S is set to be empty while $\overline{S}$ is set to include all the nodes in the network. The source node is labeled by a cost of ∞ and rest is assigned to 0 cost. The predecessors of the source node is set to 0. Next, a node, say node i in $\overline{S}$ with the largest cost is selected, added into S, being subtracted from $\overline{S}$. Next, the costs of all neighbors, $C(j)$ of this node (Note that $j \in A(i)$, where A(i) denotes the set of neighbors of node i) is updated, and node i becomes predecessor of the neighbor nodes of this node, if necessary. This procedure is repeated until destination node is included in the set, S. The returned path can be traced by predecessors vector, $\mathbf{P}$.

Basic Routing Algorithm with Time Allocation:

Note that in the previous algorithm, time allocation is not considered in selecting the node to be added into unvisited set, $\overline{S}$. In this routing algorithm, how we choose the next node to be included in $\overline{S}$ is different as the routing metric is modified to incorporate time allocations. Specifically, if the currently selected node is i and its adjacent node is $j \in A(i)$, label of node j, $C(j)$ is updated as $C(j) = \frac{C(i)R_{i,j}}{C(j)+R_{i,j}}$ as in (5.26), given that $\frac{C(i)R_{i,j}}{C(j)+R_{i,j}}$ is greater than present label of node j. Recall that in basic routing algorithm in Algorithm 3, label of node $j \in A(i)$ is updated to $\min\{C(i), R_{i,j}\}$. Basic routing algorithm with time allocation is given in Algorithm 4.

Calculate $R_{i,j} \forall i, j \in \{1, \ldots, N\}$ via (5.43);
$S = \emptyset, \overline{S} = \{1, \ldots, N\}$;
$C(1) = \infty, \mathbf{P}(1) = 0$;
$C(i) = 0, \forall i \in \{2, \ldots, N\}$;
while $N \in \overline{S}$ **do**
  Let $i \in \overline{S}$ be a node for which $C(i) = \max\{C(j), \forall j \in \overline{S}\}$;
  $S = S \cup \{i\}$;
  $\overline{S} = \overline{S} - \{i\}$;
  for $j \in A(i)$ **do**
    if $C(j) < \dfrac{C(i)R_{i,j}}{C(j)+R_{i,j}}$ **then**
      $C(j) = \dfrac{C(i)R_{i,j}}{C(j)+R_{i,j}}$;
      $\mathbf{P}(j) = i$;
    end
  end
end

Algorithm 4: Basic Routing Algorithm with Time Allocation

After termination, the routing algorithm returns a predecessors vector, $\mathbf{P}$ as the output. By tracing $\mathbf{P}$, the best path returned by the algorithm can be formed. After routing algorithm terminate, based on optimal time assignment solution

given in Algorithm 5.26, total communication time is divided between links on the selected path optimally.

5.5.2 FD Achievable Rates

We consider a network with FD nodes, where a source node is streaming packets to the destination node via FD enabled intermediate nodes. Our purpose is to 1) find the best route which produces the highest end-to-end throughput from the source node to the destination node and 2) find the optimal transmission power of the nodes on this path. These two problems should be jointly handled. Since label of permanently labeled nodes is changed due to addition of a new node on the path, the optimal path that gives the highest throughput cannot be found by label correcting algorithms such as Dijkstra's algorithm. Due to the complexity of the joint problem, the optimal path could be found, by only exhaustive search, however, this solution would be computationally costly and inefficient except for small size networks, since all candidate paths have to be considered.

We compare the performance of the following FD routing solutions:

1) Basic routing, where Algorithm 3 is used for routing and our proposed power control scheme from Algorithm 2 is applied on the determined path. This solution is referred to as $Solution1$.

2) Routing and power control proposed by Ramirez and et al in [46], where only one hop interference is considered. This scheme is referred to as $Solution2$.

3) Proposed routing algorithm in Algorithm 5 is combined with proposed power control algorithm, Algorithm 2, both of which consider full interference scenario. This scheme is named as $Solution3$.

Pseudo code of the routing solution we propose is given in Algorithm 5. This routing scheme differs from routing Algorithm 3 in updating the metric, i.e. label of nodes. Here $C(j)', j \in A(i)$ denotes the throughput of the link extending to node j from source and also passing through node i and it is calculated based on

the proposed transmission power policy given in Algorithm 2. What is basically different in this routing algorithm is that it neither assumes no interference nor one hop interference, when updating the label of the adjacent nodes. An example case showing how updating is done is given in Figure 5.14: Assume that, at an i^{th} iteration of Algorithm 5, node 5 is newly selected and included in the $\overline{S}$ and nodes 6,7 and 8 are its neighboring nodes. Assume also that predecessor nodes of node 5 to the source node have been calculated $\{1, 3, 4\}$. Algorithm 5 calculates the following rates: $R(1, 3, 4, 5, 6)$ for node 6, $R(1, 3, 4, 5, 7)$ for node 7 and $R(1, 3, 4, 5, 8)$ for node 8, where for example $R(1, 3, 4, 5, 7)$ denotes the rate of path $\{1, 3, 4, 5, 7\}$ and transmission powers of these nodes are calceulated by Algorithm 2. If these rates are larger than the current labels of the neighboring nodes $6, 7$ and 8, label of the nodes are updated to these rates, also the predecessor of the neighboring nodes is updated to 5. For example, let us assume that $R(1, 3, 4, 5, 6) > C(6)$, then $C(6)$ is updated to $R(1, 3, 4, 5, 6)$ and predecessor of node 6 is changed to 5 $(\mathbf{P}(6) = 5)$.

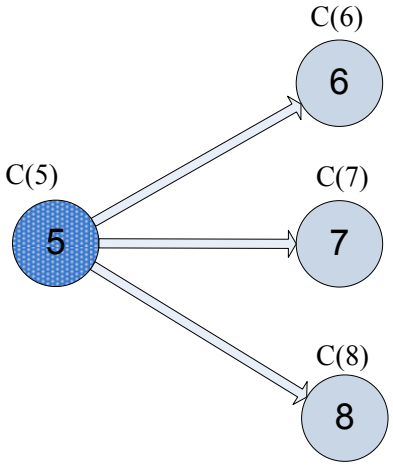

FIGURE 5.14: Label updating

Different than other routing schemes, this proposed scheme takes into account all the interfering nodes in choosing the path extension to the node i. This algorithm returns the predecessor of selected nodes on the path in $\mathbf{P}$ vector, hence the best path returned by the algorithm. We explain how routing Algorithm 5 works

in Figure 5.15 and the pseudo code of the proposed FD routing scheme that considers full interference model is given in Algorithm 5 below. Once the best path is determined, optimal power levels for the nodes on this path are assigned according to our proposed Algorithm 2, which also considers the full interference model.

Input: Channel coefficients, P_{max}, σ^2

Output: Route

$S = \emptyset, \overline{S} = \{1, \ldots, N\}$;

$C(1) = \infty, \mathbf{P}(1) = 0$;

$C(i) = 0, \forall i \in \{2, \ldots, N\}$;

while $N \in \overline{S}$ **do**

  Let $i \in \overline{S}$ be a node for which $C(i) = \max\left\{C(j), \forall j \in \overline{S}\right\}$;

  $S = S \cup \{i\}$;

  $\overline{S} = \overline{S} - \{i\}$

  for $j \in A(i)$ **do**

    Calculate $C'(j)$;

    if $C(j) < C'(j)$ **then**

      $C(j) = C'(j), \mathbf{P}(j) = i$;

    end

  end

end

Algorithm 5: Proposed FD routing algorithm based on full interference model

Complexity Analysis of Algorithm 5:

The routing algorithm given in Algorithm 5 differs from Dijkstra's algorithm in updating the labels of the selected nodes, i.e. a different metric is used in the proposed algorithm. Since our network model is represented by an all-linked graph, the complexity of the routing alone is $O(n^2)$. In each iteration of the routing, label of the neighboring nodes of the newly selected node, $C'(j)$ is calculated based on the binary search algorithm given in Algorithm 2. Assuming the initial length of the search interval is u, and that the algorithm terminates when the length of the current interval goes down below a certain interval length, ϵ, the number of

iterations taken is given by $n = \log\left(\frac{u}{\epsilon}\right)$. In each iteration of this binary search, feasibility of the current constraints is checked with a linear programming (LP) tool. Assuming that feasibility check is done via a basic LP algorithm such as Simplex algorithm, where computational time grows exponentially ($O(n) = 2^n$), complexity of the proposed algorithm is bounded by $O(2^n \log\left(\frac{u}{\epsilon}\right) n^2)$.

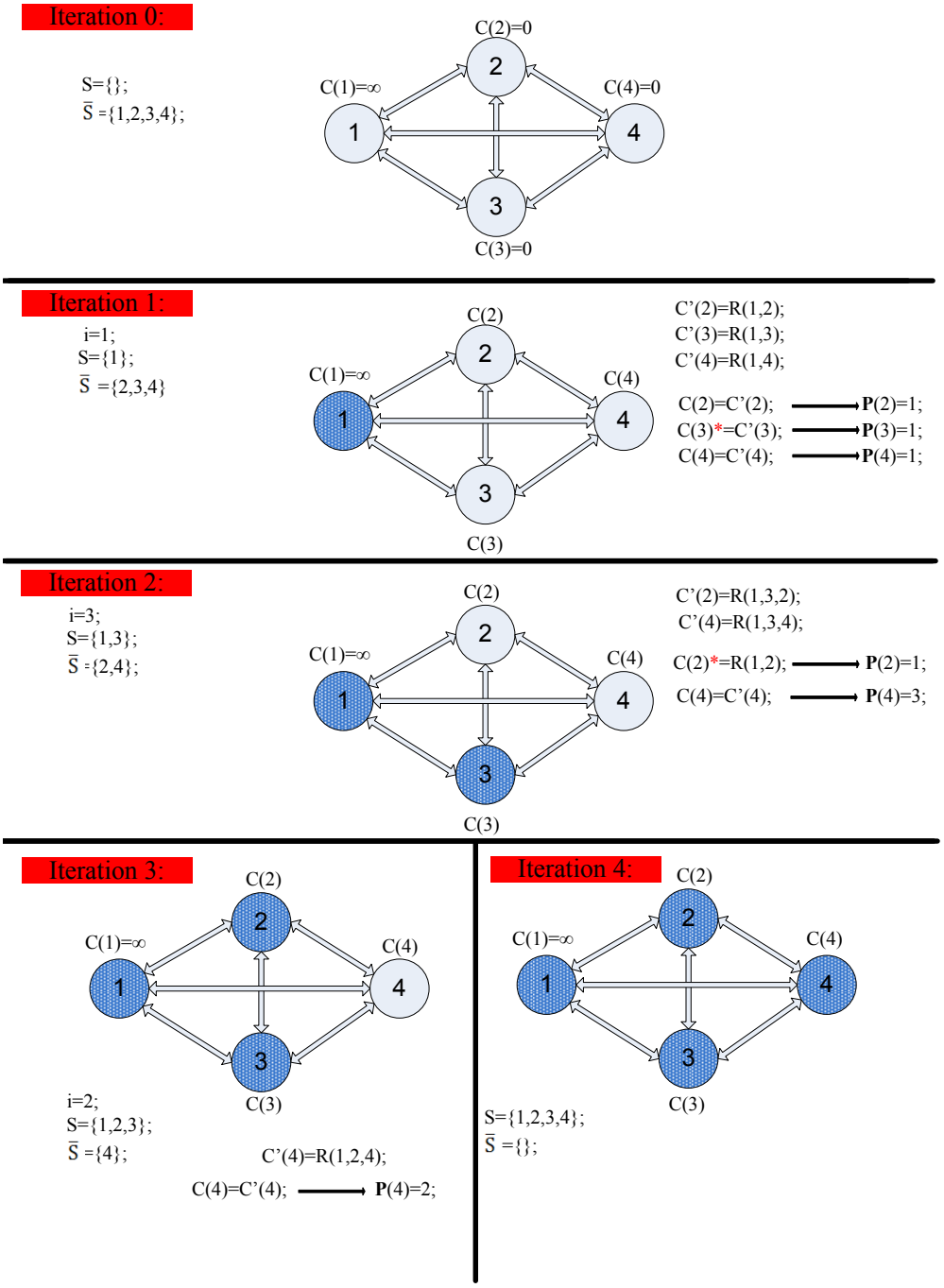

FIGURE 5.15: Execution of the proposed routing algorithm on an example network

5.5.3 Numerical Results

We dedicate this section to evaluating the performance of routing & power assignment strategies, considering several system parameters such as, maximum transmission power per node, number of the nodes, SI cancellation capability at the FD nodes, the area of the region over which nodes are strewed, path loss exponent of the environment.

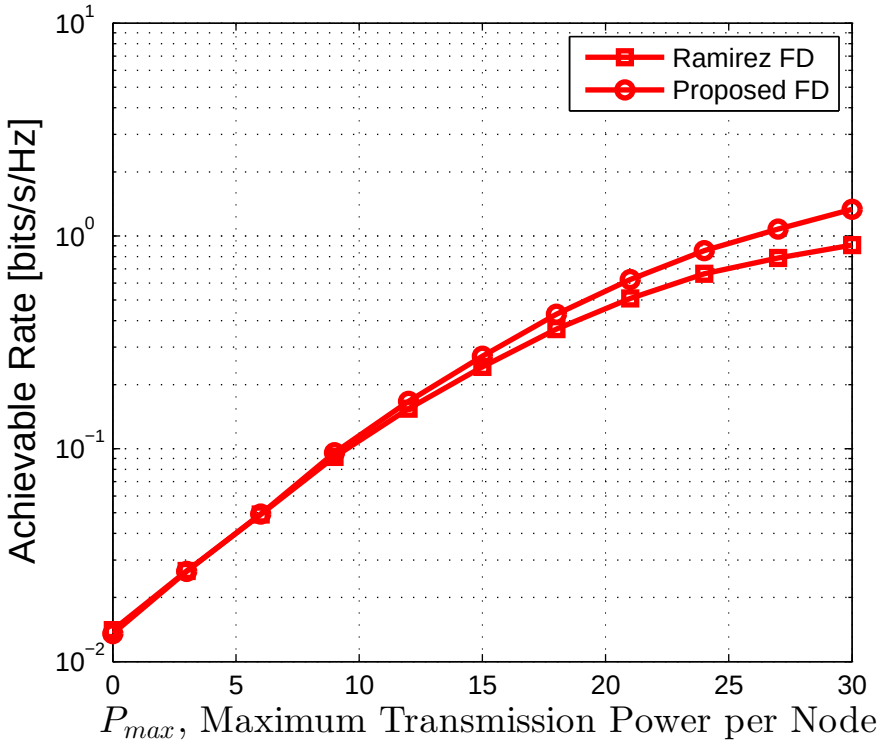

FIGURE 5.16: End-to-end throughput with respect to maximum transmission power, P_{max} $\alpha = 3, \beta = 0.01, N = 20, d = 20$

First of all, we assess the performance of Ramirez et al's proposed FD routing scheme in the test scenario investigated in their work [46] so as to ensure that we implement the power control and routing scheme proposed in [46] as accurately as it is described. In Figure 5.16, we demonstrate achievable rates offered by two strategies with respect to maximum transmission power per node. One can verify that we have obtained exactly same results as in Figure 6 of [46]. Furthermore, Figure 5.16 clearly indicates that our proposed FD routing & power control scheme produces a higher throughput in this test scenario.

For our simulations, we would rather consider a more realistic test scenario for which existing FD technologies would be more suitable in terms of SI cancellation techniques. For wide coverage, access points transmit at higher transmission power levels. From the perspective of FD implementation, transmitting with higher power obviously engenders SI signal with a greater magnitude. However, success of FD communication is substantially dependent on the SI suppression, which is quite difficult in the case of high transmission powers. As a consequence, we focus on scenarios, in which case wide coverage is not necessary, such as low power for transmissions in femto cells access points covering, only up to 10-20 meters. Additionally, the network environment is assumed be abundant of obstacles hindering the Line-Of-Side (LOS) communication and leading to a heavy path-loss attenuation. As a consequence of high path-loss attenuation introduced to the transmit signal by the environment, direct communication between source and destination node is usually not achievable and assistance of intermediate relays is required. We perform our simulations, considering a realistic test scenario with the system parameters set as listed below except for the variable that is being investigated:

TABLE 5.2: System parameters

$P_{max} = 0dBm$	Maximum transmission power per node
$N = 10$	Number of nodes in the network
$d = 100m$	Side length of the square region
$\alpha = 4$	Path loss exponent of the environment
$\beta = -80dB$	SI suppression

Simulations are performed in the following way: We first create a square region with a side length of $100m$ on a rectangular coordinate system. Then, we position source node at location (0,100) and destination node at location (100,0). Next, we randomly sprinkle the nodes, where x and y coordinate of particular node is distributed with a uniform distribution drawn from [0,100]. After the nodes are scattered, the proposed routing algorithm returns a path through which source and destination nodes communicate with, and by the proposed power control algorithm, powers of the nodes that are included in the selected path are calculated. We take 1000 realizations to take the average of the achievable end-to-end

throughput from the source node to the destination node. In order to facilitate the visualization, we provide a single realization of the positions of the nodes scattered over the square region in Figure 5.17. In this figure, source and destination nodes are labeled by numbers 1 and 10, respectively and both colored in red. Blue lines represent the wireless links between nodes. Due to the assumption that any node in the network hears others' transmission, we have an all-linked graph as the one shown in Figure 5.17.

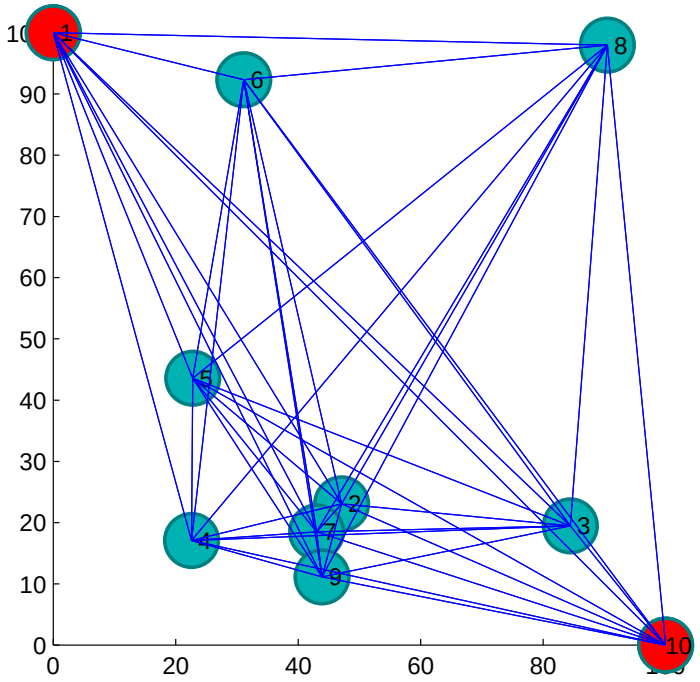

FIGURE 5.17: One realization of the nodes' positions in the square area

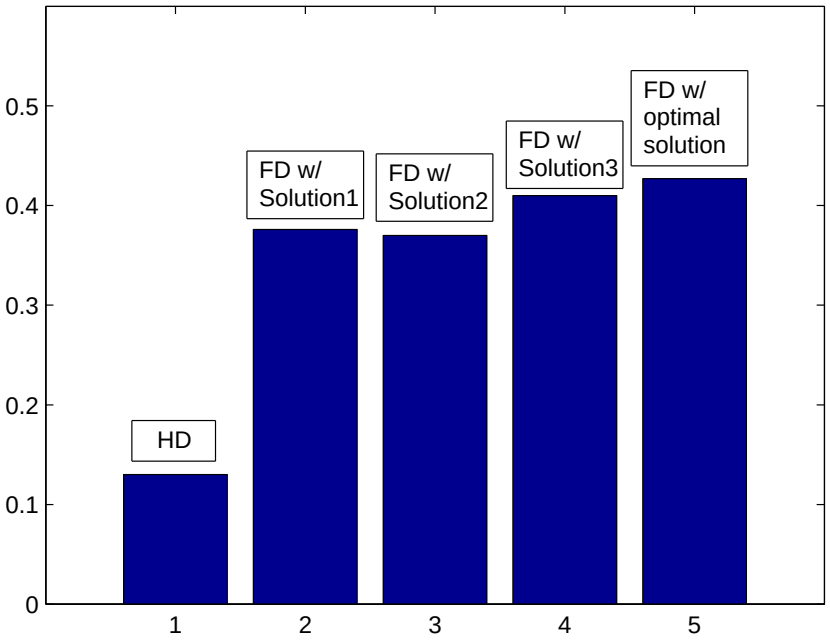

(a)

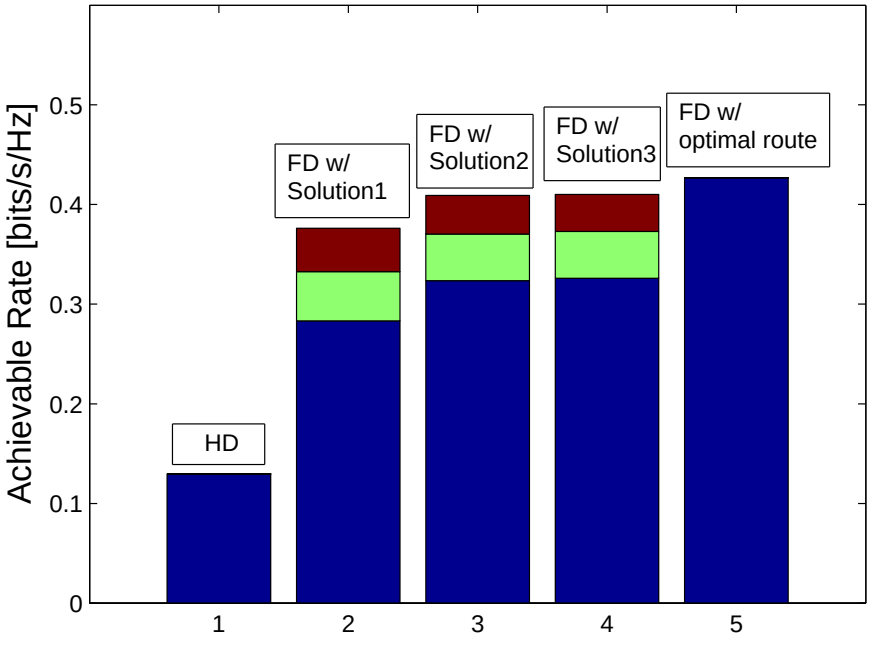

(b)

FIGURE 5.18: End-to-end throughput achieved by different transmission strategies, $N = 5, P_{max} = 0dB, \beta = -80dB, \alpha = 4$

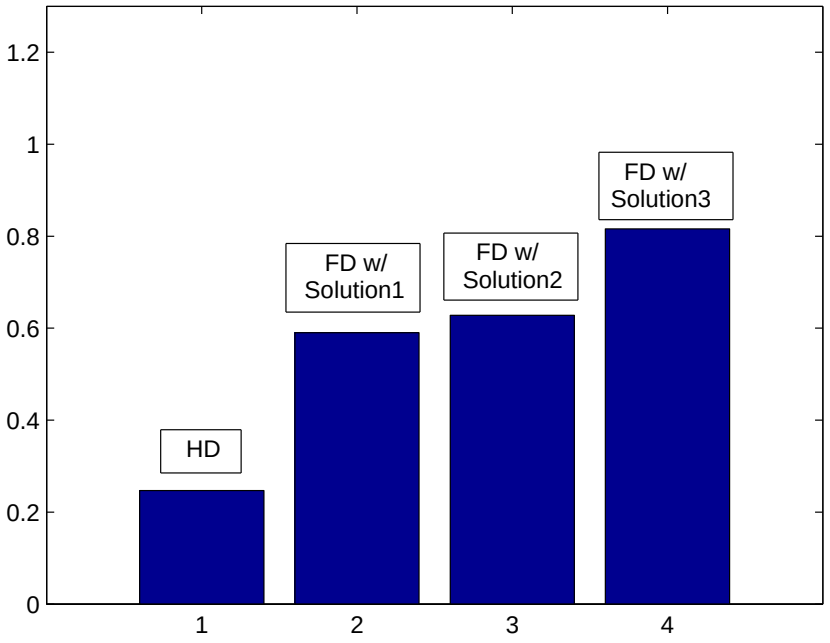

(a)

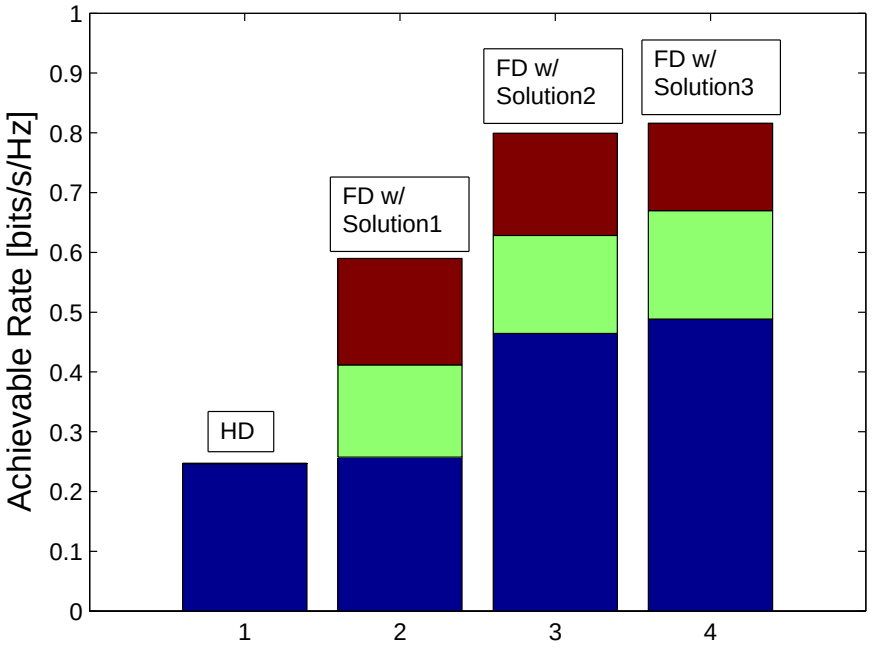

(b)

FIGURE 5.19: End-to-end throughput achieved by different transmission strategies, $N = 10, P_{max} = 0dB, \beta = -80dB, \alpha = 4$

Bar plots in Figure 5.18(a) indicates the throughput provided by HD, FD with *Solution*1, FD with *Solution*2 and FD with *Solution*3 and FD with optimal solution (optimal routing and power allocation). In Figure 5.18(b), same results are shown in a more detailed way, where bars in blue show the rate achieved by the respective routing algorithms with no power allocation scheme applied. In other words, each node transmits at P_{max}. Green bars represent the elevation in the throughput with the incorporation of transmission power allocation in [46], where only one hop interference is taken into account. Similarly, red bars indicate the improvement on the rate with the inclusion of our proposed transmission power allocation scheme. Note that Figure 5.18(a) and (b) are obtained from a scenario with $N = 5$, and shows that FD with *Solution*3 produces the highest end-to-end throughput that is also very close to the throughput obtained by the optimal solution.

In order to observe the difference between the performance of these transmission schemes in a denser network, we increase the network size to ten ($N = 10$). The results for this scenario are provided in Figure 5.19 (a) and (b). Because of the computational complexity of searching for the optimal route, FD with optimal routing & power control is not shown. Figures 5.19 (a) and (b) indicate that our proposed joint routing & transmission power control scheme produces the highest throughput among the other solutions in denser network as well, and has a gain of 1.33 over the FD with *Solution*2. It is also worthwhile to note that the most of the advantage of our proposed solution is associated with the transmission power control, rather than routing since in the case of no power control, routing in *Solution*2 and *Solution*3 yield very close throughput performance.

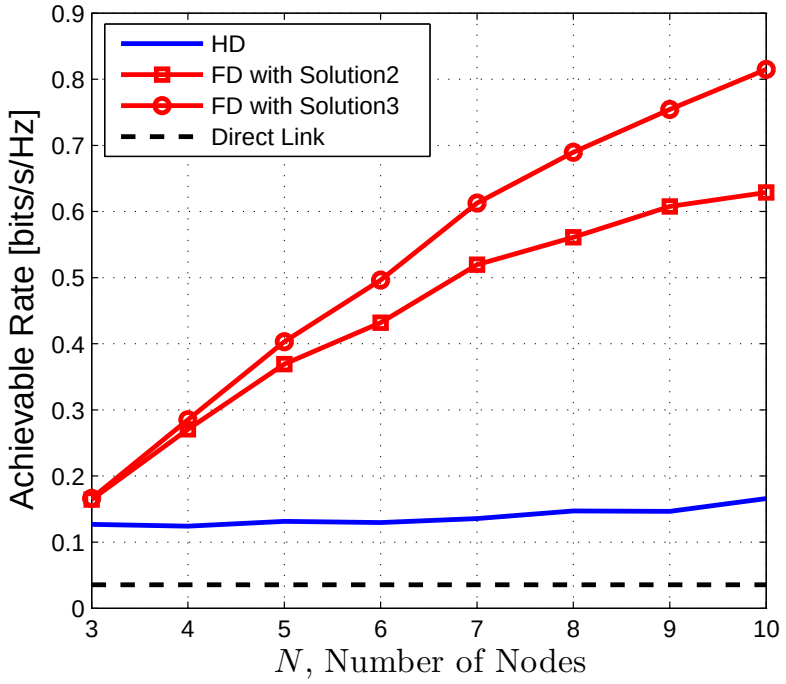

FIGURE 5.20: End-to-end throughput with respect to node density, $P_{max} = 0dBm, d = 100m\alpha = 4, \beta = -80dB$

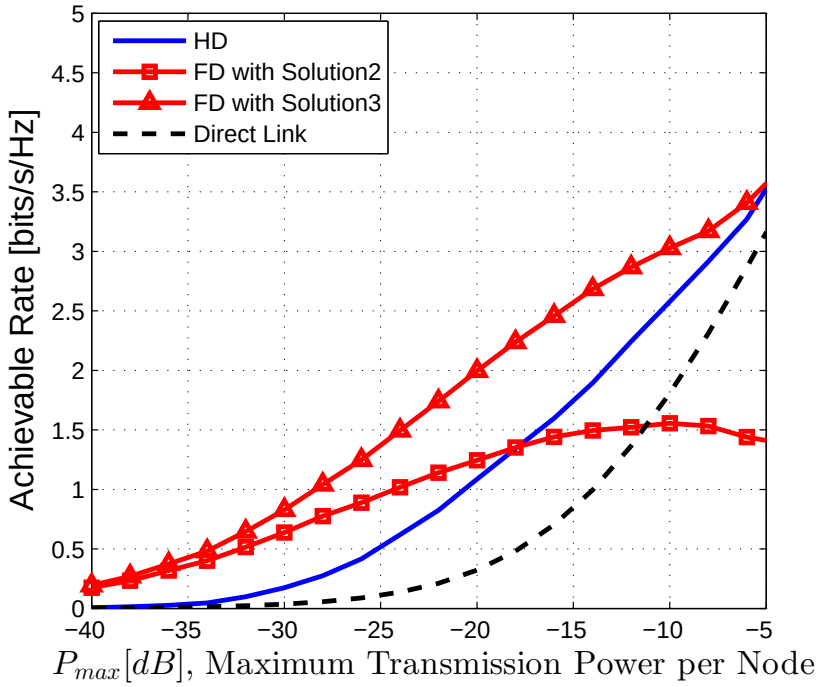

FIGURE 5.21: End-to-end throughput with respect to P_{max}, $N = 20, d = 100, \alpha = 4, \beta = -80dB$

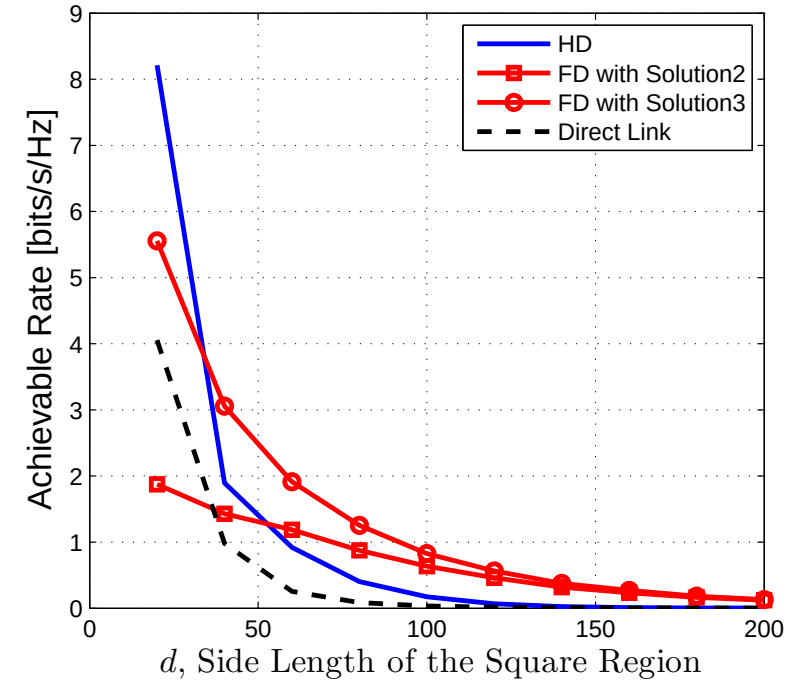

FIGURE 5.22: End-to-end throughput with respect to d, $N = 20, P_{max} = 0dBm, \alpha = 4, \beta = -80dB$

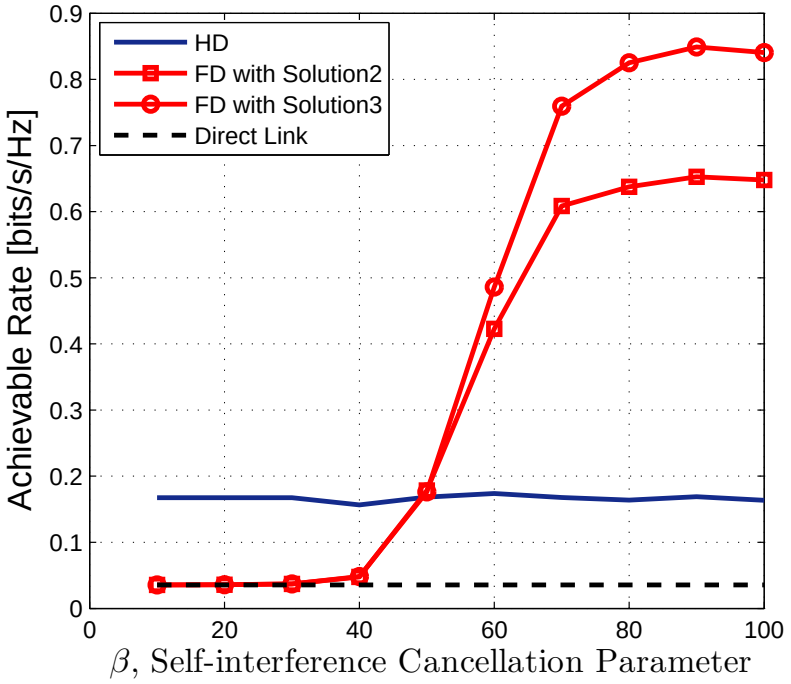

FIGURE 5.23: End-to-end throughput with respect to SI cancellation parameter, β, $P_{max} = 0dB, d = 100, N = 20, \alpha = 4$

In figures 5.20 to 5.23, we aim to observe the effect of different system parameters on these transmission strategies. For FD, we show results for *Solution*2 and *Solution*3 only. In Figure 5.20, we investigate the effect of number of nodes dropped into the area on the throughput by keeping other system parameters as stated. The results suggest that as the node density increases both proposed FD and Ramirez et al's FD yields more throughput. Also notice that proposed FD produces the highest throughput among the other transmission schemes. We plot the achievable rate curves of different communication schemes versus maximum transmission power per node, P_{max} in Figure 5.21. As clearly seen from this figure again, proposed FD offers the best performance. Note also that the performance of FD with *Solution*2 decreases after a certain power level, while performance of FD with *Solution*2 never decreases. This is because in *Solution*3 transmission power levels of FD nodes are computed optimally.

Next, we are interested in the relationship between throughput and the side length of the square region, d in Figure 5.22. What we can conclude from this figure is that HD works slightly better than other strategies for small distances. This is due to the fact that FD performance is corrupted because of strong SI in small distances. However, for $d \geq 40m$, our proposed FD turns out to produce the highest throughput.

In Figure 5.23, these transmission strategies are compared in the presence of different residual SI levels. Notice that for the SI suppression level smaller than about $50dB$, HD performs better than both FD strategies. FD outperforms HD given that SI is suppressed by at least $50dB$. Notice also that proposed FD offers a better performance than the one proposed in [46] for all SI cancellation levels. We also observe that increase in β does not improve the throughput after $80dB$ cancellation since the SI cancellation performance converges to ideal (perfect). In the case of perfect cancellation, while FD with *Solution*3 has a gain of 130% over FD with *Solution*2, it outperforms HD transmission by a factor of five in the investigated scenario.

Through the performed simulations, we compare our joint routing & transmission power solutions with existing solutions in ad hoc networks, where a pair of source and destination nodes perform a one way communication through multiple intermediate relays. We look at the performances of investigated transmission strategies, considering several system parameters such as maximum transmission power per node, node density, path loss exponent of the environment, SI cancellation capability of the FD nodes, the area of the region where the nodes are scattered. What we observe from our comprehensive investigation is that our joint routing & transmission power solution works quite satisfactorily in most of the investigated cases, producing a higher throughput than others do.

Chapter 6

Conclusions

In this thesis, we have first investigated in-band full-duplex wireless communication in fundamental wireless communication scenarios such as two way communication, one way and two way two hop communications. Through comprehensively conducted simulations, assuming same radio resource utilization (antenna conserved and RF chain conserved FD implementations), we have compared the the FD performance with that of HD, considering several system parameters. For FD, we have employed an experimentally characterized and therefore a realistic residual self-interference model in our assessment. We have also evaluated FD performance in the presence of residual self-interference with different amounts. Our results have clearly shown that FD offers a superior throughput performance over HD in two way communication and one way two communication in the case of good SI cancellation, whereas even in the perfect SI cancellation FD does not outperform HD in two way relaying given if analog network coding schemes are applied in the HD relay.

Next, we have focused on the multihop networks with linear topology to investigate the FD performance in multihop communications, where a source node sends its packets to a destination node via multiple intermediate decode-and-forward relays. It is a very well-known fact that power control plays a crucial role in maximizing the end-to-end throughput performance in multihop networks. Therefore, we have studied the problem of optimal power control in multihop relay networks. We

have initially revisited one way two hop communication with the full-interference model assumption where destination node hears both source and relay nodes. We have proposed closed form expressions for optimal power assignment policy for transmitting nodes. Then, we extend the problem to multihop networks with more than one intermediate relay. We have introduced a linear programming based algorithm for optimal power policy in multihop networks. Our simulation results have made it quite clear that FD performs satisfactorily better than HD even with the moderate SI suppression. In the investigated test scenarios, while for at low transmission power level, FD outperforms HD up to by a factor of 2.77 at low transmission power, 1.81 at high transmission power level.

We have then incorporated our proposed power control solution with routing to offer a complete solution to the problem of one way communication in adhoc networks with a single flow. We have proposed two different routing schemes on top of which we apply our power control scheme. Considering several system parameters, we have compared the performance of proposed solutions with traditional HD and the only existing FD solution in the literature. Our numerical analysis have demonstrated that as the SI cancellation capability of the nodes approaches to ideal cancellation, our joint FD routing & power control provides 30% more throughput performance than the solution proposed in [46], gain of our proposed solution over HD transmission can go up to as high as five.

As the future study, we aim to implement our joint routing and power control scheme with a cross layer, MAC and routing protocol.

Bibliography

[1] A. Sabharwal, P. Schniter, Dongning Guo, D.W. Bliss, S. Rangarajan, and R. Wichman. In-band full-duplex wireless: Challenges and opportunities. *Selected Areas in Communications, IEEE Journal on*, 32(9):1637–1652, Sept 2014.

[2] Ict Facts and Figures. `http://www.itu.int/en/ITU-D/Statistics/Pages/facts/default.aspx`. Accessed: 2015-12-22.

[3] R.A. DiFazio and P.J. Pietraski. The bandwidth crunch: Can wireless technology meet the skyrocketing demand for mobile data? In *Systems, Applications and Technology Conference (LISAT), 2011 IEEE Long Island*, pages 1–6, May 2011.

[4] G. Staple and K. Werbach. The end of spectrum scarcity [spectrum allocation and utilization]. *Spectrum, IEEE*, 41(3):48–52, March 2004.

[5] Andrea Goldsmith. *Wireless Communications*. Cambridge University Press, New York, NY, USA, 2005.

[6] Jung Il Choi, Mayank Jain, Kannan Srinivasan, Phil Levis, and Sachin Katti. Achieving single channel, full duplex wireless communication. In *Proceedings of the Sixteenth Annual International Conference on Mobile Computing and Networking*, MobiCom '10, pages 1–12, New York, NY, USA, 2010. ACM.

[7] Mayank Jain, Jung Il Choi, Taemin Kim, Dinesh Bharadia, Siddharth Seth, Kannan Srinivasan, Philip Levis, Sachin Katti, and Prasun Sinha. Practical, real-time, full duplex wireless. In *Proceedings of the 17th Annual International*

Conference on Mobile Computing and Networking, MobiCom '11, pages 301–312, New York, NY, USA, 2011. ACM.

[8] M. Duarte and A. Sabharwal. Full-duplex wireless communications using off-the-shelf radios: Feasibility and first results. In *Signals, Systems and Computers (ASILOMAR), 2010 Conference Record of the Forty Fourth Asilomar Conference on*, pages 1558–1562, Nov 2010.

[9] BTK, 4.5G ihalesini onayladi. `http://www.btk.gov.tr`. Accessed: 2015-12-22.

[10] O. Cepheli, S. Tedik, and G.K. Kurt. A high data rate wireless communication system with improved secrecy: Full duplex beamforming. *Communications Letters, IEEE*, 18(6):1075–1078, June 2014.

[11] S. Hong, J. Brand, Jung Choi, M. Jain, J. Mehlman, S. Katti, and P. Levis. Applications of self-interference cancellation in 5g and beyond. *Communications Magazine, IEEE*, 52(2):114–121, February 2014.

[12] Gan Zheng, I. Krikidis, Jiangyuan Li, A.P. Petropulu, and B. Ottersten. Improving physical layer secrecy using full-duplex jamming receivers. *Signal Processing, IEEE Transactions on*, 61(20):4962–4974, Oct 2013.

[13] M. Duarte, A. Sabharwal, V. Aggarwal, R. Jana, K.K. Ramakrishnan, C.W. Rice, and N.K. Shankaranarayanan. Design and characterization of a full-duplex multiantenna system for wifi networks. *Vehicular Technology, IEEE Transactions on*, 63(3):1160–1177, March 2014.

[14] M. Fukumoto and M. Bandai. Mimo full-duplex wireless: Node architecture and medium access control protocol. In *Mobile Computing and Ubiquitous Networking (ICMU), 2014 Seventh International Conference on*, pages 76–77, Jan 2014.

[15] Dinesh Bharadia and Sachin Katti. Full duplex mimo radios. In *Proceedings of the 11th USENIX Conference on Networked Systems Design and Implementation*, NSDI'14, pages 359–372, Berkeley, CA, USA, 2014. USENIX Association.

[16] M.E. Knox. Single antenna full duplex communications using a common carrier. In *13th Annual Wireless and Microwave Technology Conference*, Apr 2012.

[17] C.R. Anderson, S. Krishnamoorthy, C.G. Ranson, T.J. Lemon, W.G. Newhall, T. Kummetz, and J.H. Reed. Antenna isolation, wideband multipath propagation measurements, and interference mitigation for on-frequency repeaters. In *SoutheastCon, 2004. Proceedings. IEEE*, pages 110–114, March 2004.

[18] Jung Il Choi, S. Hong, M. Jain, S. Katti, P. Levis, and J. Mehlman. Beyond full duplex wireless. In *Forty Sixth Asilomar Conference on Signals, Systems and Computers*, pages 40–44, Nov 2012.

[19] Mohammad A. Khojastepour, Karthik Sundaresan, Sampath Rangarajan, Xinyu Zhang, and Sanaz Barghi. The case for antenna cancellation for scalable full-duplex wireless communications. In *Proceedings of the 10th ACM Workshop on Hot Topics in Networks*, HotNets-X, pages 17:1–17:6, New York, NY, USA, 2011. ACM.

[20] T. Riihonen and R. Wichman. Analog and digital self-interference cancellation in full-duplex mimo-ofdm transceivers with limited resolution in a/d conversion. In *Signals, Systems and Computers (ASILOMAR), 2012 Conference Record of the Forty Sixth Asilomar Conference on*, pages 45–49, Nov 2012.

[21] J.G. McMichael and K.E. Kolodziej. Optimal tuning of analog self-interference cancellers for full-duplex wireless communication. In *50th Annual Allerton Conference on Communication, Control, and Computing*, pages 246–251, Oct 2012.

[22] A.C. Cirik, Yue Rong, and Yingbo Hua. Achievable rates of full-duplex MIMO radios in fast fading channels with imperfect channel estimation. *IEEE Transactions on Signal Processing*, 62(15):3874–3886, Aug 2014.

[23] Dongkyu Kim, Hyungsik Ju, Sungsoo Park, and Daesik Hong. Effects of channel estimation error on full-duplex two-way networks. *IEEE Transactions on Vehicular Technology*, 62(9):4666–4672, Nov 2013.

[24] E. Ahmed and A.M. Eltawil. All-digital self-interference cancellation technique for full-duplex systems. *Wireless Communications, IEEE Transactions on*, 14(7):3519–3532, July 2015.

[25] D.W. Bliss, P.A. Parker, and A.R. Margetts. Simultaneous transmission and reception for improved wireless network performance. In *Statistical Signal Processing, 2007. SSP '07. IEEE/SP 14th Workshop on*, pages 478–482, Aug 2007.

[26] Byungjin Chun and Yong H. Lee. A spatial self-interference nullification method for full duplex amplify-and-forward mimo relays. In *Wireless Communications and Networking Conference (WCNC), 2010 IEEE*, pages 1–6, April 2010.

[27] Na Li, Weihong Zhu, and Haihua Han. Digital interference cancellation in single channel, full duplex wireless communication. In *Wireless Communications, Networking and Mobile Computing (WiCOM), 2012 8th International Conference on*, pages 1–4, Sept 2012.

[28] T. Riihonen, A. Balakrishnan, K. Haneda, S. Wyne, S. Werner, and R. Wichman. Optimal eigenbeamforming for suppressing self-interference in full-duplex mimo relays. In *Information Sciences and Systems (CISS), 2011 45th Annual Conference on*, pages 1–6, March 2011.

[29] J. Sangiamwong, T. Asai, J. Hagiwara, Y. Okumura, and T. Ohya. Joint multi-filter design for full-duplex mu-mimo relaying. In *Vehicular Technology Conference, 2009. VTC Spring 2009. IEEE 69th*, pages 1–5, April 2009.

[30] K. Akcapinar and O. Gurbuz. Full-duplex bidirectional communication under self-interference. In *Telecommunications (ConTEL), 2015 13th International Conference on*, pages 1–7, July 2015.

[31] N. Shende, O. Gurbuz, and E. Erkip. Half-duplex or full-duplex relaying: A capacity analysis under self-interference. In *47th Annual Conference on Information Sciences and Systems (CISS)*, pages 1–6, March 2013.

[32] T. Riihonen, S. Werner, R. Wichman, and Z.B. Eduardo. On the feasibility of full-duplex relaying in the presence of loop interference. In *Signal Processing Advances in Wireless Communications, 2009. SPAWC '09. IEEE 10th Workshop on*, pages 275–279, June 2009.

[33] S. Tedik and G.K. Kurt. Full-duplex relaying communication. In *Signal Processing and Communications Applications Conference (SIU), 2013 21st*, pages 1–4, April 2013.

[34] Yong Li, Tingting Wang, Zhongyuan Zhao, Mugen Peng, and Wenbo Wang. Relay mode selection and power allocation for hybrid one-way/two-way half-duplex/full-duplex relaying. *Communications Letters, IEEE*, 19(7):1217–1220, July 2015.

[35] Wooyeol Choi, Hyuk Lim, and A. Sabharwal. Power-controlled medium access control protocol for full-duplex wifi networks. *Wireless Communications, IEEE Transactions on*, 14(7):3601–3613, July 2015.

[36] A.S. Arifin and T. Ohtsuki. Outage probability analysis in bidirectional full-duplex siso system with self-interference. In *Communications (APCC), 2014 Asia-Pacific Conference on*, pages 6–8, Oct 2014.

[37] M. Duarte, C. Dick, and A Sabharwal. E xperiment-driven characterization of full-duplex wireless systems. *IEEE Transactions on Wireless Communications*, 11(12):4296–4307, December 2012.

[38] Yi Li, M.C. Gursoy, and S. Velipasalar. Throughput and mode selection in two-way mimo systems under queuing constraints. In *Communications (ICC), 2015 IEEE International Conference on*, pages 2271–2276, June 2015.

[39] Dinesh Bharadia and Sachin Katti. Full duplex mimo radios. In *Proceedings of the 11th USENIX Conference on Networked Systems Design and Implementation*, NSDI'14, pages 359–372, Berkeley, CA, USA, 2014. USENIX Association.

[40] M. Pashazadeh and F.S. Tabataba. Performance analysis of one-way relay networks with channel estimation errors and loop-back interference. In *Electrical Engineering (ICEE), 2015 23rd Iranian Conference on*, pages 432–437, May 2015.

[41] S. Goyal, Pei Liu, S. Panwar, R.A. Difazio, Rui Yang, Jialing Li, and E. Bala. Improving small cell capacity with common-carrier full duplex radios. In *Communications (ICC), 2014 IEEE International Conference on*, pages 4987–4993, June 2014.

[42] T. Riihonen, S. Werner, and R. Wichman. Hybrid full-duplex/half-duplex relaying with transmit power adaptation. *IEEE Transactions on Wireless Communications*, 10(9):3074–3085, Sept 2011.

[43] Sachin Katti, Shyamnath Gollakota, and Dina Katabi. Embracing wireless interference: Analog network coding. *SIGCOMM Comput. Commun. Rev.*, 37(4):397–408, August 2007.

[44] H. Alves, D. Benevides da Costa, R. Demo Souza, and M. Latva-aho. On the performance of two-way half-duplex and one-way full-duplex relaying. In *Signal Processing Advances in Wireless Communications (SPAWC), 2013 IEEE 14th Workshop on*, pages 56–60, June 2013.

[45] B. Mahboobi and M. Ardebilipour. Joint power allocation and routing in full-duplex relay network: An outage probability approach. *Communications Letters, IEEE*, 17(8):1497–1500, August 2013.

[46] D. Ramirez Dominguez and B. Aazhang. Optimal routing and power allocation for wireless networks with imperfect full-duplex nodes. In *Communications (ICC), 2013 IEEE International Conference on*, pages 3370–3375, June 2013.

[47] David Tse and Pramod Viswanath. *Fundamentals of Wireless Communication*. Cambridge University Press, New York, NY, USA, 2005.

[48] Leon Garcia. *Probability and Random Processes for Electrical Engineers*. Addison Wesley Longman, 1994.

[49] I Emre Telatar et al. Capacity of multi-antenna gaussian channels. *European transactions on telecommunications*, 10(6):585–595, 1999.

[50] T.J. Oechtering, C. Schnurr, I. Bjelakovic, and H. Boche. Broadcast capacity region of two-phase bidirectional relaying. *Information Theory, IEEE Transactions on*, 54(1):454–458, 2008.

[51] Shengli Zhang, Soung Chang Liew, and Patrick P. Lam. Hot topic: Physical-layer network coding. In *Proceedings of the 12th Annual International Conference on Mobile Computing and Networking*, MobiCom '06, pages 358–365, New York, NY, USA, 2006. ACM.

[52] R. Knopp. Two-way wireless communication via a relay station. In *GDR-ISIS meeting*, Mar. 2007.

[53] Dinesh Bharadia, Emily McMilin, and Sachin Katti. Full duplex radios. *SIGCOMM Comput. Commun. Rev.*, 43(4):375–386, August 2013.

[54] M.E. Knox. Single antenna full duplex communications using a common carrier. In *Wireless and Microwave Technology Conference (WAMICON), 2012 IEEE 13th Annual*, pages 1–6, April 2012.

[55] A. Rahmati and V. Shah-Mansouri. Price-based power control in relay networks using stackelberg game. In *Electrical Engineering (ICEE), 2015 23rd Iranian Conference on*, pages 263–267, May 2015.

[56] Yi Shi, Jiaheng Wang, K. Letaief, and R.K. Mallik. A game-theoretic approach for distributed power control in interference relay channels. *Wireless Communications, IEEE Transactions on*, 8(6):3151–3161, June 2009.

[57] T. Riihonen, S. Werner, and R. Wichman. Transmit power optimization for multiantenna decode-and-forward relays with loopback self-interference from full-duplex operation. In *Signals, Systems and Computers (ASILOMAR), 2011 Conference Record of the Forty Fifth Asilomar Conference on*, pages 1408–1412, Nov 2011.

[58] Yindi Jing and S. ShahbazPanahi. Max-min optimal joint power control and distributed beamforming for two-way relay networks under per-node power constraints. *Signal Processing, IEEE Transactions on*, 60(12):6576–6589, Dec 2012.

[59] S. Gupta and R. Bose. Joint routing and power allocation optimization in outage constrained multihop wireless networks. In *Personal Indoor and Mobile Radio Communications (PIMRC), 2013 IEEE 24th International Symposium on*, pages 2245–2249, Sept 2013.

[60] A. Sadeghi, S.H. Mosavat-Jahromi, F. Lahouti, and M. Zorzi. Multi-hop wireless transmission with half duplex and imperfect full duplex relays. In *Telecommunications (IST), 2014 7th International Symposium on*, pages 1026–1029, Sept 2014.

[61] Ravindra K. Ahuja, Thomas L. Magnanti, and James B. Orlin. *Network Flows: Theory, Algorithms, and Applications*. Prentice-Hall, Inc., Upper Saddle River, NJ, USA, 1993.